Context-dependent phenotypic switching and non-genetic memory in heterogeneous bacterial populations

Orso Maria Romano

université PARIS-SACLAY

NNT : 2017SACLS464

UNIVERSITÉ PARIS SUD
Comprendre le monde, construire l'avenir

Context-dependent phenotypic switching and non-genetic memory in heterogeneous bacterial populations

Thèse de doctorat de l'Université Paris-Saclay
préparée à l'Université Paris-Sud
au sein de l'Institut de Biologie de
l'École Normale Supérieure (IBENS)

École doctorale n°567 Sciences du Végétal : du Gène à l'Écosystème
Spécialité de doctorat: Biologie

Thèse présentée et soutenue à Paris, le 30 novembre 2017, par

Orso Maria Romano

Composition du Jury :

M. Olivier Martin Directeur de Recherche, INRA – Paris-Saclay	Président
M. Marc Lefranc Directeur de Recherche, Université de Lille	Rapporteur
Mme. Carine Douarche Maître de Conférences, Université Paris-Saclay	Examinateur
M. Nicolas Desprat Maître de Conférences, Université Paris VII	Examinateur
M. Chris Bowler Directeur de Recherche, IBENS	Directeur de thèse
Mme. Silvia De Monte Chargée de Recherche, IBENS	Co-Directrice de thèse

Thèse de doctorat

CONTENTS

ABSTRACT

Phenotypic heterogeneity is a common, complex property of microbial populations: it bridges genetics, the organism's response to the environment, and evolutionary concepts such as bet hedging.

Individual cells of isogenic microbial populations exposed to the same microenvironment can stochastically switch among discrete phenotypes as a strategy of survival. The determinants of such "phenotypic switches" between multiple stable states are often both genetic and non-genetic, and can relate to the interaction between the population and the environment.

Phenotypic multistability is often correlated with phenomena of inheritance of the phenotype from parent cells to their offspring, sometimes over several generation times. This "trans-generational persistence" of the phenotype may pave the way for the evolution of division of labour.

Pseudomonas fluorescens switching strains (switchers) are a model system to study microbial heterogeneity, phenotypic switching and transgenerational memory. The alternative phenotypic states, called CAP+ and CAP-, are related to the production of a colanic acid capsule around the cell surface.

The switchers were evolved from the *Pseudomonas fluorescens* SBW25 wild type strain by experimental evolution: the switch arises from highly specific genetic mutations on genes belonging to the pyrimidine metabolic pathway, crucial in both nucleic and colanic acid biosynthesis. Different switching strains differ in terms of growth rate and frequency of the CAP+ phenotype during exponential phase.

Populations of the switchers undergo big time variations in the fraction of cells expressing one phenotype even when they are kept in exponential growth. The amount of variation depends on the initial condition in ways that can be accounted for only if one considers that the switching rate depends on the environmental conditions created by growth of the population itself. Such a feedback gives rise to a dependence on history that can be interpreted as population-level evidence of phenotypic "memory".

Standard models whereby the genotype determines the switching rates fail to explain the observed non-monotonous dynamics of the phenotypes' frequencies, producing simple exponential decays to the asymptotic frequencies. The switching rates

need to be made non-constant, for instance by linking their value to that of an environmental cue.

We developed a model consisting of a third-order dynamical system where one of the state variables quantifies the intracellular concentration of a metabolite X synthetized by the cell and diluted along with cell division. This internal concentration works as the mediator of the coupling between population demography and switching dynamics, and the growth rate as the proxy for the ensemble of the environmental cues modulating the probabilities of switching.

This model manages to reproduce the main experimental observations (overshoot and undershoot in the frequency of the phenotypes, biphasic response to preculture conditions, long-term effect in the phenotypic composition of the population) and predicts the negative correlation between the mean growth rate and the frequency of the CAP+ phenotype in exponential phase that we observed.

In summary, a growing population of switching cells cannot be fully characterized only by the asymptotic steady state of the phenotypes' frequencies, because phenotypic switching is inextricably intertwined with demography. One possible way to model this interdependence is through internal concentrations, a choice that in our case allowed us to coherently interpret the experimental data.

From an evolutionary perspective, internal concentrations-mediated transgenerational inheritance of the phenotype may favour the emergence of bet-hedging-like strategies. Nevertheless, given the number of factors involved, only through a detailed knowledge of the ecological dynamics it is possible to draw significant conclusions on the evolutionary outcome.

Résumé en langue française

L'hétérogénéité phénotypique est un trait commun des populations microbiennes qui relie la génétique, la réponse de l'organisme à l'environnement et concepts évolutifs tels que le bet-hedging.

Des cellules individuelles de populations microbiennes isogéniques peuvent changer de façon aléatoire leur phénotype comme stratégie de survie, même quand elles sont exposées au même microenvironnement. Les déterminants de tels switch phénotypiques entre plusieurs états stables peuvent être génétiques ou non-génétiques, et souvent liés à l'interaction entre la population et l'environnement.

La multistabilité phénotypique est souvent corrélée à des phénomènes d'hérédité du phénotype, parfois à travers plusieurs générations. Cette persistance du phénotype peut ouvrir la voie à l'évolution de la division du travail.

Les souches de Pseudomonas fluorescens, appelées switchers, sont un système modèle pour étudier l'hétérogénéité phénotypique, les switch phénotypiques et la mémoire transgénérationnelle. Les états phénotypiques alternatifs, appelés CAP+ et CAP-, sont liés à la production d'une capsule d'acide colanique autour de la paroi cellulaire.

Les switchers ont été développés à partir de la souche de type sauvage *Pseudomonas fluorescens* SBW25 par évolution expérimentale : des mutations génétiques spécifiques sur certains gènes de la voie métabolique de la pyrimidine, essentielle dans la biosynthèse à la fois de l'ADN/ARN et de l'acide colanique, entraînent l'émergence du switch. Chaque souche est caractérisée par son taux de croissance et sa fréquence du phénotype CAP+ en phase de croissance exponentielle.

Même lorsqu'elles sont maintenues en croissance exponentielle, les populations des switchers présentent de grandes variations temporelles dans la fraction de cellules exprimant un des deux phénotypes. Le degré de variation dépend de la condition initiale d'une manière qui suggère que le taux de switch dépend des conditions environnementales engendrées par la croissance de la population elle-même. Une telle rétroaction donne lieu à une dépendance des conditions passées qu'on peut interpréter en termes de "mémoire" phénotypique à l'échelle de la population.

Les modèles standard qui associent à chaque génotype des taux de switch fixes ne permettent pas d'expliquer le caractère non-monotone de la dynamique des fréquences des phénotypes. Les taux de switch doivent être rendus non-constants, par exemple en reliant leur valeur à celle d'un signal environnemental.

J'ai développé un modèle sous forme de système dynamique de troisième ordre où l'une des variables d'état quantifie la concentration intracellulaire d'un métabolite X synthétisé par la cellule et dilué à travers la division cellulaire. Cette concentration interne couple la démographie et la dynamique de switch. Le taux de croissance moyen de la population fonctionne comme proxy pour l'ensemble des signaux environnementaux modulant les probabilités de switch.

Mon modèle reproduit les principales observations expérimentales et prédit la corrélation négative entre le taux moyen de croissance et la fréquence du phénotype CAP+ en phase exponentielle que nous avons observée.

En résumé, une population croissante de cellules capables de switch phénotypiques ne peut être entièrement caractérisée en déterminant uniquement l'état asympto-

tique des fréquences des phénotypes, car il se trouve que le switch phénotypique est étroitement lié à la démographie. Il est possible de modéliser cette interdépendance à travers des concentrations internes — un choix qui, dans le cas des switchers, permet d'interpréter de manière cohérente les données expérimentales.

Dans une perspective évolutive, l'héritage du phénotype par des concentrations pourrait seconder l'émergence de stratégies comme le bet-hedging. Pourtant, vu le nombre de facteurs impliqués, seule une connaissance détaillée de la dynamique écologique permet de tirer des conclusions significatives à ce sujet.

a mia mamma

CHAPTER 1

INTRODUCTION

Phenotypic heterogeneity, i.e. the variability in observable traits across members of a sympatric population, is ubiquitous among living organisms. Genetic, environmental and epigenetic factors affect phenotypic variability in a wide variety of ways, weaving a complex cloth of interactions, from the molecular scale, up to the behavioral one.

Isogenic populations of microbes, too, display heterogeneity at the phenotypic level, which proves to be advantageous from an evolutionary perspective. Microbial phenotypic heterogeneity often takes the form of alternative, discrete phenotypes whose adaptive value resides in allowing the organism to respond to changes in the environmental conditions, or anticipate them by stochastically generating phenotypic variants. The latter strategy, where individual cells stochastically switch between the possible alternative states, is adaptive when the environment is hardly predictable, and can be interpreted as an attempt of the population to hedge its "survival bets".

Most mathematical models for the study microbial phenotypic heterogeneity draw a dychotomous distinction between responsive and stochastic variability. Nevertheless, the examples of hybrid responsive-stochastic phenotypic switch are manifold, bacterial persistence being the most eminent one. By using *Pseudomonas fluorescens* as model organism for populations of phenotypically switching units, in this Thesis I explore the general framework through a mixed theoretical-experimental approach.

This research develops two main themes. First, I will address the mutual dependence between phenotypic variability and the demography of populations of switching units. As already mentioned, under certain circumstances, variability can be advantageous for those populations adopting it. Besides, many are the instances of environmental cues affecting population growth that can be associated with a change in the phenotypic composition of the population. However, the evolution of phenotypic switch is seldom studied beyond the cases of simple demographic regimes (e.g. populations artificially held in exponential phase). This is a reasonable simplification, for the sake of simplicity and power of prediction, unless the switching behaviour proves to be influenced by the state of growth of the population.

A second theme tackled in this Thesis is the relation between phenotypic switching and trans-generational, non-genetic heritability of the phenotype. Indeed, it can be noticed that often the phenomena of maintenance of the phenotype throughout generations are correlated with the presence of multistability. This is true in other fields, too — such as physics and neurobiology: the existence of multistable states is considered to be strictly linked to "memory" (metastability). If this is a general property, is it possible to establish a link between trans-generational memory and the existence of the switch? I will investigate the consequences on the population-level history-dependence of having a context-dependent stochastic switch.

In summary, by the use of mathematical models and experiments on *Pseudomonas fluorescens* switching populations, this Thesis aims at investigating the mechanisms that might underpin the interplay between population demography and phenotypic variability, and its possible ecological outcomes. This is realized by going beyond the classic dualistic view where context-independent stochastic switch is in opposition to a responsively-tuned switching behaviour.

Questions addressed by this thesis

More in detail, this Thesis tackles the aforementioned general problems by addressing the following questions:

- Can the phenotypic switch performed by *Pseudomonas fluorescens* populations be considered as purely stochastic or environmentally-driven? How is it possible to discern between these two scenarios through population-level measurements?
- Which are the relevant observables to describe the phenotypic state of a collection of switching units? How can these quantities be measured?
- What are the ecological processes influencing phenotypic heterogeneity in populations of *P. fluorescens* switchers? Is population growth one of them? If yes, which interplay exists between the time scales of the cellular switch and that of population growth?
- How is phenotypic variability maintained and sustained in growing populations of *P. fluorescens*? Can a non-genetic trans-generational transmission of the phenotypic state be inferred from measurements of the phenotypic composition of the population? If yes, what are the ecological conditions influencing it?

Outline of this Chapter

This Introduction to my Thesis starts by providing an overview on phenotypic heterogeneity, focusing on the cellular mechanisms that can influence its emergence and on the functions that this significant property can provide (Section 1.1). I then discuss what mathematical models can bring to the understanding of the ecological and evolutionary consequences of phenotypic heterogeneity (Section 1.2). Finally, *Pseudomonas fluorescens* is presented as an appropriate model system for the study of microbial phenotypic heterogeneity (Section 1.3).

1.1 Phenotypic heterogeneity in microbial populations

Natural selection acts on phenotypes, and phenotypic variation is its raw material. Indeed, a gene is affected by the action of natural selection only if the latter differentially influences the phenotypes expressed by the former. In the long run, competition among phenotypes results in the perpetuation or elimination of the whole underlying genotype from the population pool [58]. In other words, natural selection makes the genetic pool of a population more and more adapted to the environment if at least part of the phenotypic variation has a genetic basis.

Along with genetic information, environmental cues are fundamental in the determination of phenotypic heterogeneity [99]. It was shown that extreme environmental changes, just as high mutation rates, tend to increase phenotypic variation[1]. This raises the question: Is variation due to mutations and due to environmental change equivalent? A positive answer is suggested by studies introducing the concept of "equivalence" (or "interchangeability") [103]: this phenomenon — empirically discovered in a phylogeny study on sex determination in turtles and lizards [50] — consists in the fact that a (great) change in gene expression can be equally induced by genetic mutations or by (extreme) environmental change, and is one of the strongest pieces of evidence in support of genetic assimilation [97].

Genetic assimilation *phenotypic trait fixation due to a genetic change in regulation following a persistent selection for that trait, usually environmentally induced*

In other words, gene expression, the means through which biological information is processed, is indifferent to its causes, let them be endogenous or external. If we consider variability in a phenotypic trait as a distinct phenotypic trait itself, then we should conclude that genetic and environmental factors might result in the same degree of phenotypic variability. As it will become evident later on, the focus of this work is phenotypic variation in isogenic bacterial populations, thus independent of genetic mutations as sources of variability at the phenotype level. Moreover, the study of bacteria rules out complications associated to using animals or plants as model organisms, such as long generation times, large genome size, polyploidy and sex.

For further simplicity, the (more general) problem of continuous traits tackled by quantitative genetics is reduced here to the case of alternative phenotypes. Phenotypic alternatives fall into two broad categories, in terms of the selective contexts that give rise to them and (in some cases) induce their expression: alternatives fundamentally due to the response to environmental heterogeneity or change, and alternatives expressed *a priori*, enabling to escape from strong intraspecific competition for resources (e.g. nutrients, space, or mates) [98]. In either case, alternative phenotypes represent the epitome of the ability of living beings to respond and adapt to, or anticipate, any change in their surroundings [99].

Increased levels of phenotypic heterogeneity can evolve in the laboratory, driven by experimentally imposed fluctuating selection [51, 15, 63, 11]. In a social context, where cells are arranged in groups of interacting elements, phenotypic heterogeneity can be at the basis of the division of labour between individuals and therefore in-

[1] A classical example are *Drosophilae*, see [97] and *cf.* [46]: "In addition to the average phenotypic change by genetic mutation, the observed increase in phenotypic fluctuation acts as an evolutionary strategy to produce an extreme phenotype under severe selective environments.".

crease, through group performance, the rate at which populations grow or the range of functions that they can perform [79]. The role of selection regimes is there crucial: experimental evolution on the trans-generational persistence of heterogeneous collectives showed that, counterintuitively, a regime where the lowest fitness phenotype at the cell level attributes an enhanced fitness to the lineage (and thus has a greatest evolutionary potential) is favoured on the one where the low-fitness phenotype is purged from the population pool [45]. Other cases where heterogeneity/division of labour emerged in the lab can be found in yeast evolution experiments [81].

Alternative phenotypes
discrete options for a particular function, always divergent from each other due to selection under the different conditions of their expression

Section 1.1.1 reviews what is known about the role of genes on the determination of phenotypes and their variability. In Section 1.1.2 the ability to tune the phenotype in response to the environment, called phenotypic plasticity, is discussed. Section 1.1.3 is devoted to detailing the role of stochasticity in the determination of phenotypic heterogeneity. Examples of alternative phenotypes, and a review on the possible mechanisms underpinning their expression and evolutionary consequences are expounded in Section 1.1.4. Finally, the role of mechanisms allowing microbial populations to transfer information throughout generations is discussed in Section 1.1.5.

1.1.1 The genotype-to-phenotype relationship

The genotype is at the same time the physical substrate and the information at the basis of phenotypic determination. All factors linking the genotype with the expression of phenotypes are of extreme importance for evolution.

Since the Danish botanist and genetics pioneer William Johannsen in 1906 formalized the relation between genotype and phenotype (later described as a "map"), the mechanisms shaping and controlling it have been the subject of intense debate [3, 76]. Although a "one genotype, one phenotypic trait" correspondence is often assumed for parsimony and simplicity, a large body of experimental observations indicate that in many important circumstances tno univocal relationship between the genotype and expressed phenotype can be established, for example in populations living in unpredictable environments.

It is well known that genes and their level of expression affect not only the mean phenotypic trait values (making them more or less adapted to the specific environment), but also their variability. Theoretical and experimental studies indicate the existence of a positive correlation between the variability of a phenotype across a population and the average response of such phenotype to a given genetic change. Kunihiko Kaneko and collaborators performed an evolutionary experiment in bacteria in which they selected for increased fluorescence of a protein and measured a positive correlation between the phenotypic fluctuation of the fluorescence over clone bacteria (inter-individual variability) and the speed of fluorescence evolution (response to the genetic change) [85]. In other words, the closer the system is to "perfect" adaptation, the lower is the trait improvement due to mutations, as well as the variance of the trait variation around the mean phenotype, a conclusion which is analogous to Fisher's theorem on gene and trait variation [36].

1.1.2 The role of environment: phenotypic plasticity

Phenotypic (intraspecific) variation can be classified according to different properties: its responsive/stochastic character [16], the continuous/discrete nature of the trait [39], or depending on whether the phenotypic variability has a purely genetic origin or not. About the last categorization, in 1963 Mayr introduced a distiction between *polymorphism* (genetically-induced phenotypic heterogeneity) and *polyphenisms* (non-genetically-induced phenotypic heterogeneity), which can be regarded as the extreme ends of a continuous spectrum of phenotypic outcomes due to genes, environment and their interaction.

Phenotypic plasticity
the ability of an organism to react to an environmental input with a phenotypic change

When dealing with environmentally-induced variation alone, phenotypic heterogeneity is usually named phenotypic plasticity. Phenotypic plasticity is the ability of a single genotype to produce more than one alternative form of morphology, physiological state, and/or behaviour in response to the environmental conditions [98]. Plasticity is a concept borrowed from developmental biology, and it can be interpreted as time-dependent intra-individual variability [99].

In other words, one given trait (and, by extension, also a strain or a population) is plastic if the possible phenotypes produced by that single genotype when exposed to different environmental conditions are more than one [77, 39]. Together with control mechanisms like genetic canalization and developmental stability, plasticity contributes to the tuning of phenotypic variation induced by all the sources of variability (genes, environment and stochasticity). It also modulates the level of competition between sympatric populations [98].

1.1.3 The role of stochasticity: from noise to bet hedging

Finally, some instances of phenotypic heterogeneity cannot be ascribed neither to genes, nor to the environment or their interaction, and appear to be generated by random processes: stochastic phenotypic heterogeneity is found both in continuous traits (e.g. seed dormancy in annual plants [19]), and in discrete ones (e.g. the offspring size in chicken [29]).

Stochasticity is generated at the molecular scale by fluctuations in the number of key cellular components, such as transcription factors in gene expression [92, 30]. Noise in gene expression has been classified into extrinsic or intrinsic [93, 31]: extrinsic noise refers to stochasticity in gene expression due to fluctuations in other cellular compounds or processes (cell age, cell cycle phase) affecting the expression of the gene of interest, while intrinsic noise consists in the stochasticity in the expression of a particular gene all other factors being equal. Intrinsic variability is typically attributed to stochastic fluctuations in the number of molecules involved in gene expression, when these are present in small numbers within cells.

Noise in gene expression can underpin heterogeneity only under certain genetic network architectures [17, 75, 66]. Seemengly, some of these modular gene regulation topologies, called *motifs*, evolved across different clades due to the fitness increase that they can supply to the organism [5]. Furthermore, noise in gene expression might bestow a selective advantage to organisms under stress, as high levels of fluctuations can generate a library of different metabolic possibilities, thus phenotypic diversifica-

tion. Noise-induced enhancement in a population's adaptive potential highlights the potentially fundamental role of stochastic mechanisms in the evolution of microbial survival strategies [38].

For the scope of this work, the most relevant adaptive value of stochastic phenotypic heterogeneity resides in the fact that it allows some individuals of a population to survive sudden changes in selective conditions, thereby eliciting persistence of the underpinning genotype in ever-changing, unpredictable environments. In this perspective, the stochastic generation of variant phenotypes is interpreted as a bet-hedging strategy [88] (see [94] for a review).

Bet hedging
random assignment of the possible phenotypes to recurrent but unpredictable environments, on the chance that some will fall into an environment where they are adapted and thus save the lineage from the decline or extinction

In adaptive bet hedging, the mean individual fitness of an isogenic population or brood is lowered by the expression, in some individuals, of maladaptive phenotypes. Rather than those perfectly adapted to their current environment, though, selection may favor populations expressing some of those phenotypic alternatives, thus reducing the chances of a complete failure in the future. In other terms, homogeneous populations adapted to the most favourable environment (the "good year specialists") maximize their arithmetic fitness, while by adaptive bet hedging a population maximizes the fitness geometric mean over the set of possible environmental conditions.

Bet-hedging strategies can enhance the success of microbial infections, with populations of infectious microbes performing division of labour in order to optimize timing and spreading of their infections. This was observed for populations of *Salmonella typhimurium* [2, 24] and *Pseudomonas aeruginosa* [25]. Typically, such populations are poorly susceptible to classic countermeasures like antibiotics exposure, the most noteworthy example being persistence to antibiotics treatment in *E. coli* [8].

Theoretical and experimental studies show that bet hedging evolves as a response to unpredictably fluctuating environments over a time scale usually longer than a generation time. Other solutions are instead preferable with other patterns of environmental variation. When the changes in the environmental conditions are predictable, then genetically encoding for a sort of developmental program, or heterochrony [43], might be a preferred strategy. When the changes occur on a time scale faster than individual generation time, thus "detectable" by single individuals, sensing is the preferred strategy [54]. Spatially heterogeneous enviroments as well favour genetically-driven differentiation (polymorphisms) over bet hedging [87].

1.1.4 Alternative phenotypes and switching

As reviewed in the previous Sections, phenotypic heterogeneity shows a great deal of variety in terms of determinants and functions. Here and throughout this work, I focus on a simple yet general instance of phenotypic heterogeneity, that is the case of discrete phenotypic states for qualitative traits, also known as polyphenisms or alternative phenotypes. Alternative phenotypes can either be induced by environmental cues, or stochastically determined [99]. The expression of alternative phenotypes can be seen as a clear manifestation of the "principle of divergence" [23]: the advantage of adopting opposite, extreme phenotypes or tactics enables individuals to escape, partially at least, competition with conspecifics that would otherwise be their closest rivals.

In the microbial domain, alternative phenotypes are everywhere. Instances of alternative phenotypes are often distinguished between *responsive* and *stochastic*. Responsive alternatives are elicited by the assessment of the environmental conditions through sensing mechanisms, and generate a response to match the new environment. Stochastic alternatives rely on the intrinsic stochasticity of the gene circuits involved in the determination of the phenotype of interest, and allow microbial populations to hedge their survival bets and prevent extinction in the case of very rare or completely unpredictable events.

Quorum sensing
bacterial cell to cell communication involving the production, detection, and response to autoinducers, i.e. signaling molecules produced and excreted by cells

One of the most fascinating example of responsive alternative phenotypes in microbes is quorum sensing [84]. In pathogenic bacteria, the response to population density can for instance consist in the ability of tuning the transcription of genes related to virulence [18, 2], allowing some bacteria to maintain a benign persistent infection in their host. Such persistence possibly facilitates the evolution of mutualistic relationships [32].

In turn, examples of noise-generated phenotypic bistability can be found in bacterial persistence in *Escherichia coli* and genetic competence in the soil bacterium *Bacillus subtilis*. Persistence is provided by a phenotype that is rarely expressed in bacterial isogenic populations. Cells in the persistent state are characterized by a very low growth rate but also by the capacity to stand exposure to antibiotics for a very long time. Once the antibiotics cycle is over, these cells restore normal cell division, therefore allowing the genotype to survive. Populations grown from such surviving bacteria are not resistent to antibiotics, and the proportion of susceptible cells does not change after the first cycle of antibiotics, which proves the phenotypic nature of the switch between the persistent to the susceptible state and vice versa [8].

In stationary phase, around 10% of cells in genetically identical *B. subtilis* populations gain the ability to take up naked DNA from the environment (genetic competence). Bistability results from noisy expression of the *comK* gene: while in exponential phase its product ComK is rapidly degraded in all cells, when stationary phase is reached, a quorum sensing cascade leads to the expression of ComS, a protein that protects ComK from degradation. Cells reaching a threshold level of ComK spontaneously switch to the competent state (and those that drop below the ComK threshold switch back to the non-competent state) ([60], reviewed in [26]).

It should be pointed out, however, that such a distinction between responsive and stochastic switching is nothing but an oversimplification, as sensing and noise are often tangled mechanisms. An example is provided by diauxic shifts, i.e. the production of morphologically distinct dormant stages in response to starvation [65, 91]. The classic view identified its main cause in the modification of metabolic fluxes induced by the exhaustion of one nutrient source, while recent studies on *Lactococcus lactis* and *Klebsiella oxytoca* revealed how much stochasticity and response can be intertwined [89, 86]. *Lactococcus lactis* presents populations able to grow on two sugar sources always present two coexisting stable cell types with alternative metabolic strategies. The fraction of each metabolic phenotype depends on the level of catabolite repression and the metabolic state-dependent induction of stringent response, as well as on epigenetic cues [89]. These examples of environment-dependent stochastic bistability find all a common factor in the presence of growth rate differences, which result on an

effective reduction of population-averaged production of cells in exponential phase. I will tackle this problem in Chapter 3.

Whatever the mechanisms underpinning their behaviour, phenotypically switching microbial populations are often described in terms of multistable systems whose global state (the ensemble of the variables[2] of the system, like population size and frequency of the alternative phenotypes across the population) depends on few environmental or internal parameters [26]. Multistability encompasses the concepts of fluctuation (the variance of some quantity) and response (the average change of that quantity for a given parameter change). With a theoretical approach, Kaneko and collaborators proposed a proportionality relationship between fluctuation and response in biological systems, analogous to the fluctuation–dissipation theorem in physics [85], suggesting a quantitative way to interpret evolutionary strategies such as the production of extreme phenotypes [46].

A most striking signature of multistability is hysteresis, whereby the history of the system influences its response to a same input or signal [94]. As environmental conditions (e.g. concentrations of available nutrients, or selective agents) change, relative frequencies of phenotypes in a phenotypically heterogeneous isogenic microbial population are susceptible to vary in a hysteretic fashion, as was shown for the expression of the *lac* operon in *Escherichia coli* [73], or genes subjected to mutual repression in a synthetic circuit [20].

At the cellular level, both responsive and stochastic polyphenisms work through a mechanism that makes individuals change their phenotypic state: I refer to any kind of process allowing the transition between discrete alternative states with the term "switch". Typically, individual cells in microbial heterogeneous populations switch phenotype on a temporal scale faster than that of genetic mutations (see [74] and references therein). Such a time scale depends on that of environmental change, directly in the case of responsive switching, and indirectly for stochastic bet-hedging strategies [54].

In either case, switching has an influence on fitness and long-term population growth [1] whenever the alternative phenotypes are not equivalent (neutral) with respect to the environment. The long-term success of an exponentially growing population can be assessed on the basis of the probabilities of switching between phenotypes [57]. Indeed, if one of the two phenotypes is more adapted than the other to a given environmental state, it will grow faster and/or reach a higher population size in that environment, while the reverse occurs when conditions become favourable to the other phenotype. The average growth rate of the isogenic population of switchers, which can be computed as the weighted average of the growth rate of its phenotypically diverse components, is therefore influenced by the population composition.

[2]Here and later in this Thesis, I will refer to time-dependent observables characterizing the state of the system with the term *variable*, and I will adopt the term *parameter* for observables specifying a condition of the system, influencing the variables of the system and in principle externally controllable.

1.1.5 Non-genetic trans-generational phenotypic "memory"

Due to its relevance in the study of phenotypic variability in bacterial populations, in this Section I present and discuss another main topic of modern evolutionary synthesis: the heritability of the phenotype, that is the trans-generational persistence of phenotypes, herein also referred to as non-genetic "memory". Indeed, (each kind of) variability needs to be heritable in order to be the raw material for selection. As proved by the ubiquitous existence of epigenetic mechanisms (even excluding behaviour or cultural transmission), heritability in its broader sense is partly non-genetic and has a very strong impact on evolution [47]. In other terms, the problem consists in answering the following question: How does the behaviour of single cells scale up to history-dependence at the population level?

In the presence of stochastic phenotypic switching, it is usually possible to associate characteristic persistence times to each of the possible phenotypic states. Experimental evidences on microbes showed that there exist two main qualitatively different classes of phenotypes in terms of their persistence time distributions across the members of the population [72]: "memoryless" states (whose duration follows a negative exponential distribution, like radioactive decay), and "time-controlled" states (whose duration is distributed around a characteristic persistence time). In either case, an average persistence time can be defined: when such a characteristic time scale exceeds the generation time, then the phenotypic persistence can be interpreted as the result of trans-generational memory mechanisms.

When the division rate of the individual depends on its phenotypic state (thus when the fitness of the population depends on inter-individuals heterogeneity), tuning the time scales of the switch between alternative states and the efficacy of phenotypic "memory" becomes essential for microbial populations to cope with the inevitable changing nature of their environments [48]. Many examples about multiple phenotypes associated with trans-generational "memory" support this idea: microbial populations are known to respond faster to a change of nutrient source when the forthcoming nutrient source has been presented in the recent past ("nutrient shifts", [56]), and to display increased survival to a given level of stress when previously exposed to sub-lethal levels of the same stress ("stress response", [7] and [64]).

As I will discuss in detail in Section 1.3, *P. fluorescens* is an excellent biological model organism to study phenotypic heterogeneity and trans-generational persistence of the phenotype: several phenotypically heterogenous phenotypes have been obtained through experimental evolution in controlled conditions, and the phenotypic states that they can express persists for several generations. These features make this bacterium an ideal candidate to study the relation between phenotypic heterogeneity and population eco-evolution.

1.2 Theoretical models of phenotypic heterogeneity

If the "book [of Nature] is written in mathematical language" [40], biology makes no exception. The study of living systems is all about the assessment of variations (in number, shape, pattern…, both in time and in space) and, although biology had remained a mostly observational and conjectural discipline for centuries, only rigorous quantification and analysis has so far permitted to compare and discuss the results on an objective ground.

Models, i.e. convenient schemes of reality, can be effective tools to investigate natural phenomena in a systematic way, as they spell out the hypotheses of a given interpretation framework, and make testable predictions. When the relations between the qualities of the object of study are written in mathematical terms, the expression mathematical model is used. Their formalism must accomodate the characteristics of the system to be studied and be appropriate to answer the relevant questions. Classic examples can be found in the use of systems of ordinary differential equations for the population dynamics of two interacting species [59], or in the application of agent based modelling to the study of collective motion [82].

The elaboration of a mathematical model proceeds by inductive reasoning, and aims to an arbitrarily good description of the phenomena of interest. Once attained the desired level of precision in its descriptive power, a mathematical model is queried for quantitative predictions about the behaviour of the real system under different conditions, whose correctness and accuracy can then be experimentally tested. The analysis of the deviations between theoretical predictions and results of the experimental tests usually reveals to be useful for the refinement (or, eventually, the utter refutation) of the model itself.

In this Section, I discuss the variety of approaches typically used to describe the generation and the maintainance of phenotypic heterogeneity in microbial populations. I will disregard the case where evolved regulatory units (such as operons and regulons) enable an almost immediate adaptation to a new environment [49], corresponding to *homogeneous* populations in fixed environmental conditions. Instead, my focus will be on populations with a standing phenotypic diversity, where cells cannot tune exactly their state to match the surrounding environment.

Concerning the mechanisms of switching underpinning sustained *heterogeneous* populations at fixed environmental conditions, different possible criteria of classification can be used. The most relevant for the aim of this work concerns the relationship between the intrinsic stochasticity of the system and the role of external factors. I start by discussing a first case where the switching behaviour has only stochastic causes, and the environment can have consequences on the differential survival probability of the alternative phenotypes (context-independent switch, Section 1.2.1). I then focus on a second class of models where changes in the environmental conditions affect both the expression of the alternative phenotypes and their survival (context-dependent phenotypic switch, Section 1.2.2). As more thoroughly examined in Chapter 3, the relevance of the classification of phenotypic switches according to the role of the environment resides in the difference in the resulting temporal dynamics of the phenotypic variability across the population (Fig. 1.1).

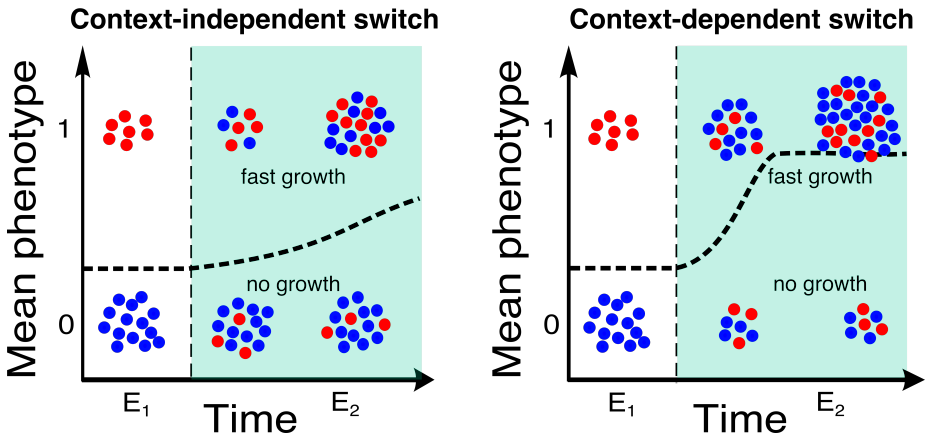

Figure 1.1: Environmental change can elicit different dynamics in heterogeneity depending on its role on the phenotypic switch mechanisms. Even when the switch is independent of the environment (left panel), the mean phenotype of the population (measured in terms of the frequency of one of the alternative phenotypes, dashed line) can still be altered by an environmental change (E1 to E2) if the new conditions favour one phenotype over the other one. In context-dependent switches (right panel) this effect can be magnified (reduced) if the probability of transition to the more adapted state increases (decreases) from the old to the new environment. Depending on the relationship between the time scales of the switch and of cell division, these two scenarios can as well give rise to different transient regime of the phenotypic dynamics.

1.2.1 Pure stochastic switchers

In models where all extrinsic sources of variability are neglected, the switching behaviour is characterized by constant rates of transition between phenotypic alternatives. Therefore, the typical way of modelling it is to consider the switch between the possible states as a Markovian process with fixed transition rates [12]. As all other Markovian processes, this does not display any kind of memory.

Dealing with pure stochastic switching does not mean that the environment has no effect whatsoever on the system: for example, the fitness of alternative phenotypes may be differentially affected by the state of the environment (usually summarized by one or few environmental proxies), in terms of rate of survival or division.

Models of pure stochastic switching behaviour typically aim at predicting the long-term growth rate and the evolution of the population under conditions of exponential growth, thus effectively neglecting transient periods and interactions between phenotypic state and demography [7]. The evolutionary benefit of an environment-independent stochastic switch strategy relies in differentiating (bet hedging), in environments where the conditions do not change too frequently [95].

Many are the examples of systems modelled as pure stochastic switchers in the recent literature. One notable example is provided by a particular instance of bacterial persisters, that is the *Escherichia coli* high persistence *hipQ* mutant, isolated in a screen for high persistence to norfloxacin treatment [100]. Balaban *et al.* showed that their phenotypic dynamics is well described by a model with constant switching

rates between the persistent and the normal cell state, and characterized by one order of magnitude of difference between the normal cell type's division rate and that of the persistent state. Such a difference was observed to occur before and after the antibiotic treatment, indifferently [8].

The relationship between the environmental fluctuations and the stochastic switch are also very important for the long-term fitness of the population: a seminal paper by Kussell & Leibler mathematically proved that the optimal strategy for a population of phenotypically switching microbes consists in tuning the inter-phenotype switching rates to the frequency of environmental change [54]. This was afterwards confirmed in an experimental study where fast- and slow-switching populations of *Saccharomyces cerevisiae* competed in both slowly and rapidly changing environments [1].

The feedback between the environment and the switching strategies makes a full circle when the environment is responsive to the state of the population, for example in the case of "catastrophic responsive environments" [96], analogous to some instances of host immune response [71]. A theoretical model by Allen and collaborators explored the scenario in which the individuals can switch between a fast-growing but susceptible state and a slow-growing non-susceptible one, and in which the environmental state flips and strongly reduces the fast-growing susceptible subpopulation with a probability depending on the difference between its relative size in the population and a given threshold. They found that, when the environment is responsive, two alternative strategies can be followed to maximize the population fitness: never switch to the non-susceptible state (and thus maximize growth), or switch at an optimal rate. The degree of the sharpness of the environmental response to the population state affects both the optimal switching rate and which of the two strategies is the most favourable [96].

1.2.2 Context-dependent switchers

With respect to mathematical models of pure stochastic switch, allowing the switch to be affected by the environmental context can lead to more complicated phenotypic dynamics, which can display dependence on the previous states explored by the system, and therefore bearing evolutionary consequences.

These models interpret the interaction between cells and environment as the result of the mediation of cell physiology, via metabolism, genetics, or a combination of the two. Measurable properties such as growth rate, rate of synthesis or degradation of proteins, and concepts such as density- or frequency-dependence, are then introduced to explain the behaviour of heterogeneous populations [55]. The level of "resolution" can scale up to describing how genes or gene networks influence the cell response to the environmental inputs [5, 53].

A quintessential case of environment-dependent switch was identified by Balaban *et al.* in *Escherichia coli hipA7* mutant [69]. The bimodal distribution of growth rates in the *hipA7* population, which can be appreciated also prior to the environmental trigger (in that case, antibiotic exposure), appears to be at the basis of the phenotypic variability: after the antibiotic ceases to be provided to the population, persister cells exit their state of arrested growth and can generate a newly sensitive population

[8]. Balaban *et al.* decided to model this system as a two-state chain where the two transition probabilities can each assume two fixed different values, depending on the presence or absence of the antibiotic. Moreover, the switch is unidirectional in the exponential regime of population growth, the transition rate to the persistent state being set to zero [8].

Other known examples of models of microbial responsive diversification through phenotypic switching can be found in the study of the operon *lac*, whose discovery by Jacob and Monod [49] set the bases for the extraordinary development of molecular and systems biology. Across the decades, the case study of *lac* operon in *Escherichia coli* inspired the development of mathematical models at the different levels of description, from population dynamics, to cellular metabolism and gene expression, as reviewed in [95]. In pivotal works on the *lac* operon switch, single-cell imaging allowed to unveil the distribution of the individual phenotypes across an isogenic population. Environmental conditions, in terms of extracellular concentrations of carbon sources, were shown to elicit a hysteretic response. A model by Ozbudak *et al.* provided a quantitative and predictive description of the intracellular state's dependence on lactose availability, in the form of a bistable dynamical system [73].

In biological systems of context-dependent switch, trans-generational "memory" of the individually-expressed phenotypic states can take the form of hysteresis due to the gene networks wiring conferring an intrinsic bistability to the system [73]. Again, the relation between the time scales of the switch and of the environmental variation can have implications on the evolutionary time scale: Lambert *et al.* showed that all possible combinations of the average duration and variability shape a phase diagram for memory optimization where evolutionary phase transitions between "constitutive", "memoryless" and "finite memory" responses can be defined [56].

To conclude, in this scenario phenotypic heterogeneity is an observable changing dynamically in time, which means that a complete characterization of the system requires the assessment of variability both across individuals and in time. Environmental change can be determined by the growth of the population itself, as actually happens to microbial populations in less artificial settings than those devised to study only the stochastic or the responsive component of a switch. In the next Section, I present *Pseudomonas fluorescens* as an appropriate model system for this study.

1.3 *Pseudomonas fluorescens* switchers: a model system for diversity

Pseudomonas fluorescens is a common plant-colonizing, aerobic bacterium [78], which has been widely used in evolutionary genetics because of its ability to rapidly generate a wide variety of mutants under novel environmental conditions [68]. Mutants strains are easily screened by examining the morphology of clonal colonies grown on agar plates. Wild-type strains indeed form smooth translucent colonies with a regular round shape. Mutants, on the other hand, typically display a variety of wrinkled, rugged colony shapes that are generated when cells secrete unsoluble compounds, such as colanic acid or cellulose. These compounds also elicit identification of mutants at the single-cell level.

Selection for survival in unstructured and structured environments showed that while the wild type morphology was maintained over evolutionary time in the the former case, spatial structure supported an extraordinary rapid diversification. Indeed, competition for limiting oxygen, consumed as the population grows to saturation, selects mutant genotypes that secrete polymers on the scale of a few days. These "Wrinkly Spreader" mutants are particularly efficient in building a biofilm to the air-water interface, thus creating a new niche from which wild-type cells are, temporarily at least, excluded. Biofilm formation, and the related wrinkly colony morphology, are achieved by the excretion of cellulose, that acts as a "glue" able to keep cellular mats together and prevents them to sink by sticking to the vessel's walls [80, 90].

Phenotipically heterogeneous isogenic strains have been subsequently evolved in two different set of experiments from the same wild type strain SBW25 in the lab of Paul Rainey. Of the two alternative phenotypes, one is always morphologically identical to the wild-type. However, the genetic underpinning and morphology of the alternative phenotypes depend on the features of the selection regime under which evolution took place.

Selection for phenotypic novelty at the moment of plating produced cells that were able to produce both smooth and wrinkled colony shapes, so that at every selection cycle a novel phenotype was produced even in genetically uniform populations [11]. Interestingly, this solution was found after a number of generations when novelty was brought in by genetic mutations analogous to those observed in the previously mentioned adaptive radiation experiment [80, 90]. However, once the potential of variation originated from knocking out unessential pathways was reduced, the best solution has been for cells to exploit stochastic variations of their phenotype.

Selection for survival in an experimentally imposed life-cycle, with alternating growth in structured and unstructured environments [45], gave rise to cells that alternated between a wild-type, smooth phenotype, and a WS-like phenotype, thus they were able to easily generate biofilms when the environmental context gave to such an arrangement a selective advantage.

Although the complete genetic and molecular characterization of the second type of switchers is underway, both in the case of the exclusion rule and in that of the life-cycle experiment, the phenotype alternative to the wild type had similar features, and produced opaque sectors in growing colonies. However, as far as the first experiment

is concerned, as I will discuss more in detail later, the polymer that was excreted was colanic acid and not cellulose, because the exclusion rule gives no advantage to stickiness per se. I will call these "capsulation" switchers, because the excreted polymer forms a thick capsule outside the cell wall.

In the rest of this Section, I will present the genetic and metabolic underpinning of the latter type of *Pseudomonas fluorescens* switchers, and provide more details on the experimental exploration of their phenotypic heterogeneity. After a brief description of the two phenotypes and a recall of the current knowledge about the mechanisms involved in the switch (Section 1.3.1), I detail the experimental evolution protocol giving rise to the *Pseudomonas fluorescens* capsulation switchers (Section 1.3.2). Then, I discuss the role of the genotype and of the environmental conditions on the switching behaviour (Section 1.3.3), and finally present the results of experimental observations which proved that phenotypic heterogeneity displayed by populations of switchers depends on the time of the observation and on the past history of the population (Section 1.3.4). These observations were instrumental for the development of a mathematical model aimed at describing the observed phenomenology and infer its implications, which will be the object of the next Chapters.

1.3.1 The alternative phenotypes of the capsulation switchers

The alternative phenotypes expressed by the *Pseudomonas fluorescens* "capuslation switchers" are called CAP- and CAP+. The CAP- phenotype corresponds to the wild type prevalent morphology, whereas the CAP+ phenotype is characterized by a massive capsule of excreted polymers that can be directly imaged by staining (Figure 1.2). Capsulated cells can be also identified by fluorescent microscopy, thanks to the transformation of the switching strain with a fluorescent marker, put under the promoter of the operon producing the polymer (see Chapter 2). The measure of this level of fluorescence allows to quantify the fraction of cells in the population that have switched on the polymer production, either by direct imaging of fluorescence under a microscope, or by automatic counting via FACS.

The capsulated phenotype CAP+ is expressed by around 1:10000 cells in wild type SBW25 populations, and its expression was found to be caused by the activation of an operon responsible for the production of colanic acid-like polymers [42]. More in detail, transposon mutagenesis demonstrated that the structural basis of the capsule is a polymer encoded by a specific locus (Pflu-3656-wzb). There exists a link with smooth (SM) / wrinkly spreaders (WS) colony morphology heterogeneity: the WS mats are mainly made of ACP (acetylated cellulosic polymer), coded by a 10-gene operon called *wss*. The CAP+ polymer consists of a mix of ACP and an acidic polymer encoded by *wzb*, and was found to belong to the 5th group, that of the M-antigens [80]. The biosynthesis of a variety of excreted polymers as a response, for instance, to stress is well-documented in other bacterial strains (e.g. *Vibrio parahaemolyticus* [33], *Vibrio cholerae* [101]).

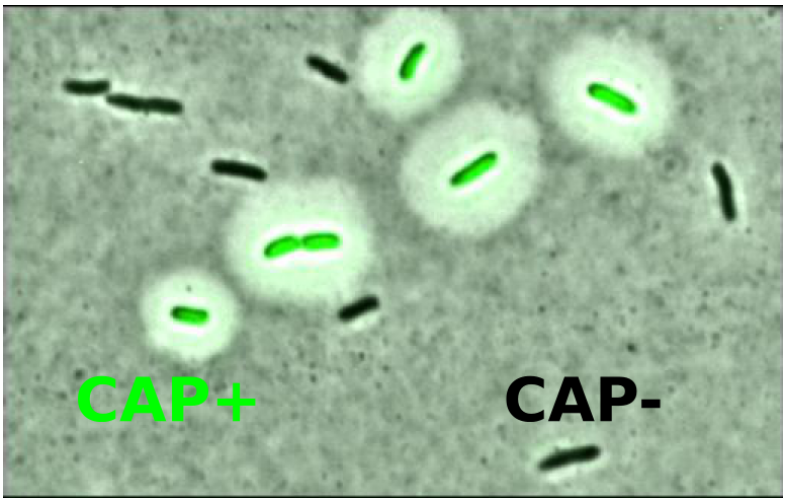

Figure 1.2: Microscopy image of *Pseudomonas fluorescens* "capuslation switchers". These isogenic populations express two alternative capsulation phenotypes: along with the normal cellular state CAP-, they can express an alternative phenotypic state called CAP+. CAP+ cells present a capsule around the cell surface (visible after staining with indian ink) and present green fluorescence due to the insertion of the *gfp* gene under the control of the same promoter of the operon responsable for the capsulation. The image was obtained through the superposition of bright-field and GFP fluorescent microscopy images (courtesy of Philippe Remigi).

1.3.2 The evolution of the capsulation switchers

Via a process of artificial selection, Rainey and collaborators evolved *Pseudomonas fluorescens* strains able to express the CAP+ phenotype at a much higher frequency with respect to the wild type ($\sim 10^{-1}$ vs $\sim 10^{-4}$) [11].

The evolution experiment consisted in subjecting 12 identical populations of *Pseudomonas fluorescens* SBW25 to successive rounds of alterned growth regimes and selection through single-colony bottleneck based on phenotypic novelty, that is by restarting a new culture in fresh medium from the colony whose morphology was the most different from the prevalent one (Fig. 1.3, top panel). After nine rounds, in two lines out of twelve a noticeable increase in the frequency of uncommon morphotypes was observed. This shift coincided with the appearance of a switching mutant, which managed to be largely overrepresented among cells that survived the exclusion rule, thus rapidly making up the totality of the population.

When let grow for longer times on agar plates, such high-frequency switching lines produced sectored colonies (Figure 1.3, mid panel). The colony morphology reflected two features of the cell-level phenotypic behaviour that I will more extensively treat in Chapter 3. First, individual cells are found in one of the two alternative phenotypic states (Fig. 1.3, bottom panel). Second, since the lineage descending from a newly switched cell creates a sector in the colony, the phenotypic state must persist for several generations, so that the whole descendence of a cell tends to express, at least over a sufficiently short time scale, the same phenotype.

One of the main insights that the exclusion rule of the evolution experiment pro-

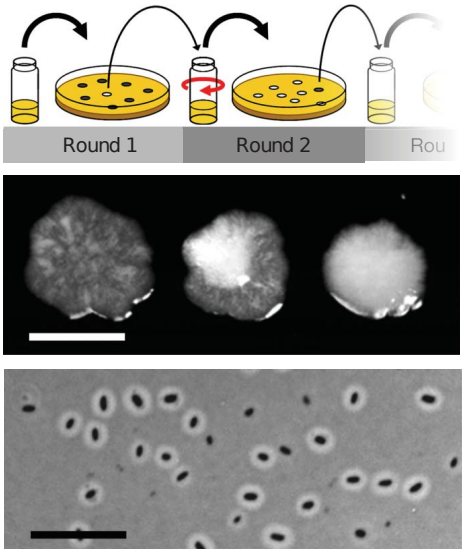

Figure 1.3: Scheme of the evolution experiment. Top panel: *Pseudomonas fluorescens* SBW25 populations were propagated in static or shaken (red arrow) microcosms, and small aliquots of them periodically plated to obtain novel colony types, before transfering one of them into the opposing environment ("exclusion rule"). Mid panel: colonies of 1w4, one of the evolved bet-hedging genotypes, display variably sectored colonies, suggesting that the phenotypic composition changes along with genetic background and context. Scale bar, approximately 2 mm. Bottom panel: 1w4 sectored colonies are composed of a mixture of CAP+ and CAP- cells (phase-contrast light microscopy with negative capsule staining). The proportions of CAP+ cells produced in the evolved switching strain 1w4 were three orders of magnitude higher than both the original ancestor SBW25 and the immediate ancestor of 1w4. Scale bar, approximately 10 µm. Figure from [11].

vided about *Pseudomonas fluorescens* CAP+/CAP- phenotypic switch was the role of contingency: each round of the evolution experiment led to the selection of a mutation giving rise to phenotypic novelty at the colony level, and each successive mutation participated in creating the genetic substrate for the last, decisive mutation to happen. Indeed, genetic studies provided the list of mutations needed to evolve the CAP+/CAP- phenotypic switch. The switching behaviour, however, could be directly obtained by artificially inducing the last mutation on the right locus of the wild type genome [42].

Re-evolved switchers

When dealing with microbes, it is possible to 'replay the tape of life' and explore the role of contingency in evolution [14]. In the case of the CAP switchers, after each round of selection a sample from the selected, morphologically novel colony was taken and frozen. Restarting the evolution experiment from the immediate precursor of 1w4 (one of the two switching lines obtained), six more switching strains were evolved.

Each of the independently re-evolved strains displayed a high degree of phenotypic variability [41]. The causal mutations all involved a couple of genes (*carB* and *pyrH*) along the pyrimidine pathway, although they affect different loci (Fig. 1.4).

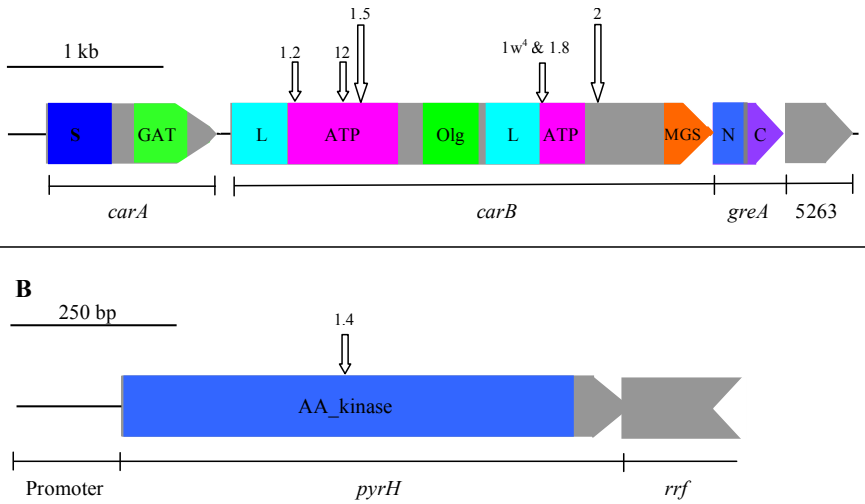

Figure 1.4: Genes involved in the final mutation endowing *Pseudomonas fluorescens* strains with the capacity of expressing the CAP+ phenotype at high frequency. Although the affected genes are always *carB* and *pyrH*, the loci where such final mutations take place can vary across 1w4 and the switchers re-evolved from its direct predecessor (white arrows). Figure from [42].

Such mutations seem to be responsible for a disequilibrium in the flux of UDP and UTP along the pyrimidine pathway, before a branching point where metabolites are partitioned between DNA/RNA production and colanic acid biosynthesis (Fig. 1.5). This checkpoint might be a safety measure to prevent cells from starting division without the minimum amount of resources to accomplish it [42], and is thus likely to be related to the response of bacterial cells to starvation. As I will discuss later, modifications of such response might involve an imbalance in a number of intracellular compounds, from precursors of biomolecules to ribosomes.

On the basis of these observations, a first interpretation of the origin of the switching behaviour was given in [42]: there may exist a threshold in the intracellular concentration of UTP, lower than the homeostatic value for the wild type cells, above which cells express the capsulated phenotype. For the mutant genotypes, for which such a homeostatic value might be lower, stochastic fluctuations are enough to cross the threshold and switching to the capsulated state. The presence of control mechanisms, elicited when the polymer production is exceedingly high, might allow cells to recover to the CAP- state. The exact nature of such control mechanisms remains, however, unclear.

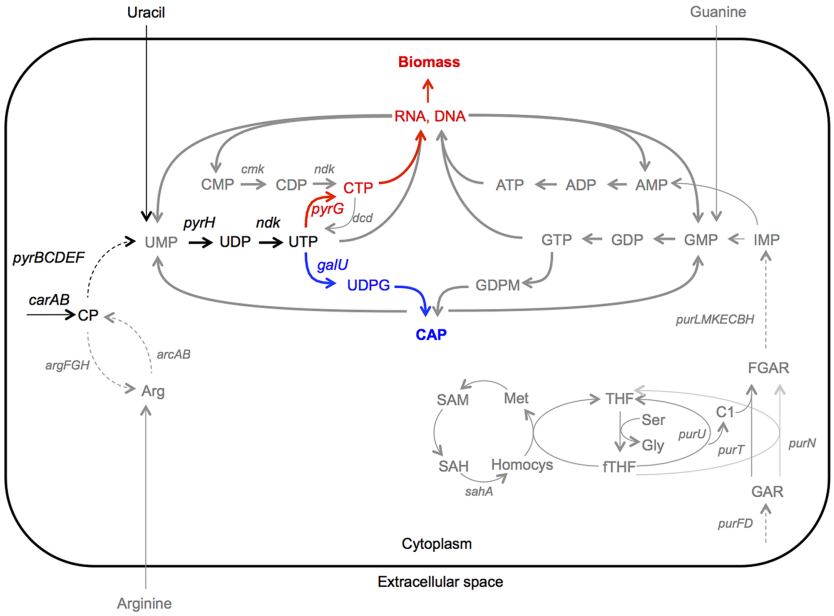

Figure 1.5: Intracellular metabolic pathways downstream of *carB* gene. The switch-eliciting *carB* mutation reduces concentrations of intermediates in the pyrimidine biosynthesis pathway (shown in black), exposing a decision point at which uridine triphosphate (UTP) is used either by *PyrG* for nucleotide biosynthesis (leading to the CAP- phenotype, components in red), or by GalU for polymer biosynthesis (generating CAP+ phenotype, components in blue). Figure from [42].

1.3.3 Genetic and environmental sources of heterogeneity

The availability of several strains achieving, through the same path, the same ability to switch between the capsulated and the uncapsulated phenotypes, allows to address the genetic and environmental bases of heterogeneity within bacterial populations.

Different "switchers" can be quantitatively compared in terms of the amount of capsulated cells they produce, of their average growth rate or demographic dynamics. As explained in more detail in Chapter 4, Section 4.1.2, the switching strain 1w4 and the 6 re-evolved strains differ in their demographic features and in the frequency at which the alternative phenotypes are expressed. This may indicate that the degree of sensitivity of the switch to random fluctuations varies depending on genetic background.

The conditions in which bacterial cultures are grown also affect both the average growth rate of the population and the proportion of capsulated cells. In isogenic populations of 1w4 grown in different environmental conditions, a higher proportion of capsulated cells was associated to lower temperatures, older cultures, and uracil enrichment in the medium (Jenna Gallie, Philippe Remigi and Paul Rainey, unpublished, and [41]). However, no systematic study has so far been conducted to quantify how the population composition scales with an externally controllable parameter. Therefore, a causal connection between the mechanisms underpinning the switch and the population-level outcome cannot be easily established.

Some qualitative expectations based on the mechanistic picture illustrated in Section 1.3.2 have been nonetheless verified. According to Jenna Gallie's model cited above, when the UTP/UDP balance is altered by addition of UDP to the extracellular medium, the probability that stochastic fluctuations bring the cell above the switching threshold is expected to increase. Accordingly, more capsulated cells are observed in UDP-enriched cultures. To what extent this is actually due an increased rate of transition to CAP+, rather than on a slowdown of the rate at which the CAP- phenotype is recovered, could not be assessed with this kind of measure.

Another expectation that has been only documented in a case of colony growth on agar, is that capsulated cells divide slower that non-capsulated ones. It is reasonable to assume that this holds true also in liquid medium, as the production of a bulky polysaccharide capsule should divert resources from growth, and thus entrain a cost. This individual cost should be measurable at the population level in terms of growth reduction, so that conditions giving rise to a higher number of CAP+ cells should be associated to a slower average growth rate, and may also reflect in a lower cell concentration at stationary phase. In Chapters 3 and 4, I will discuss our current understanding of the relation between growth rate and phenotypic state of the population, and how some of these intuitions might be misleading when comparing populations in different phases of their growth.

A particular instance of contextual dependence of the phenotypic composition of a *Pseudomonas fluorescens* switcher population is detailed in the following Section, and will constitute the benchmark for the theoretical work of Chapter 3 of this Thesis.

1.3.4 Time- and history- dependent phenotypic heterogeneity

Considering the dependence of the population phenotypic state on the environmental context, one can wonder to what extent a genotype defines the probability of finding cells in one of the two alternative phenotypes. In other words, whether it is possible to map the genotype not to one phenotype, but to a definite percentage of cells that are found in each of the phenotypic states. In this case, the phenotypic composition of the population could be considered, similarly to what happens in multicellular organisms with differentiated cells, as a manifestation of the underlying genotype. Understanding when and how the environment acts on the determination of the population composition is essential for the comprehension of the selective advantage of a switching genotype.

As seen in the previous Section, *Pseudomonas fluorescens* switching strains seem to respond to changes in the environment. In fact, for microbial populations grown in batch culture, the environmental state is determined not only by externally controlled parameters, but it is influenced by the population demography itself. The possibility that population growth affects phenotypic composition was explored by Dr. Philippe Remigi and Prof. Paul Rainey at NZIAS, Auckland, New Zealand, in an experiment that I recapitulate here, and that will be described in detail in Chapter 3, where I propose a model for describing the observations.

This experiment consisted in monitoring over several bacterial generations the total size and the proportion of capsulated cells in a population held in a closed reactor.

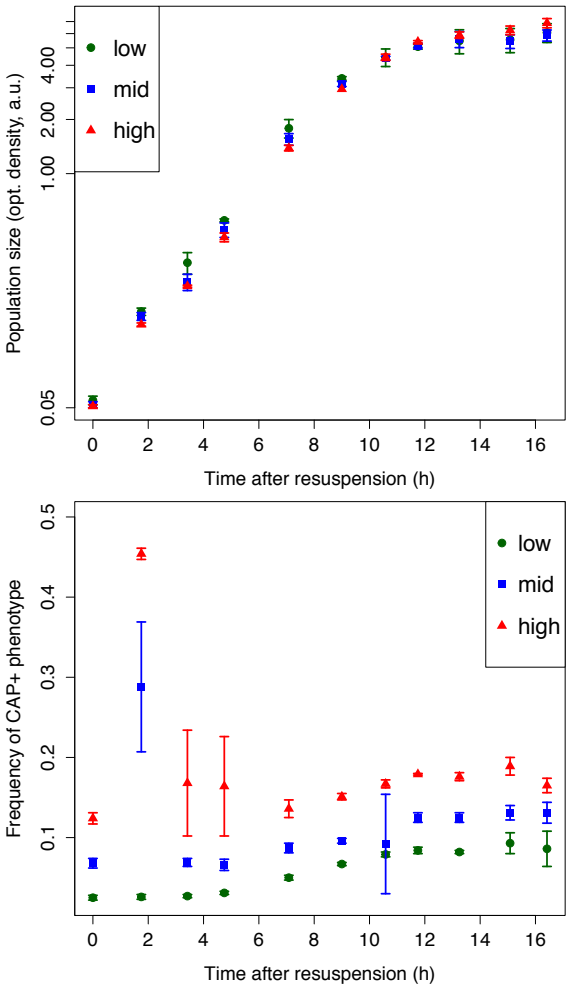

Figure 1.6: Demographic and phenotypic dynamics of a population of a *Pseudomonas fluorescens* "switcher" over several bacterial generations (lasting, in exponential phase, around 40 minutes). Population size is measured through optical density (top panel), and CAP+ frequency through flow cytometry (bottom panel). Three different treatments, corresponding to different final population densities of the precultures they were replicated from, are shown: "low" (preculture OD $\simeq 0.3$, green circles), "mid" (preculture OD $\simeq 1.0$, blue squares), "high" (preculture OD $\simeq 1.5$, red triangles). All treatments were diluted to the same population size at the beginning of the measurement phase (OD $= 0.05$). Each of the points corresponds to the mean value over three statistical replicas, and error bars indicate standard deviation.

While the population size followed a standard logistic growth, eventually attaining the stationary phase (Fig. 1.6, top panel), the proportion of CAP+ cells changed in time in ways that were not only qualitatively variable, but sometimes had dramatic non-monotonic variations (Fig. 1.6, bottom panel). Even more interestingly, treatments initiated with the same cell density, but derived from cultures at different stages of their growth (early, mid, or late exponential phase) presented quantitatively and qualitatively different behaviours in terms of the temporal variation of their phenotypic composition. Indeed, whereas the culture replicated from an early exponential phase preculture underwent a gradual and slow increase in the fraction of capsulated cells after resuspension in fresh medium, cultures replicated from precultures having reached later stages of growth expanded of several folds their fraction of CAP+ phenotype in just a few bacterial generations. Such fast augmentation then ended almost as abruptly as it originated, and at the onset of stationary phase the three cultures behaved alike, with the difference that cultures initiated from an "older" preculture still conserved their higher percentage at the end of the experiment.

To conclude, these results proved that a genotype does not univoquely determine the phenotypic composition of a population, but the whole phenotypes' frequency and population size dynamics are necessary to fully characterize a switching *Pseudomonas fluorescens* genotype. In Chapter 3, I will present a mathematical model that, integrating the information on the metabolic nature of the switch, can quantitatively describe the observed time- and history-dependence of the CAP+ frequency, and proposes a possible link between population growth and phenotypic composition.

1.4 Thesis outline

Materials and Methods (Chapter 2) In the next Chapter, I present a compendium of the materials and methods employed to investigate phenotypic heterogeneity in *Pseudomonas fluorescens* switching strains. The lists of the bacterial strains, plasmids, antibiotics, culture media and microscopy material used all along the experimental part of my work (Section 2.1) are followed by a review of the experimental techniques and protocols, with a particular focus on the genetic manipulations performed on the strains to mark the CAP+ phenotype with the green fluorescent protein (Section 2.2). Finally, I review the numerical methods used to simulate the mathematical model and analyze the results of the experimental assays (Section 2.3).

Theoretical Results (Chapter 3) In Chapter 3, I present and discuss the main theoretical results of my work. After the presentation of the general formalism used (Section 3.1), I prove that the coupling between population growth and phenotypic expression observed in the experiment of Section 1.3.4 cannot stem from a purely stochastic switch, even in the presence of a constant growth rate difference between the two alternative states (Section 3.2). I therefore propose a deterministic mathematical model suggesting one simple way to implement context-dependence in the switch that can reproduce the observed non-monotonous dynamics of the phenotypic composition of the population (Section 3.3). The results of the "overshoot" experiment are extensively discussed (Section 3.4) and quantitatively fitted by the mathematical model (Section 3.5). Finally, I present the predictions of the model on phenotypic variability across populations characterized by different average growth rates (Section 3.6) and discuss the main implication of the results (Section 3.7).

Experimental Results (Chapter 4) Chapter 4 deals with the experimental observations that provided the premises of my theoretical work, and with the results of the experimental assays aimed at testing its validity. First, I present the evidences I collected about the existence of a significant negative correlation between the average growth rate and the levels of expression of the CAP+ phenotype in exponential regime of growth (Section 4.1). Although the model of Chapter 3 predicts the negative sign of such correlation, I show that it cannot account for the most part of the observed variability in the CAP+ frequency, unless the ratio between the maximum switching rates depends on the growth rate in a nonlinear fashion (Section 4.2). Finally, I discuss a physiological interpretation of the mathematical model that might justify why such nonlinear scaling yields to an improved prediction of the degree of the variability in the expression of the CAP+ phenotype in exponentially growing populations of switchers (Section 4.3).

Discussion (Chapter 5) In the last Chapter I review the main results of this Thesis and discuss their implication on phenotypic heterogeneity in *Pseudomonas fluorescens*. In particular, I explore the combined role of genetic, environmental

and stochastic factors in the expression of the CAP+ phenotype and its variability. I end this work by putting into a general context the choice of modelling context-dependence through intracellular concentrations of proteins, as population growth alone can provide the sufficient information on the environment to yield transient variations in the phenotypic composition of the population.

CHAPTER 2

MATERIALS AND METHODS

After having contextualized the problem of phenotypic heterogeneity in microbial isogenic populations, the variety of mechanisms and that of the evolutionary consequences, in this Chapter I present the biological material used to perform the experimental part of my work, together with the genetic, microbiology and computational techniques acquired and employed to advance the project.

In Section 2.1 I inventory all the bacterial strains, plasmids, antibiotics, culture media and microscopy material I needed for the experimental side of this work. Section 2.2 is devoted to a review of the experimental techniques used and protocols followed, with a particular focus on the genetic manipulations performed on the switching strains to have the CAP+ phenotype marked with the green fluorescent protein. Finally, in Section 2.3 I present the basic ideas behind the development of the numerical methods needed to simulate the mathematical model and analyse the results of the experimental assays.

2.1 Materials

2.1.1 Bacterial strains

The study of microbial phenotypic heterogeneity was experimentally addressed by means of a series of experiments on *Pseudomonas fluorescens* strains characterized by a phenotypic switch related to the production of a capsule around the cellular wall [11]. Starting from the wild type SBW25, Rainey and collaborators evolved strains switching at high frequency via an experimental evolution protocol ("re-evolved switchers" see Chapter 1, Section 1.3.2 for details). Following the approach set by Jenna Gallie [41], I contributed to transform seven of the re-evolved switchers by marking the capsulated phenotype with the insertion of *gfp*. A couple of specific *Escherichia coli* strains (donor and helper) were needed to accomplish this task. All bacterial strains used are listed in Table 2.1 and were stored at -80° C in 45% glycerol saline solution.

Strain	Genotype and characteristics	Reference
Pseudomonas fluorescens		
SBW25	Wild type, isolated from beet leaves (Oxfordshire, 1989)	[78]
SBW25xGFP	Wild type constitutively expressing GFP	[41]
SBW25 1w4	9th strain of the REE, line 1 switcher	[11]
SBW25 6w4	9th strain of the REE, line 6 switcher	[11]
SBW25 Re1.2	Switcher re-evolved from 1s4, P144L mutation on *carB*	[11], [41]
SBW25 Re1.4	Switcher re-evolved from 1s4, R123C mutation on *pyrH*	[11], [41]
SBW25 Re1.5	Switcher re-evolved from 1s4, T279I mutation on *carB*	[11], [41]
SBW25 Re1.8	Switcher re-evolved from 1s4, R674C mutation on *carB*	[11], [41]
SBW25 Re2	Switcher re-evolved from 1s4, N826S mutation on *carB*	[11], [41]
SBW25 Re12	Switcher re-evolved from 1s4, C232Y mutation on *carB*	[11], [41]
SBW25 1w4xGFP	CAP-GFP expression SBW25 1w4 strain	[42]
SBW25 6w4xGFP	CAP-GFP expression SBW25 6w4 strain	This study
SBW25 Re1.2xGFP	CAP-GFP expression SBW25 Re1.2 strain	This study
SBW25 Re1.4xGFP	CAP-GFP expression SBW25 Re1.4 strain	This study
SBW25 Re1.5xGFP	CAP-GFP expression SBW25 Re1.5 strain	This study
SBW25 Re1.8xGFP	CAP-GFP expression SBW25 Re1.8 strain	This study
SBW25 Re2xGFP	CAP-GFP expression SBW25 Re2 strain	This study
SBW25 Re12xGFP	CAP-GFP expression SBW25 Re12 strain	This study
Escherichia coli		
DH5$\alpha - \lambda pir$	Donor strain carrying pUIC3 plasmid with mutated DNA	[41]
DH5α (pRK2013)	Helper strain carrying pRK2013 plasmid (tra+, Km^R)	[41]

Table 2.1: Designations and characteristics of bacterial strains used.

2.1.2 Plasmids and transposons

Two plasmids were needed to realize the aforementioned insertion of *gfp* into the genome of the re-evolved *Pseudomonas fluorescens* switching strains, called pRK2013 and pUX-BF13. The former is needed as a mobilization helper, so that the latter, the one inserting the *gfp* sequence thanks to the Tn7 transposon, could deliver the insert in the chromosome. The plasmids and the transposons used in this study are listed in Table 2.2.

Name	Characteristics	Reference
Plasmids		
pRK2013	Km^R, IncP4, *tra*, *mob*; mobilization helper for tri-parental mating	[35]
pUX-BF13	Mini-Tn7 delivery plasmid, providing the Tn7 transposase proteins	[9]
Transposons		
Tn7	High-frequency bacterial transposon	[22]

Table 2.2: Designations and characteristics of plasmids and transposons used.

2.1.3 Antibiotics

Three antibiotics were needed in different phases of the project. Tetracycline and Nitrofurantoin were used after the tri-parental mating process to select for the transformed bacteria (see later, Section 2.2.1). On the other hand, Gentamycin was added to all *Pseudomonas fluorescens* switchers cultures to prevent the invasion of cells having lost the *gfp* insert. The antibiotics used in this study are listed in Table 2.3.

Antibiotic	Purpose	Conditions of use
Tetracycline (Tc)	selection of *gfp*-transformed cells	10 µg ml^{-1} final (in 1:1 ethanol:water)
Nitrofurantoin (NF)	*E. coli* growth inhibition	100 µg ml^{-1} final (dissolved in DMSO)
Gentamicin (Gm)	counterselection of *gfp* cassette loss	10 µg ml^{-1} final (liquid culture media)

Table 2.3: Designations and characteristics of antibiotics used.

2.1.4 Media and culture conditions

Three main types of media were used in the series of experiments performed for this work (Tab. 2.4). Lysogeny broth (LB) was needed to grow *Escherichia coli* populations during the conjugation process, while King's Broth (KB) and King's Broth Switcher (KBS) were the preferred culture media to grow *Pseudomonas fluorescens*. The latter, in particular, was found to signficantly enhance the capacity of *Pseudomonas fluorescens* switchers to express the CAP+ phenotype because of a different uracil content (see Chapter 4 for further details and measurements).

Medium	Chemical composition (g/L)	Reference
Lysogeny Broth (LB)	10 NaCl, 10 tryptone, 5 yeast extract	[13]
King's Broth (KB)	10 glycerol, 20 Prot. Peptone No.3, 1.5 K2PO4, 1.5 MgSO4	[52]
King's B Switcher (KBS)	10 glycerol, 20 Prot. Tryptone, 1.5 K2PO4, 1.5 MgSO4	[42]

Table 2.4: Designations and composition of culture media used.

Pseudomonas fluorescens cultures were grown with shaking at 120 rpm at 28° C unless expressly mentioned. The culture microcosms consisted either of 250 ml glass microcosms containing 50 ml of culture medium or 50 ml Falcon plastic tubes containing 10 ml of culture medium. Overnight cultures were grown for 16 hours unless specified.

2.1.5 Microscopy materials

Cell-level microscopy was performed using a Zeiss Axio Observer inverted microscope. Samples were prepared on standard microscopy slides and mounted onto the high precision 130x100 Scanning Stage, surrounded by a heated chamber warmed at 28° C and at controlled air humidity. All images were collected through the Zeiss 60x oil immersion objective with 1.6x Optovar magnification changer and the Definite Focus.2 system for maintenance of focus over time. GFP proteins present in the

samples were excited with the 495 nm line from a 230 W X-cite 120LED lamp and collected with a dichroic mirror (Chroma #49002) and a 525/50 nm emission filter. Images were acquired with a Hamamatsu ORCA-Flash4.0 LT Digital CMOS camera. The *xyz* position of the stage, the objective, the choice of the excitation light channel (phase contrast or GFP), the exposition time, and the camera were all controlled with Micro-Manager Open Source Microscopy software.

2.2 Experimental methods

2.2.1 Bacterial conjugations

Bacterial conjugation is a mechanism of artificially induced horizonthal gene transfer (inter-strain exchange of genetic material) by direct cell-to-cell contact or via pili. Individual cells of the so-called *recipient* strain receive mobilizable genetic material from the cells of the *donor* strain. Under certain circumstances, the presence of a third strain (*helper*) is needed to facilitate the process by providing a conjugative plasmid coding for the genes required for conjugation and DNA transfer (*triparental mating*).

In this work, triparental mating was used to transform *Pseudomonas fluorescens* re-evolved switchers (Re1.2, Re1.4, Re1.5, Re1.8, Re2, Re12) with the insertion of a promoter-*gfp*-vector to mark capsule expression with GFP, as already accomplished on 1w4 by Prof. Rainey and Dr. Gallie [42].

Triparental mating

Pseudomonas fluorescens of various genotypes are crossed with a 1:1 mixture of DH5$\alpha-\lambda pir$ carrying pUIC3 containing mutated DNA and an *Escherichia coli* helper strain DH5α (pRK2013) (tra+, Km^R). 500 µl of *Pseudomonas fluorescens* cells in an Eppendorf tube are heat-shocked at 45° C for 20 minutes. 500 µl of *Escherichia coli* donor in LB and 500 µl of *Escherichia coli* helper in LB are mixed 1:1 and pelleted. Cells are washed once in 1 ml of LB broth and then resuspended in 1 ml LB broth. Following heat-shock, *Pseudomonas fluorescens* cells are pelleted and resuspended in the *Escherichia coli* mix. Cells are again pelleted, resuspended in 30 µl of LB broth, and the 30 µl droplet transfered to the surface of an LBA plate, pre-heated to 28° C. The spot was allowed to dry before being transferred to the 28° C growth room to incubate overnight. The next day, spots are harvested by scraping up cells with the edge of a sterile tip and resuspending in 1 ml LB in an Eppendorf tube. Bacterial suspensions were diluted to 10^{-1} in 1 ml LB, and 25, 50, and 100 µl aliquots (respectively) of each dilution (10^0 and 10^{-1}) are spread onto LBA plates containing 10 µg/ml tetracycline, and 0.1 mg/ml nitrofurantoin (NF). NF is prepared fresh when the plates are poured by dissolving 0.08 g of NF in 2 ml of DMSO and adding this to 800 ml of LB agar. Tetracycline selects for the pUIC3 vector in *Pseudomonas fluorescens*, while nitrofurantoin selects against *Escherichia coli*. pUIC3 cannot replicate in *Pseudomonas fluorescens* so all recombinants should have plasmid insertions in the cloned region of interest carried on pUIC3 (Fig. 2.1).

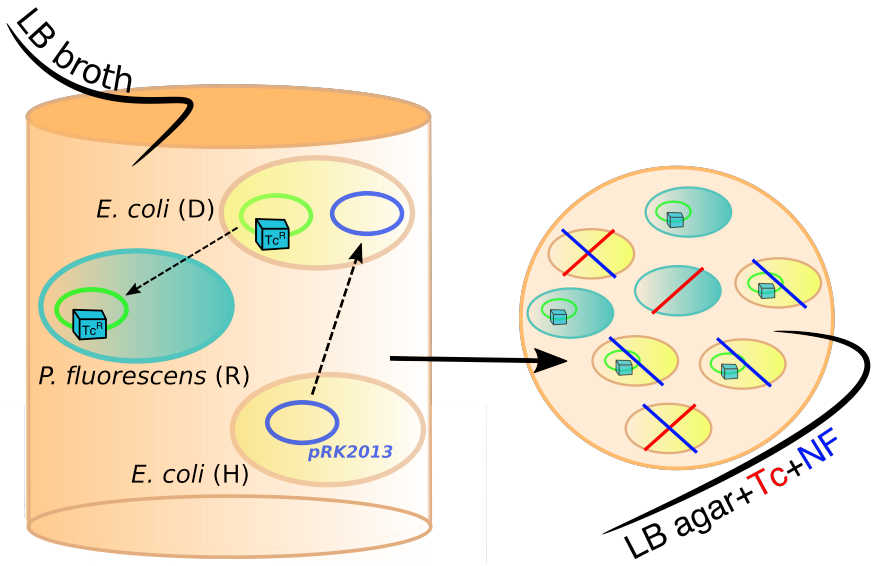

Figure 2.1: Scheme of the procedure followed to insert the *gfp* gene in the *Pseudomonas fluorescens* switching strains. The previously amplified promoter of CAP biosynthetic locus gene pflu3655 and the gfp-expressing gfpmut3 gene were ligated, and the vector+insert introduced into the re-evolved switchers by conjugation (with helper plasmids pRK2013), downstream of the glmS stop codon. Two *Escherichia coli* strains were used as donor (D) and helper (H): the donor strain provided the *gfp* insert (integrated on a plasmid along with the Tetracycline resistance cassette), while the helper was needed to pass the pRK2013 plasmid to the donor, to let it produce pili. After having been mixed together in LB broth (left panel), the cells were exposed to selective medium (LB agar + Tetracycline + Nitrofurantoin): Tetracycline selected for bacteria with the Tc^R (Tetracycline resistance) cassette, and Nitrofurantoin selected against *Escherichia coli* (right panel).

2.2.2 Biological assays

Optical density curves in bulk through spectrometry

Three statistical replicates from each of the three biological replicates per strain per time point are prepared by extracting an aliquot of $\sim$ 1 µl of the the correspondent culture and diluted in fresh KB or KBS medium depending on the experiment. Optical density of each of the statistical replicates was then measured through a portable WPA Biowave spectrometer. The exact quantities of cellular culture and fresh medium were chosen as to obtain a dilution allowing to measure OD in the optimal range for the instrument (OD < 1).

Optical density curves in TiCan 96-wells plates

Three statistical replicates for each of the three biological replicates of the eight strains were inoculated into 81 of the 96 wells of the plates at our disposal. The TiCan reader ran over 42 hours, getting optical density data every 10 minutes. Resulting growth profiles were analyzed with simple routines written in the R programming language

and devoted to perform linear fit of the logarithm of the measured OD in a chosen time window (to select time points corresponding to exponential phase).

Flow cytometry

Flow cytometry allows a higher throughput in counting assays with the possibility, among the many options, to distinguish between cells expressing or not a fluorescent protein. Here I present the protocol designed by Dr. Philippe Remigi to assess the frequency of CAP+ cells in any sample of a growing population of *Pseudomonas fluorescens*. For each of the eight analysed strains, three independent overnight cultures were prepared by inoculating KBS microcosms directly with glycerol stock, except for the only replica for the control strain 1w4 (without the GFP marker). After 24 hours one tube per strain was prepared: between 5 and 10 µL of the night culture, previously washed and diluted in PBS, was vortexed and then added to 1 mL of PBS, adjusting the quantity according to the flow rate the fluocytometer revealed during each pre-measurement (which had to be around 1000 and 4000 particles per second). A blank sample (2 mL of PBS) was analyzed to get information about the intrinsic noise of the measurements. The machine was calibrated with the use of 350 µL of CST, that is a solution of fluorescent beads, whose intensity spectrum is well-known, in PBS. Each tube was then passed to the flow cytometer until 50000 events (particles) had been revealed and measured, where cells were counted and sorted for the characteristics of their fluorescent spectrum. The auto-fluorescence of CAP- individuals and the GFP signal coming from CAP+ cells appeared on the screen as partially superposing gaussian profiles.

Counting assays

The counting technique developed by Dr. Jenna Gallie in her Ph.D. thesis to assess the frequency of capsulated cells in the population revealed to be extremely useful for the scope of this work, too. At the time point during exponential phase at which the measurement of the frequency of the CAP+ phenotype in the population is performed, ~ 2 µl of the bacterial culture are put onto a microscope slide and covered with a plastic coverslip after one minute (to let the sample dry a little and force cells to adhere to the microscope slide). The so-prepared sample is brought under the Zeiss microscope, where phase contrast and GFP pictures were taken under the 60x objective endowed with a 1.6x Optovar magnification changer. Around 20-30 photos were collected for each biological replicate, for each genotype or temperature, so to reach a minimum statistics of bacteria per replicate (then estimated in around 500-1000 cells). The total number of cells, along with that of CAP+/GFP+ cells, was then established by automatic procedures through embedded ImageJ routines (segmentation and counting).

Time-lapse microscopy

Through time-lapse microscopy it is possible to track the growth of a microcolony of bacterial cells growing on agar pads and the phenotype expressed by the individual cells, over a long time span and in an automatic fashion. In this work, technical issues prevented me from efficiently using time-lapse movies to assess the expression of the

alternative phenotype. Nevertheless, time-lapse microscopy allowed me to test some hypotheses of the mathematical model about the role of the phenotype in the determination of the cellular division rate. Overnight cultures of the strains were started from -80° C, around 18 hours before the start of the acquisition of the first images. The microscope slide had been carefully cleaned and then prepared by the application of an adhesive strip onto it, resulting in a well. Then, $\sim$ 350 µL of 1.5% agarose KBS gel was poured into the well and immediately leveled by the superposition of another microscopy slide. Once the gel had cooled down and solidified, the upper slide was removed and the blue adhesive strip opened and cut to form a channel through which air could flow to let obligate aerobic *P. fluorescens* bacteria live. Finally, $\sim$ 1.5 µL of a 10^{-3} dilution in KBS of the original night culture is added to both sides of the channel and, once dried out, covered with a thin microscopy slide which had to firmly adhere to the adhesive strip. The system is then ready to be observed at the Olympus microscope, where around 10 bacterial microcolonies (founded by a single cell) were photographed every 20 minutes for a total time of more than 6 hours. Growth of the microcolonies were assessed via the segmentation of the successive pictures with the ImageJ software. The areas of the microcolonies, much simpler than the tracking of several divisions, was measured for every time point. As for the ImageJ algorithm, here are the steps followed to segment the files sorted out by the microscope software:

- split gfp and phase contrast channels (an example of phase contrast image is presented in Fig. 2.2, top-left panel);
- Image $\rightarrow$ Adjust $\rightarrow$ Brightness/contrast;
- save images as 8bit;
- Process $\rightarrow$ Substract background (30 pixel radius): images must be very clean, requiring to perform a series of this step when necessary;
- Image $\rightarrow$ Adjust $\rightarrow$ Brightness/contrast (Fig. 2.2, top-right panel);
- Image $\rightarrow$ Adjust $\rightarrow$ Threshold: adjust the threshold to try to get as much surface as possible (keeping white background and black colonies, Fig. 2.2, bottom-left panel);
- Process $\rightarrow$ Binary $\rightarrow$ Fill gaps (Fig. 2.2, bottom-right panel);
- Analyze $\rightarrow$ Measure particules (size: $0.01 - \infty$).

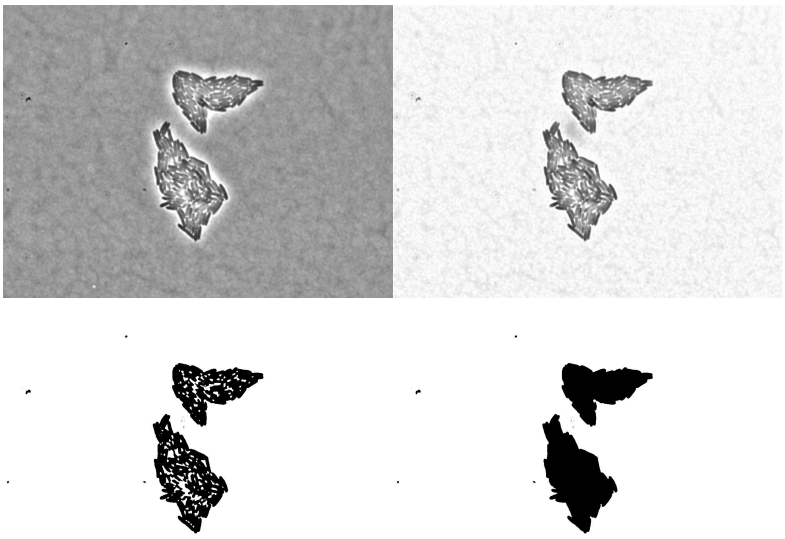

Figure 2.2: Image analysis of time-lapse pictures with ImageJ in four phases. The contrast of the original picture (top left) is enhanced with the specific built-in command (top right). Then, an appropriate threshold allows to individuate the area of the two microcolonies (bottom left). Finally, the gaps of the so-created binary mask are filled in via another built-in function (bottom right). The last image is then ready to be analyzed through the "Measure particles" command.

2.3 Numerical methods

2.3.1 Simulation of the dynamical system

The dynamical systems defined by the mathematical models of Chapter 3, developed to describe the transient phenotypic dynamics were simulated via *ad hoc* Python routines written by the Author. The first part of such routines consisted of the declaration and the initialization of the main parameters and variables defining the model. Modular definitions of the functions followed (e.g. setting the functional form of the switching rates). Code modularity allowed to make the routines easily adaptable to different variations of the model. The system of ordinary differential equations was integrated with the *odeint* routine present in the ScyPy Python scientific package. The plot of any output of the Python routines were produced through specific Python modules embedded in the main code. All Python routines were run through the Enthought Canopy 1.4.1 (Academic License version) graphical user interface.

2.3.2 Fit of the overshoot experiment

To evaluate the goodness of the mathematical models elaborated to describe and interpret the results of the overshoot experiment, I wrote specific Python routines comparing the experimental data with the theoretical predictions. After selecting those regions of the parameter space considered of particular interest given the biological

assumptions of the models, an alternating direct search followed: successive combinations of the free parameters were simulated and the output (the temporal dynamics of the three variables (N, f, c)) evaluated in terms of the deviation from the measurements of the dynamics of the population size N and of the CAP+ frequency f. The combination of the parameters that best fitted the experimental data was found by extracting, from the log file collecting the results, the one scoring the minimum χ^2, through simple AWK scripts.

2.3.3 Analysis of the results of the biological assays

The whole statistical analysis of the data obtained from the biological assays and experimental tests of the model was performed through R routines written by the Author and run through the Enthought Canopy 1.4.1 (Academic License version) graphical user interface. The operated statistics mainly consisted in bivariate analysis (linear or exponential fit, linear correlation analysis). All graphs of experimental data and tests were produced with R unless specified.

CHAPTER 3

MODELLING NONLINEAR GROWTH-AND-SWITCH DYNAMICS

BJECT OF THIS CHAPTER is the study of *Pseudomonas fluorescens* "switchers" (Chapter 1, Section 1.3) as a particular instance of context-dependent phenotypic switch. After having introduced the *Pseudomonas fluorescens* "switchers" evolved by experimental evolution [11] as a convenient biological model system for the study of phenotypic heterogeneity (Chapter 1), I present here a general modelling framework to tackle the problem of how phenotypic heterogeneity varies in time in a growing population of switching units. Once introduced the general problematic and the mathematical tools, I carry out the comparison between the two classes of models discussed in Chapter 1, Section 1.2 in terms of their predictive power of the phenomenology presented in Section 1.3.4, that is between mathematical models of context-independent and context-dependent phenotypic switch.

The questions addressed in this Chapter are the following:

- Given the experimental observations on the temporal variation of phenotypic composition of growing populations of switchers, can their phenotypic heterogeneity be interpreted in terms of a context-independent stochastic switch?
- If not, which are the essential features that simple models of context-dependent phenotypic switching need in order to reproduce the experimental observations, in terms of the dynamics of the phenotypic composition of the population?
- What would a context-dependent switch mediated by internal concentrations imply on the variation of phenotypic expression across different genotypes characterized by different growth rates?

After having presented the general formalism in Section 3.1, in Section 3.2 I mathematically prove that the observed coupling between population growth and phenotypic expression cannot be the result of a pure stochastic switch, even in the presence

of a constant growth rate difference between the two alternative states. In Section 3.3 I propose a deterministic mathematical model corresponding to one simple way to implement context-dependence in such systems. By linking the phenotypic dynamics with demography through internal concentrations of proteins, the observed non-monotonous dynamics of the frequency of the two alternative phenotypes can be reproduced. The results of the "overshoot" experiment, whose salient features were reviewed in Chapter 1, Section 1.3.4, are extensively discussed in Section 3.4, and the mathematical model's quantitative fit of such results are the subject of Section 3.5. Finally, in Section 3.6 I discuss the prediction, provided by the model, of the existence of a negative correlation between the growth rate and the expression level of the CAP+ phenotype in exponential phase, which will be experimentally tested in Chapter 4.

3.1 Representations and formalism

In this Section, I discuss which of the measurable quantities (observables) of the biological system are needed in a model describing a growing population of switching units (Section 3.1.1), introduce a general notation allowing a straightforward comparison between the classes of mathematical models discussed in the following (Section 3.1.2), and finally recall the experimental terminology that is used in this Chapter (Section 3.1.3).

3.1.1 From observables to variables and parameters

The first phase in the elaboration of any mathematical model describing a natural phenomenon is the assessment of which measurable characteristics of the system, or *observables*, to take into account and how to partition those between *variables* (usually those assuming different numerical values during the observations) and *parameters* (intrinsic constants or accurately controllable properties of the system whose variation can qualitatively change the behaviour of the system).

In a study on phenotypic heterogeneity in growing populations of switching units, the observables related to the *demographic* state of the population (e.g. population size, the population growth rate) can be distinguished from those characterizing the *phenotypic* state of the population (e.g. the frequency of one phenotype, the time scale associated to the switch).

3.1.2 General modelling framework

In this work the analytical methods chosen for a quantitative description of growing populations of switching units belong to dynamical systems theory. In particular I make use of ordinary differential equations, the most natural choice when dealing with the variation of continuous quantities in time.

Although at a first thought the most straightforward way to model demography and the phenotypic state of the population is to track the time variation in the *number* of cells expressing the alternative states, in this work I make use of the alternative,

equivalent description where the state of the system is written in terms of the *total number* of cells and of the *frequencies* of the alternative phenotypes.

The passage between the two formalisms can be easily demonstrated. Let N_+ and N_- be the total number of CAP+ and CAP- cells, respectively, $R_+(t)$ and $R_-(t)$ the time-dependent maximal growth rates associated with the two phenotypes, and $S_+(t)$ and $S_-(t)$ the (in general time-dependent) switching terms. The dynamics of the system in terms of *numbers* of CAP+ and CAP- is given by:

$$\dot{N}_+ = D(N_+ + N_-)\left[R_+(t)N_+ + S_+(t)N_- - S_-(t)N_+\right] \tag{3.1}$$

$$\dot{N}_- = D(N_+ + N_-)\left[R_-(t)N_- - S_+(t)N_- + S_-(t)N_+\right] \tag{3.2}$$

where the change in the number of CAP+ (CAP-) cells is either due to growth or to a change in phenotype of CAP- (CAP+) cells. A density-dependent factor, called $D(N) \in [0, 1]$, is assumed to be equal in both growth and switching terms and thus factored out. This corresponds to the assumption that switching can only occur as long as cells can divide, and slows down as stationary phase is approached, as one would expect for any metabolically related cell process.

By rewriting the system in terms of the *total number of cells* $N = N_+ + N_-$ and of the *fraction* of CAP+ cells $f = \frac{N_+}{N}$, the dynamical system defined by Eqs. 3.1 and 3.2 gives:

$$\dot{N} = \dot{N}_+ + \dot{N}_- \tag{3.3}$$

$$\dot{f} = \frac{\dot{N}_+ N - N_+ \dot{N}}{N^2} \tag{3.4}$$

which yields

$$\dot{N} = \left[R_-(t) + \left(R_+(t) - R_-(t)\right) f\right] D(N)N \tag{3.5}$$

$$\dot{f} = D(N)\left[\left(R_+(t) - R_-(t)\right) f(1-f) + S_+(t)(1-f) - S_-(t)f\right] \tag{3.6}$$

or, by defining the difference in growth rate $\Delta R(t) = R_+(t) - R_-(t)$,

$$\dot{N} = \left[R_-(t) + \Delta R(t) f\right] D(N)N \tag{3.7}$$

$$\dot{f} = D(N)\left[\Delta R(t) f(1-f) + S_+(t)(1-f) - S_-(t)f\right]. \tag{3.8}$$

The total number of cells N thus follows a density-dependent growth of speed $R_-(t)D(N)N$, corrected by a time-dependent term if the two phenotypes have different growth rates. The frequency of the CAP+ phenotype changes due to both population growth and phenotypic switch. However, when the two phenotypes are identical with respect to growth, this dependence reduces to a density-dependent modulation of the switching rates.

3.1.3 Experiment-related terms

The terminology related to the experimental evidences presented in Chapter 1, Section 1.3.4 is here recalled, given its relevance in the construction of the mathematical models.

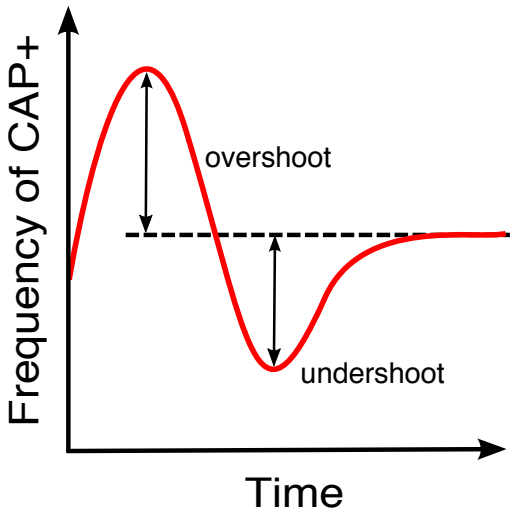

Figure 3.1: Overshoot and undershoot in the phenotypic dynamics. Non-monotonic variations of the frequencies of the alternative phenotypes can be observed in populations of *Pseudomonas fluorescens* "switchers". In this work, the term "overshoot" designates the transitory values assumed by one frequency exceeding its final value. After the overshoot, the transitory values of the frequency below its final value are indicated with the term "undershoot".

The "overshoot" experiment consisted of two successive *rounds* of growth, called 0 and 1. *Round 0* corresponded to a preculture stage, during which identical populations of switchers were grown until they reached different population densities. Bottlenecking these populations and diluting them to the same population density provided different inocula for the subsequent measurement stage (*round 1*). Measures of cell density (through optical density) and of population composition (through fluocytometry) started after these inocula were resuspended into fresh medium.

Three different treatments were realized, that differed only in the time of sampling in round 0, therefore in the age of the culture and its optical density. The names "low", "mid" and "high" will in the following designate experiments started on round 1 with inocula from early, mid, and late exponential phase of growth in round 0. Set aside this difference in the history of the culture, all treatments undergo the same protocol. Culture in round 1 are started by dilution to the same initial cell density, which is sufficiently low for populations to recover exponential growth for several hours, before entering the stationary phase about 10 hours after dilution. The mean population growth rate in exponential phase is indicated by ρ. During the first hours of exponential growth, an *overshoot* in the fraction of CAP+ cells was observed for the "mid" and "high" treatments. This term indicates a transient non-monotonic increase in the frequency, as illustrated in Fig. 3.1. When, after the overshoot, the frequency of capsulated cells (CAP+) decreases below the level that it would assume at the end of the experiment, the term *undershoot* is used.

In the following Section, I will assess to which extent such experimental observations can be explained by simple models of stochastic switching, where the temporal variation of the switching rate is limited to a density-dependence common to the two phenotypes.

3.2 Models for context-independent switching

In this Section, three mathematical models of pure stochastic switching are presented (Fig. 3.2) and shown to fail to describe the basic features of the experiment. Indications about the missing characteristics needed to model the phenotypic dynamics of a growing populations of switchers will be drawn.

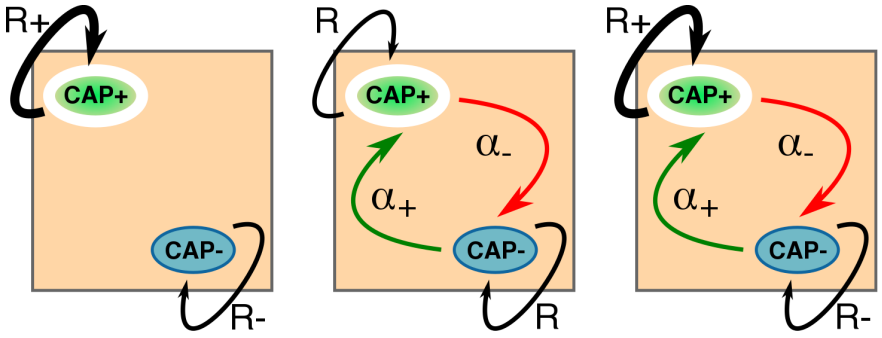

Figure 3.2: Scheme of three instances of simple mathematical models of context-indepedent switch. From left to right: "differential growth", "pure switch", and a mixed model with constant switching rates and a difference in growth rate between CAP+ and CAP-.

3.2.1 Growth rate difference, no switch ("differential growth")

Looking for the most parsimonious set of hypotheses to explain the experimental observations presented in Chapter 1, Section 1.3.4, the simplest option consists in considering fixed growth rate differences between phenotypes, and that – in the short-term at least – there is no switch in the cellular phenotype (Fig. 3.3). The rapid initial increase in CAP+ cells may thus result from a combination of a higher initial proportion of capsulated cells in the "mid" and "high" treatments, and a faster growth of the CAP+ phenotype. The frequency dynamics of capsulated cells would be driven in this case by the differential demography of the two subpopulations.

If switching between phenotypic states is not allowed ($S_+(N,f) = S_-(N,f) = 0$), then the equations ruling the dynamical system become:

$$\dot{N}_+ = R_+(t)D(N_+ + N_-)N_+ \tag{3.9}$$
$$\dot{N}_- = R_-(t)D(N_+ + N_-)N_-. \tag{3.10}$$

In terms of the total number of cells and of the fraction of CAP+ cells, I obtain:

$$\dot{N} = \left[R_-(t) + \Delta R(t) f\right] D(N) N \tag{3.11}$$
$$\dot{f} = D(N)\Delta R(t) f(1-f). \tag{3.12}$$

The expression for the temporal variation of the frequency of the CAP+ phenotype (Eq. 3.12) is slaved to demography through the density-dependence term $D(N)$, which is always positive. Such factor acts as a time scale modulation of the dynamics of frequencies, but it neither changes its equilibria, nor alters the sign of the variation of f, as it would be necessary to have an overshoot.

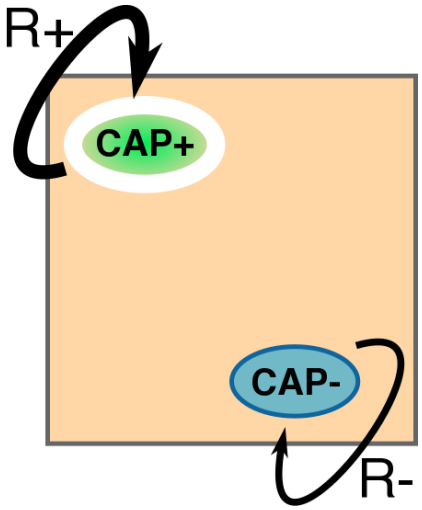

Figure 3.3: First null model: in the "differential growth" model no switch between the two states is allowed and the subpopulations expressing the alternative phenotypes differ only in terms of the growth rate. Both mathematical and biological considerations exclude that this model could account for the observed phenotypic dynamics.

The qualitative dynamics of the system is thus determined by the dependence of the frequency variation on the frequency itself. As no 1-D dynamical system can display a dynamics like the one experimentally observed, the equilibria being always attained monotonously, this model cannot explain the overshoot/undershoot dynamics. I can nevertheless discuss which stead-state is predicted by this model, and establish if such a model could be appropriate for describing the first couple of hours of the experiment, when the population grows exponentially and the fraction of capsulated cells dramatically explodes.

Phenotypic equilibria in exponential phase

In early exponential phase, when $D(N) \simeq 1$, Eqs. 3.12 and 3.11 become:

$$\dot{N} = [R_-(t) + \Delta R(t) f]\, N \tag{3.13}$$

$$\dot{f} = \Delta R(t) f (1 - f). \tag{3.14}$$

In early exponential phase the growth rates of the CAP+ and CAP- phenotypes are constant and equal to their maximum values r_+ and r_-, respectively. By letting ρ be the average growth rate $\rho = r_+ f + r_-(1 - f)$ and dr the (constant) difference in growth rate between CAP+ and CAP- $dr = r_+ - r_-$, it follows:

$$\dot{N} = \rho N \tag{3.15}$$

$$\dot{f} = dr f (1 - f). \tag{3.16}$$

The exponential phase phenotypic equilibria (setting $\dot{f} = 0$ in Eq. 3.16) correspond to the fixation of either phenotype: $f^* = 0$ or $f^* = 1$. These phenotypic equilibria do not depend on the absolute growth rates, but only on their difference: the fastest-growing phenotype gets fixed in the population, again in contradiction with the experimental findings.

Quantitative comparison with observations

Though failing to describe the whole temporal course of the experiment, one could still think that growth rates differences are still the factor most likely to account for the observed initial increase of CAP+ frequency f. For this reason, I made a quantitative comparison with the initial data of the overshoot experiment to estimate what should be the growth rate difference dr compatible with the increase in frequency between the initial value and the first measure.

By solving Eq. 3.16, one obtains:

$$f(t_1) = f_{R0}e^{(r_+ - \rho)t_1}, \tag{3.17}$$

where ρ corresponds to the average growth rate $\rho = r_+ f_{R0} + r_-(1 - f_{R0})$, r_+ to that of CAP+ cells, t_1 the first time point of round 1 and f_{R0} and $f(t_1)$ the frequency of CAP+ measured at resuspension and at t_1, respectively. Solving for r_+ yields:

$$r_+ = \rho + \frac{ln(f(t_1)/f_{R0}}{t_1} \tag{3.18}$$

and conversely for CAP- cells (whose frequency is given by $1 - f(t)$):

$$r_- = \rho + \frac{ln((1 - f(t_1))/(1 - f_{R0}))}{t_1}. \tag{3.19}$$

The results of this analysis, obtained by informing Eqs. 3.18 and 3.19 with the measured values ρ, f_{R0}, $f(t1)$, are summarized in Table 3.1: in the "mid" and "high" treatments the CAP+ cells should divide around 4 and 7 times faster than the CAP-, respectively.

Preculture	f_{R0}	$f(t_1)$	$r_+(h^{-1})$	$r_-(h^{-1})$
low	0.025	0.026	0.472	0.449
mid	0.068	0.288	1.275	0.296
high	0.124	0.454	1.192	0.180

Table 3.1: Growth rates of CAP+ and CAP- cells estimated from the data under the hypothesis that their growth rates are constant and their average growth rate does not change at the beginning of round 1.

Although not impossible, this scenario is highly unlikely, since it would lead to a very marked difference in the growth curves between treatments, whose effects are not evident in the growth curve (see Section 3.4 for the experimental growth curves and Section 3.3.4 for a more detailed analysis). Furthermore, such a hypothetical high difference in growth rate between the two phenotypes was never observed during microscopic observations realized over a big spectrum of experimental conditions. Finally, one would expect that the growth rate difference between phenotypes should be treatment-invariant.

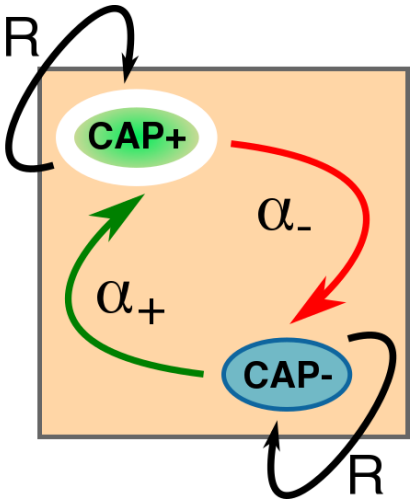

Figure 3.4: Second null model: the basic way to interpret a biological system expressing two phenotypes and able to switch back and forth is a Markov chain. This is a stochastic system where the individuals can switch between the two states at any time with a non-zero (constant) probability, regardless of the previous states assumed (no memory). A constant term R, the same for both phenotypes, guarantees population growth without affecting the phenotypic composition.

3.2.2 Constant switching rates, same growth rate ("pure switch")

In the absence of growth rate differences, the frequencies of the alternative phenotypes in the population may change if cells are allowed to change their phenotypic state via a switching mechanism. A classic way of representing a phenotypic switch consists then in assigning fixed transition probabilities between the phenotypic states [54].

Transition probabilities per unit of time (from now on, "switching rates") are in this case held constant, and independent of the time elapsed from the previous transition, the time of last cellular division or of the previous states' time series. The switch can therefore be modelled as a Markov process [44], defined by the switching rates to the CAP+ and the CAP- states (called α_+ and α_-, respectively). The growth rates of the CAP+ and of the CAP- subpopulations are moreover assumed to be equal and constant (Fig. 3.4).

Hence, setting $R_+(t) = R_-(t) = R(t)$ (or, equivalently $\Delta R(t) = 0$) and $S_-(t) = \alpha_-$ and $S_+(t) = \alpha_+$, Eqs. 3.1 and 3.2 for the numbers of CAP+ and CAP- cells become,

$$\dot{N}_+ = D(N_+ + N_-)\,[R(t)N_+ + \alpha_+ N_- - \alpha_- N_+] \tag{3.20}$$

$$\dot{N}_- = D(N_+ + N_-)\,[R(t)N_- - \alpha_+ N_- + \alpha_- N_+]\,. \tag{3.21}$$

In terms of the total population size $N = N_+ + N_-$ and of the frequency of CAP+ cells $f = N_+/N$, this dynamical system can be written as:

$$\dot{N} = R(t)D(N)N \tag{3.22}$$

$$\dot{f} = D(N)\,[\alpha_+(1-f) - \alpha_- f]\,. \tag{3.23}$$

The dynamics of the phenotypic composition of the population described by Equation 3.23 is again essentially determined by a 1-D system. Indeed, the positive factor $D(N)$ sets the time scale at which the equilibria are attained, and cannot cause a change in the sign of the frequency variation. As already discussed for the case of the "differential growth" model, no such first-order dynamical system can display any non-monotonic dynamics in the frequency of either phenotype.

Phenotypic equilibria in exponential phase

In exponential phase, when the average growth rate assumes its maximum value ρ and $D(N) \simeq 1$, Eqs. 3.22 and 3.23 become:

$$\dot{N} = \rho N \tag{3.24}$$

$$\dot{f} = \alpha_+(1-f) - \alpha_- f. \tag{3.25}$$

From Eq. 3.25 the exponential phase equilibria for the fraction of CAP+ cells can be easily obtained by setting $\dot{f} = 0$:

$$f^* = \frac{\alpha_+}{\alpha_+ + \alpha_-}, \tag{3.26}$$

meaning that the equilibrium frequency of CAP+ in exponential phase is proportional to the CAP- to CAP+ transition probability per unit of time. Furthermore, the equilibrium is independent of the mean growth rate ρ, like in the previous null model.

Quantitative comparison with observations

The "pure switch" model can be regarded as a first approximation of the *Pseudomonas fluorescens* switching populations. By setting the switching rate constant, and by ignoring the possibility of differences in population growth for the three preculture conditions "low", "mid" ad "high", this model allows to compute a rough estimate of the CAP- to CAP+ switching rate. Indeed, for $f \simeq 0$ (the situation at the beginning of the experiment) Eq. 3.25 yields

$$\dot{f} \simeq \alpha_+, \tag{3.27}$$

which allows to estimate the switching rate from the CAP- to the CAP+ phenotype (Table 3.2).

Preculture density	f_{R0}	$f(t1)$	$\frac{f(t_1)-f_{R0}}{t_1} \sim \alpha_+(\mathrm{h}^{-1})$
low	0.025	0.026	$5.7\ 10^{-4}$
mid	0.068	0.288	0.126
high	0.124	0.454	0.189

Table 3.2: In the "pure switch" model, when the initial frequency is small the switching rate from the CAP- to the CAP+ phenotype can be approximated by the derivative of the CAP+ frequency at time 0. The values in the Table must therefore be considered overestimates of the switching rate α_+.

In summary, to account for the experimental data in a "pure switch" scenario, the populations started from the dilution of low-density precultures should have a CAP- to CAP+ switching rate 3 orders of magnitude lower than in the other treatments. This is unrealistic in cases where the transition rates are a property of the phenotype alone, as assumed in most models of phenotype switching, and point to the role of other variables in determining the speed at which the transitions between phenotypes occur.

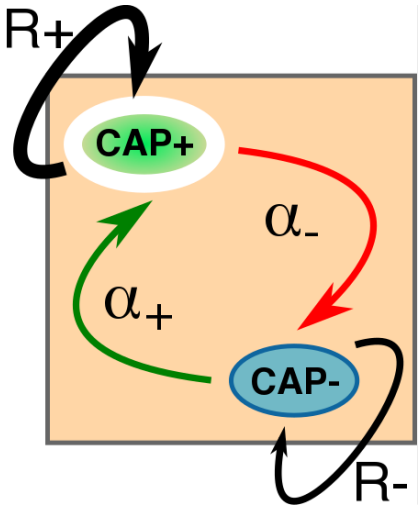

Figure 3.5: Third null model: a growth rate difference between CAP+ and CAP- cells is added to the switching process. Like the "differential growth" and the "pure switch", this model fails to describe the overshoot in the phenotypic dynamics during exponential phase.

3.2.3 Constant switching rates with growth rate difference

By combining the two previous models ("differential growth" and "pure switch"), I will explore the possibility that a combination of constant switching rates and growth rate difference is sufficient to produce a non-monotonous increase in CAP+ frequency at the beginning of exponential phase (Fig. 3.5).

In this scenario, Eqs. 3.1 and 3.2 write:

$$\dot{N}_+ = D(N_+ + N_-)\left[R_+(t)N_+ + \alpha_+ N_- - \alpha_- N_+\right] \tag{3.28}$$
$$\dot{N}_- = D(N_+ + N_-)\left[R_-(t)N_- - \alpha_+ N_- + \alpha_- N_+\right], \tag{3.29}$$

and in terms of the total number of cells N and of the frequency of CAP+ f:

$$\dot{N} = D(N)\left[R_-(t) + f\Delta R(t)\right]N \tag{3.30}$$
$$\dot{f} = D(N)\left[\Delta R(t) f(1-f) + \alpha_+(1-f) - \alpha_- f\right]. \tag{3.31}$$

It can be noticed that for $\alpha_+ = \alpha_- = 0$ this model corresponds to the "differential growth" (Eqs. 3.15 and 3.16), and for $r_+ = r_-$ to the "pure switch" one (Eqs. 3.24 and 3.25).

The phenotypic dynamics described by Equation 3.31 is decoupled from the demographic one (Eq. 3.30), except from a time-rescaling that does not change the direction of the flow along a trajectory: this model fails to provide a quantitative explanation for the overshoot, too.

Phenotypic equilibria in exponential phase

Even if it does not produce an overshoot, this model may however be used to predict the phenotypic composition of the population in the exponential phase of growth. In this phase, $D(N) \simeq 1$, and the growth rates attain their maximum, so that $R_-(t) =$

r_-, $R_+(t) = r_+$. Defining $r_+ - r_- = dr$, I obtain:

$$\dot{N} = (r_- + fdr)N \tag{3.32}$$

$$\dot{f} = drf(1-f) + \alpha_+(1-f) - \alpha_- f. \tag{3.33}$$

By setting $\dot{f} = 0$, from equation (3.33) I obtain:

$$f^*_{1,2} = \frac{dr - (\alpha_+ + \alpha_-) \pm \sqrt{(dr - (\alpha_+ + \alpha_-))^2 + 4dr\alpha_+}}{2dr}. \tag{3.34}$$

Unlike the previous null models, the exponential phase phenotypic equilibrium now depends on demographic parameters, therefore capturing one of the features of the *Pseudomonas fluorescens* switchers (Chapter 1, Section 1.3.3):

$$f^* = \frac{\alpha_+ + \rho - r_-}{\alpha_+ + \alpha_- + \rho - r_-}. \tag{3.35}$$

Under conditions in which such equilibrium fraction is positive for every ρ, this model thus predicts that f^* increases with the average growth rate ρ. As I will discuss in Chapter 4, this is at odds with independent observations of the biological system.

3.2.4 Conclusions about context-independent switch models

Both the "differential growth" and the "pure switch" null models are qualitatively inconsistent with the observations of Chapter 1, Section 1.3.4 as they cannot account for the experimentally observed non-monotonic phenotypic dynamics in the exponential growth regime. Moreover, when trying to provide a quantitative justification of the increase in the CAP+ frequency in the first two hours after resuspension in round 1, their parameters should assume disproportionate differences between CAP+ and CAP-.

The third null model, wherein a growth rate difference between the two states complexifies the Markovian switching process, cannot reproduce the non-monotonic phenotypic dynamics either. Unlike the previous ones, however, this model predicts the frequency of CAP+ during exponential phase to depend on the mean growth rate of the population (Eq. 3.35), but such dependence goes in the opposite direction with respect to independent observations.

To summarize, standard models whereby the genotype determines the switching rates between alternative phenotypic states are not apt to explain the whole phenotypic dynamics of a growing population of *Pseudomonas fluorescens* "switchers". To reproduce the non-monotonicity in the dynamics of the phenotypes' frequencies, the switching rates need to be made time-dependent, for example by linking their value to a demography-related variable.

3.3 Model of demography-dependent switching

In this Section, I present a model coupling phenotypic switching at the cell level with population demography, based on the hypothesis that internal concentrations of proteins or other metabolic compounds are the mediators of such an interaction. Indeed, changes in the population growth rate, corresponding to variations in the division time of individual cells, modulate the process of dilution of proteins and other molecules inside the cellular volume, potentially triggering a concentration-dependent switch between alternative phenotypes.

Mathematically, this is accomplished by adding, alongside the total number of cells and frequency of CAP+ cells, a third state variable: the concentration of a metabolite X synthesized by the cell, accumulated inside the cellular volume, and diluted through cell division. This internal variable works as a proxy for the ensemble of metabolic processes affecting the switching dynamics, and does not refer to any specific compound. Under this assumption, the switching rates come to depend on the overall population growth state: balance between production and dilution of the X metabolite will be altered when the population demography, along with the generation time, changes — and this will in turn modify the switching rates.

A similar model including growth-switch feedback mediated by internal concentrations as a basis for bistability has been proposed by Herbert Levine and collaborators in a setting when the difference in growth rate between phenotypes was central, that of bacterial persisters [8]. They showed that the dynamics of *Escherichia coli* persisters can be interpreted in terms of differential dilution of toxin/antitoxin (TA) molecules between the growing (and susceptible) state and the dormant (thus, persister-like) one [34].

Here, I will instead mostly focus on the limit of negligible growth rate differences, so that both phenotypes grow at a comparable rate. This approximation is relevant for differential, rather than binary (dead/alive), responses to selection.

A general mathematical representation of the model will be initially presented: when the subpopulations expressing different phenotypes do not share the same growth rate, dilution will affect differently the internal concentrations in individual cells of either phenotype. Moreover, the two phenotypes might in principle differ in terms of the production rate of the X metabolite, too. As a result, *two* more equations with respect to the models presented in Section 3.2 would be needed to describe the internal concentrations in capsulated (CAP+) cells and in non-capsulated (CAP-) cells. In order to simplify the analysis of the system, I will however assume for most part of the Chapter that growth rate differences between phenotypes are negligible, and show that the essential features of the experimentally observed dynamics are reproduced by a system of three equations.

3.3.1 Alternative phenotypic states and intracellular bistability

In phenotypically switching microbial populations, individual cells are often described in terms of multistable systems whose state depends on few environmental or internal "parameters". Signature of such multistability is hysteresis: the history of the system influences its state [94]. As environmental conditions (e.g. concentrations of nutrients

or antibiotics) change, relative frequencies of phenotypes in an isogenic microbial population are susceptible to vary in a history-dependent fashion.

In *Pseudomonas fluorescens* switching strains, the two alternative states are related to the expression of an operon responsible for the production of a capsule around the cell surface (Chapter 1). Analogous to Ozbudak *et al.*'s experiment, these strains were transformed so that an inserted *gfp* gene was stably co-expressed with the capsule operon, resulting in a coincidence between CAP+ and GFP+ phenotypes (Chapter 2).

Back in Chapter 1, Section 1.3.3, I reviewed how the expression of the CAP+ and CAP- phenotypes can be altered by environmental conditions such as temperature, cell density and extracellular concentration of uracil. The data gathered on the response to environmental cues having an effect on the intracellular state supported the idea of introducing a third state variable c, corresponding to the intracellular concentration of an unknown metabolite X synthesized by cells. This concentration would act as a "control variable" on the bistable phenotypic dynamics, possibly as a proxy for the overall cell metabolic state.

As commonly done for many different experimental systems [20, 73, 34], I choose to model the intracellular state as a bistable hysteretic dynamical system, where the probability of expressing one or the other cell phenotype is a function of the intracellular concentration $c(t)$ (Fig. 3.6). When the concentration c is controlled by the external environment as in [73], it determines the range and location of the region where two distinct stable equilibria exist and the magnitude of their basins of attraction. Here, on the other hand, the intracellular concentration c is one of the variables of the system affecting the switching dynamics.

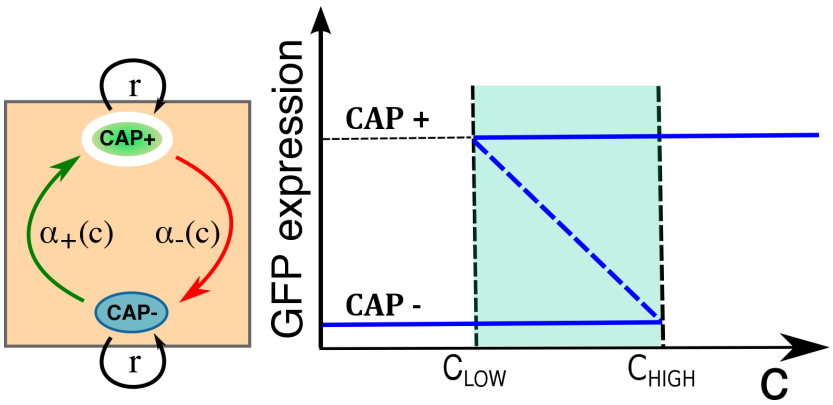

Figure 3.6: The alternative phenotypes in populations of *Pseudomonas fluorescens* "switchers" can be modelled as the two stable equilibria of a bistable system. I decided to consider an internal variable (the intracellular concentration c of a generic metabolite synthesized by the cell) in analogy with the control parameter of bifurcation diagrams with fixed environmental conditions. The bistability region is bound by two threshold values of c, called c_{LOW} and c_{HIGH}. Being the CAP+ phenotype marked with the insertion of a *gfp* gene under the control of the promoter of the same capsule-related operon, CAP- and CAP+ cellular states can be set apart in terms of intensity of GFP fluorescence.

Bifurcation diagram for the intracellular dynamics

In the theory of bifurcations of dynamical systems, bifurcation diagrams represent the qualitative changes in the orbits of a (system of) differential equation(s) as a consequence of continuous variations in one (or more) parameters. These are commonly called control parameters because of the possibility of observing such qualitative changes by externally tuning their value [6]. A famous example of an actual bifurcation in microbial heterogeneity is that of *Escherichia coli lac* operon: Ozbudak *et al.* demonstrated that a bistable dynamical system accounting for the genetic architecture of the operon regulation could quantitatively explain the relation between extracellular concentrations and the proportion of cells that were in either phenotypic state [73]. It could moreover predict that the bistable regime would be lost under different conditions, where a change in the carbon source concentration would not elicit an on-off change in the cell phenotype.

Similarly, bifurcation theory was used by Gardner *et al.* to demonstrate that, in a synthetic gene circuit, mutually inhibiting repressible promoters are able to give rise to a region of bistability, that they quantitatively quantified based on measures of intracellular rates [20].

In the case of *Pseudomonas fluorescens* switchers, the knowledge of the intracellular architecture eliciting the switching behaviour is not sufficiently advanced to allow a quantitative modelling of the intracellular regulation. I thus assumed that a qualitatively similar dynamical system could account for the phenotypic switch. Instead of being a control *parameter*, c will more generally be a control *variable* determining the probability of switching between phenotypes. The concentration c can be interpreted as a proxy encompassing all the sources of modification in the switching probabilities between the CAP- and CAP+ states. In Figure 3.6 the stable equilibria, corresponding to the two cellular states CAP- and CAP+, are represented with solid lines. In the bistability region, for the same value of c, the system has two stable alternative equilibria, and an intermediate unstable equilibrium marks the border of their basins of attraction, if the feedbacks stabilizing the alternative equilibria act on a fast time scale. As a consequence of intrinsic intracellular stochasticity, however, the cell may switch equilibrium, with a probability that is by simplicity assumed to be proportional to the magnitude of the relative basin of attraction relative to that of the alternative equilibrium. This representation allows us to avoid specifying the precise sources of stochasticity and to model the system with a deterministic system of equations.

I chose, again for the sake of simplicity, a piecewise linear bifurcation diagram where the relation between basins of attraction is easily obtained (see next paragraph). This way, any fine-scale variation in the degree of GFP expression among cells with a CAP+ phenotype can be neglected, and analogously for phenotypes that do not express the fluorescent protein at all. The description of the phenotype through a binary variable is a good approximation of reality, as the fluorescence peaks obtained by FACS are well separated, supporting the assumptions that when cells change basin of attraction, they decay fast to the new equilibrium.

Switching rates as a function of intracellular concentration

The compound X is assumed to enhance the probability of expressing the CAP+ state. As a consequence, the higher is c, the larger the switching rate towards the capsulated state equilibrium, and the lower the switching rate to the non-capsulated phenotype. For the simplified bifurcation diagram illustrated in 3.6, the switching rates depend linearly on c inside the bistability region. Figure 3.7 illustrates the relation between the bifurcation diagram and the Markov chain representation:

- for low values of c (below a threshold value called c_{LOW}), the CAP- to CAP+ switching rate α_+ is set to zero, while the CAP+ to CAP- switching rate α_- is maximum;
- for high values of c (over a threshold value called c_{HIGH}), α_+ assumes its maximum value, while α_- is set to zero;
- for intermediate values of c (between the two threshold values c_{LOW} and c_{HIGH}), α_+ and α_- are both non-zero and are an increasing and a decreasing function of c, respectively, corresponding to the relative extension of the basins of attraction of the two alternative equilibria.

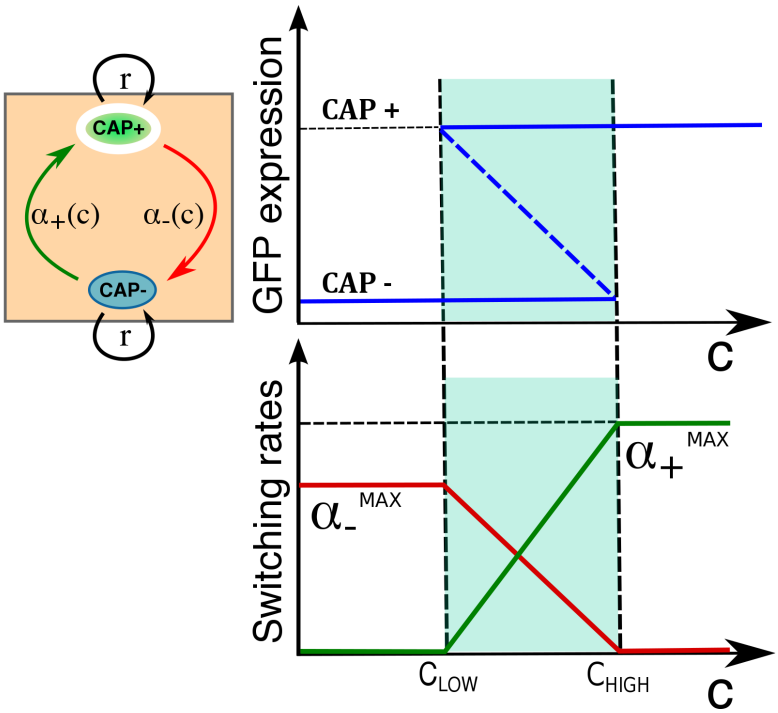

Figure 3.7: Switching rates are proportional to the width of the basins of attraction of the two stable equilibria (i.e. the CAP- and the CAP+ phenotypic states). For intermediate values of the intracellular concentration c a cell is inside the "bistability region" where the switching rates are both non-zero. Outside the bistability region the switching rates assume their maximum or minimum values (the latter arbitrarily set to zero).

This description bears similarities to neural models such as that by FitzHugh-Nagumo [37]: one variable (in this case c, playing the role of the recovery variable), whose dynamics is slow, controls the steady-state of another one (the phenotypic state CAP-/CAP+, corresponding to the membrane potential of neurons), whose dynamics is faster. The response of excitable systems to stochastic process that occur on fast time-scales is known to encompass, among other dynamical behaviours, transient dramatic changes in a systems variable, analogous to what observed in the overshoot experiment.

3.3.2 Protein concentrations can couple demography and switch

The variable c, corresponding to an intracellular protein concentration, works as the mediator of the impact of the population state on phenotypic heterogeneity and connects demography (population size and its dynamics) and physiology (probability of switching) in *Pseudomonas fluorescens* populations.

This assumption is consistent with the experimental evidences presented in Chapter 1 and in agreement with previous works: even in isogenic populations, different regimes of population growth are known to cause cell-to-cell phenotypic variability, for example via variation in gene expression and regulation [67]. Phenotypic switching, such as the persisters or our *Pseudomonas fluorescens* switchers, makes no exception [34, 42].

Intracellular concentrations can be coupled to the population state in many different ways. Here, I will consider the simplest one, that is assuming no direct effect of population size except the one due to dilution. This assumption is certainly too crude for proteins that are controlled by the wild-type genetic circuit, which are most likely to be subjected to different kinds of regulation so as to keep their expression synchronized with growth. However, since phenotypic switchers in *Pseudomonas fluorescens* are newly evolved, it is well possible that purifying selection had no time to optimize the modified intracellular circuits, thus resulting in a minimalistic regulation of some of its components. In this way, switching rates are essentially influenced not by the cell density, but by its differential, the population growth rate, which provides a "measure" for the demographic state of the population. Differences in division time can in this way affect intracellular properties through changes in the dilution of cellular internal content. These simple assumptions retain some of the scaling properties of more complicated models which take into account the relationship between growth rate and other processes such as transcription or translation rates [53].

A faster (slower) growth regime will be mathematically translated into higher or (lower) dilution factor in the equation ruling the dynamics of the internal concentration c, causing the system to move towards the left- (right-) hand side of the bifurcation diagram of Figure 3.7. Following this modelling choice, I will write the dynamics of the internal concentration c as the combination of a production and a dilution term: their (dynamically changing) relative importance will be responsible for the states explored by the system.

3.3.3 General 4-D dynamical system

A general form of a model with switching rates depending on an internal variable whose magnitude is a function of a dilution term (proportional to the growth rate) must take into account that, in principle, CAP- and CAP+ cells might not share the same growth rate. In this general case, two separate equations will describe the two concentrations c_+ and c_-, assumed to be equal in all CAP+ and all CAP-, respectively.

The equations for the intracellular concentrations will be coupled to the population equations from the "constant switching rates with growth rate difference" null model, through the switching rates S_+ and S_-. These will from now on depend on the intracellular concentration of X, according to Fig. 3.7:

$$\dot{N} = D(N)\left[R_+(t)f + R_-(t)(1-f)\right]N \tag{3.36}$$

$$\dot{f} = D(N)\left[\Delta R(t)f(1-f) + S_+(c_-)(1-f) - S_-(c_+)f\right]L(t) \tag{3.37}$$

$$\dot{c}_+ = P_+(c_+,t) - D(N)R_+(t)c_+ \tag{3.38}$$

$$\dot{c}_- = P_-(c_-,t) - D(N)R_-(t)c_- \tag{3.39}$$

where $D(N)$ represents a density dependence term, $R_+(t)$ and $R_-(t)$ are the time-dependent growth terms for CAP+ and CAP-, respectively, $\Delta R(t) = R_+(t) - R_-(t)$ is their difference, $L(t)$ is a time-dependent factor corresponding to the lag phase, P_+ and P_- are the rates of synthesis of the X product for the two phenotypes, and $S_-(c_+)$ and $S_+(c_-)$ the concentration-dependent switching rates to the opposite state.

In the next paragraph I discuss the role of the density-dependence term $D(N)$, which translates the hypothesis that the switch is gated at cell division, and that of the time-dependent modulation of the growth rates $L(t)$, under the hypothesis that switch and cell division are strictly linked processes.

The "switch at cell division" hypothesis

The density dependence term $D(N)$ can be written as a logistic factor $(1-\frac{N}{K})$, where N is the total population size and K the carrying capacity of the ecological system. $D(N)$ sets the time scale not only for the demographic dynamics, but also for the intracellular one: by reducing population growth at the entry of stationary phase, it dampens the dilution of the internal concentrations c_+ and c_-, making the switch to the CAP+ state more likely, and that to the CAP- state less so.

By multiplying both switch terms S_+ and S_- by $D(N)$ in the equation for the CAP+ frequency f (Eq. 3.37), I model the hypothesis that the phenotypic switch does not occur with the same probability at any time during the cell cycle, but it is likely to be concentrated around the division time. Cell division is indeed the moment during the cell cycle when stochastic fluctuations in protein number are maximum, due to the possible assymetric repartition of low density molecules between the daughter cells. Stochastic fluctuations are known to be at the basis of phenotypic switching, for example by changing the concentration of a key regulator across a critical threshold in an appropriately designed genetic circuit allowing bistability (e.g. via a positive feedback loop or a double negative regulation). An example is provided by the opaque/white switch in *Candida albicans* colony morphology: stochastic fluctuations

in the expression of the *wor1* gene can move the concentration of its product *Wor1* (a master transcriptional regulator) below or above the level triggering the cellular switch that underpins the variability at the colony level [102]. At cell division such fluctuations increase, making the switch more likely to happen.

The effect of conditions slowing cell division thus lowers the switching rates as well, under the hypothesis that the switch can only occur at cell division. The effects of relaxing the hypothesis of a cell-cycle triggered phenotypic switch will be later discussed in Section 3.5.2.

Different time-dependent terms were introduced so as to encompass the effect on growth and switching of the lag phase that characterizes the beginning of the demography of cultures close to stationary phase, when they are resuspended. The growth terms $R_-(t)$ and $R_+(t)$ are thus assumed constant and equal to the maximum growth rates r_-, r_+, except when growth is arrested. Arrested growth is here modelled by a lag factor $L(t)$:

$$L(t) = \theta(t - \tau) \tag{3.40}$$

where τ represents the length of the lag phase experienced by cells after resuspension into fresh medium and $\theta(x)$ is the Heaviside step function, defined as:

$$\theta(x) = \begin{cases} 0, & \text{if } x < 0 \\ 1, & \text{if } x \geqslant 0. \end{cases} \tag{3.41}$$

As a consequence, the time-dependent maximal growth rate is:

$$R_+(t) = r_+ L(t) \tag{3.42}$$

$$R_-(t) = r_- L(t). \tag{3.43}$$

At times $t < \tau$, where τ is the the duration of the lag phase at resuspension, growth is impeded ($\theta(t - \tau) = 0$ and therefore $\dot{N} = 0$); for times after the end of the lag phase ($t \geq \tau$) the equation for the demographic dynamics of the population resumes the classic Verhulst form of logistic growth.

The lag phase (whose early discovery in *Salmonella enterica* was motivated by the research on the effects of temperature on bacterial growth [70]) can be defined as the stage preceding the beginning of exponential growth, during which bacterial cells are not able to grow or divide. Several, more and more refined interpretations of this fact have been so far proposed: lag as the time needed for bacteria to adapt to a novel environment [61], to recover from molecular damage accumulated in stationary phase [27], or corresponding to transient sensitivity to oxidative stress generating iron accumulation [83].

In this study, one primary difference in the three treatments ("low", "mid", "high") is actually the time of suspended growth after cells get resuspended, the longer the closer the preculture was to stationary phase. In Section 3.4 I show that in Dr. Philippe Remigi's experiment a delay in the onset of the exponential growth phase is present. I make the hypothesis that the phenotypic dynamics, as well as the demographic one, is completely interrupted in lag phase: for this reason, the factor $L(t) = \theta(t - \tau)$ multiplies the equation for $\dot{f}$, too. This is consistent with the previously discussed coupling between switching and cell division. With respect to the production of X, though, I

assume that this process is not impeded during lag phase: indeed, although unable to divide, cells are metabolically active during lag [62], meaning that the processes of transcription and translation of X can be assumed to occur even before maximum, exponential growth is restored (*cf.* also the model by Baranyi & Roberts [10]).

Production and dilution of the intracellular compound X

The internal state of CAP+ and CAP- cells is described in terms of the concentration of a metabolite X that cells are able to synthesize and that is diluted through cell division. The equations for c_+ and c_- each include a term of *production* of the X metabolite (indicated above with $P(t)$) and a term accounting for the *dilution* process.

As for *production* term $P(t)$, I make the hypothesis that concentrations get regulated proportionally to the ratio between their instantaneous values c_+ (or c_-) and their maximum allowed value K_c – which I suppose to be the same for CAP+ and CAP-. During the lag phase, the production rate is considered to be maximal and unregulated (*cf.* previous paragraphs). In formulas:

$$P_+(t) = \begin{cases} b_+, & \text{if } t < \tau \\ \left(1 - \frac{c_+}{K_c}\right) b_+, & \text{if } t \geqslant \tau \end{cases} \tag{3.44}$$

$$P_-(t) = \begin{cases} b_-, & \text{if } t < \tau \\ \left(1 - \frac{c_-}{K_c}\right) b_-, & \text{if } t \geqslant \tau; \end{cases} \tag{3.45}$$

As for *dilution*, I assume that the average single cell volume can be considered constant across the experimental time: although it is known to actually fluctuate, this happens on a fast time scale, that is that of the cell cycle [21], much faster that the whole duration of the dynamics tracked in the experiment. Dilution is therefore described by an exponential decay process, whose exponent is proportional to the growth term $R_+(t)$ or $R_-(t)$, itself dependent on the cellular phenotype. In summary, the *production*/*dilution* balance will depend on population demography as follows:

DURING LAG cell division is prevented and therefore no dilution is possible. Internal concentrations will exponentially increase as the result of the unregulated production of X:

$$\dot{c}_+(t) = b_+ \tag{3.46}$$

$$\dot{c}_-(t) = b_- \tag{3.47}$$

IN EXPONENTIAL PHASE as the population grows at its maximum rate, the X metabolite gets diluted at the highest rate possible. Production starts being regulated. If the *dilution* term is greater than the *production* one, internal concentrations can decrease:

$$\dot{c}_+(t) = \left(1 - \frac{c_+}{K_c}\right) b_+ - r_+ c_+ \tag{3.48}$$

$$\dot{c}_-(t) = \left(1 - \frac{c_-}{K_c}\right) b_- - r_- c_- \tag{3.49}$$

IN STATIONARY PHASE population growth slows down, and the internal concentrations might increase again as a result of having a production term greater than the *dilution* one:

$$\dot{c}_+(t) = \left(1 - \frac{c_+}{K_c}\right) b_+ - \left(1 - \frac{N}{K}\right) r_+ c_+ \tag{3.50}$$

$$\dot{c}_-(t) = \left(1 - \frac{c_-}{K_c}\right) b_- - \left(1 - \frac{N}{K}\right) r_- c_-. \tag{3.51}$$

In other words, this mathematical model includes a differential equation describing the temporal variation of the intracellular concentration of a protein which, in principle, is not constitutively expressed, given the observed variation in the capsulation generated by environmental change. The dilution factor is modelled as a linear function of the growth rate, and the rate of production of the protein as a saturating function of the concentration itself.

Fully-coupled equations

By taking into account these choices about how to formalize the different parts of the model, the system of ordinary differential equations writes:

$$\dot{N} = \left(1 - \frac{N}{K}\right) \left[r_+ f + r_-(1-f)\right] N\theta(t-\tau) \tag{3.52}$$

$$\dot{f} = \left(1 - \frac{N}{K}\right) \left[(r_+ - r_-) f(1-f) + \alpha_+(c_-)(1-f) - \alpha_-(c_+) f\right] \theta(t-\tau) \tag{3.53}$$

$$\dot{c}_+ = \left(1 - \frac{c_+}{K_c}\theta(t-\tau)\right) b_+ - \left(1 - \frac{N}{K}\right) r_+ c_+ \theta(t-\tau) \tag{3.54}$$

$$\dot{c}_- = \left(1 - \frac{c_-}{K_c}\theta(t-\tau)\right) b_- - \left(1 - \frac{N}{K}\right) r_- c_- \theta(t-\tau) \tag{3.55}$$

where the functional dependence of the switching rates from the intracellular concentrations is given by the following equations:

$$\alpha_+(c_-) = \begin{cases} 0, & \text{if } c_- < c_{LOW} \\ \alpha_+^{MAX} \frac{c_- - c_{LOW}}{c_{HIGH} - c_{LOW}}, & \text{if } c_{LOW} \leq c_- < c_{HIGH} \\ \alpha_+^{MAX}, & \text{if } c_- \geq c_{HIGH} \end{cases} \tag{3.56}$$

$$\alpha_-(c_+) = \begin{cases} \alpha_-^{MAX}, & \text{if } c_+ < c_{LOW} \\ \alpha_-^{MAX} \frac{c_{HIGH} - c_+}{c_{HIGH} - c_{LOW}}, & \text{if } c_{LOW} \leq c_+ < c_{HIGH} \\ 0 & \text{if } c_+ \geq c_{HIGH}. \end{cases} \tag{3.57}$$

This model can be easily simulated, however the large number of non directly quantifiable parameters related to the intracellular state makes its use for quantitative fitting complicated and questionable, because of the risk of overfitting. I will thus proceed to study the dynamics of a simpler 3-D approximation of the model. The next Section provides the experimental justification for assuming that such 3-D system is a relevant approximation of the complete 4-D model in the regimes that I am studying.

3.3.4 Analysis of a reduced three-dimensional model

The four-dimensional model presented in the previous paragraphs can be made significantly simpler under the assumption that CAP+ and CAP- cells do not differ in terms of division time under the same conditions. The results of experimental assays presented in the last Section showed indeed no evidence of big differences in growth rate between microcolonies founded by CAP+ and CAP- individual cells.

I thus consider, as a first approximation, $R_+(t) = R_-(t) = R(t)$, or $\Delta R(t) = 0$, which implies the fact that the dilution term in the equations of the model is phenotype-invariant. Now the internal state of all cells is described by one concentration $c(t)$ instead of two:

$$\dot{N} = D(N)R(t)N \tag{3.58}$$

$$\dot{f} = D(N)\left[S_+(c)(1-f) - S_-(c)f\right]L(t) \tag{3.59}$$

$$\dot{c} = P(c,t) - D(N)R(t)c. \tag{3.60}$$

Following the same modelling choices as for the four-dimensional model:

$$\dot{N} = \left(1 - \frac{N}{K}\right) rN\theta(t-\tau) \tag{3.61}$$

$$\dot{f} = \left(1 - \frac{N}{K}\right) \left[\alpha_+(c)(1-f) - \alpha_-(c)f\right]\theta(t-\tau) \tag{3.62}$$

$$\dot{c} = \left(1 - \frac{c}{K_c}\theta(t-\tau)\right) b - \left(1 - \frac{N}{K}\right) r\, c\, \theta(t-\tau) \tag{3.63}$$

with

$$\alpha_+(c) = \begin{cases} 0 & \text{if } c < c_{LOW} \\ \alpha_+^{MAX} \frac{c - c_{LOW}}{c_{HIGH} - c_{LOW}} & \text{if } c_{LOW} \leq c < c_{HIGH} \\ \alpha_+^{MAX} & \text{if } c \geq c_{HIGH} \end{cases} \tag{3.64}$$

$$\alpha_-(c) = \begin{cases} \alpha_-^{MAX} & \text{if } c < c_{LOW} \\ \alpha_-^{MAX} \frac{c_{HIGH} - c}{c_{HIGH} - c_{LOW}} & \text{if } c_{LOW} \leq c < c_{HIGH} \\ 0 & \text{if } c \geq c_{HIGH}. \end{cases} \tag{3.65}$$

The demographic dynamics $\dot{N}$ is now independent of both f and c, and the intracellular dynamics $\dot{c}$ does not depend on f. The former observation justifies looking for the equilibria of the sub-system $(\dot{c}, \dot{f})$ even when the population demography has not yet reached its steady-state, and to study how the uncoupled demographic dynamics acts as a master of the slaved subsystem. Since the equation for the concentration is independent of $f(t)$, the variation in the phenotypic frequency is"controlled" by the intracellular state. In exponential phase, when density-dependent modulation is not present, $f(t)$ and $c(t)$ will thus have a unique equilibrium.

3.3.5 Three-dimensional model: equilibria and their stability

Beside the asymptotic steady state, which corresponds to the situation attained by the system at growth arrest in stationary phase, I am interested in the study of the quasi-

steady states the system may reach during exponential or early-stationary phase. Indeed, in the experiments, the biggest changes in frequency of the phenotypes takes place while cells are still exponentially dividing (see Fig. 1.6).

If the intracellular and phenotypic dynamics described by the $(\dot{c}, \dot{f})$ sub-system takes place on a faster time-scale than that of population growth, c and f will attain a quasi-equilibrium before the population size reaches the carrying capacity. In other words, if the dynamics of $\dot{N}$ is slow enough (with respect to the intracellular one) the time scales can be separated and the quasi-steady states studied as a function of population size N. Population size can then be treated as a measure of time, being $N(t)$ an invertible function of t (Verhulst logistic function).

On the other side, the asymptotic steady-state in stationary phase might not correspond to the fact that the fluxes between phenotypic rates are zero. Indeed, due to the multiplicative factor $D(N)$, the phenotypic dynamics will halt because of population growth arrest, and in that case the system "freezes" in an equilibrium that is different from the quasi-equilibrium for the fast subsystem. By taking the general form of the (c, f) sub-system (Eqs. 3.59 and 3.60) and equaling all the expressions to zero, if $D(N) \neq 0$:

$$f^* = \frac{S_+(c^*)}{S_+(c^*) + S_-(c^*)} \tag{3.66}$$

where c^* is the solution of

$$P(c^*, t) = D(N)R(t)c^*. \tag{3.67}$$

The existence of equilibria for the frequency of CAP+ depends on the existence of equilibria for c, that is the existence of times for which the concentration c multiplied by the *dilution* factor $D(N)R(t)$ balances the *production* term $P(t)$.

For times t belonging to the exponential phase and neglecting lag (which does not occur when exponentially dividing cells are diluted into fresh medium), the quasi-steady states for the intracellular and phenotypic dynamics can be written as:

$$f_E^* = \frac{\alpha_+(c_E^*)}{\alpha_+(c_E^*) + \alpha_-(c_E^*)} \tag{3.68}$$

$$c_E^* = \frac{1}{\frac{r}{b} + \frac{1}{K_c}}. \tag{3.69}$$

Taking the linear switching rates (Eqs. 3.64 and 3.65) and considering $K_c \in [c_{LOW}, c_{HIGH}]$, the exponential phase quasi-equilibria for f and c are:

$$f_E^* = \left[1 + \frac{\alpha_-^{MAX}}{\alpha_+^{MAX}} \frac{\left((\frac{r}{b} + \frac{1}{K_c})c_{HIGH} - 1\right)}{\left(1 - (\frac{r}{b} + \frac{1}{K_c})c_{LOW}\right)}\right]^{-1} \tag{3.70}$$

$$c_E^* = \frac{1}{\frac{r}{b} + \frac{1}{K_c}}. \tag{3.71}$$

In stationary phase the model allows an infinity of neutrally stable (initial conditions dependent) equilibria: if the concentration reaches its steady, regulated value

K_c before the population enters stationary phase, then the (quasi-)equilibria read:

$$f_S^* = \frac{\alpha_+(c_S^*)}{\alpha_+(c_S^*) + \alpha_-(c_S^*)} \tag{3.72}$$

$$c_S^* = K_c \tag{3.73}$$

and, again, considering Equations 3.64 and 3.65 and considering $K_c \in [c_{LOW}, c_{HIGH}]$:

$$f_S^* = \left[1 + \frac{\alpha_-^{MAX}}{\alpha_+^{MAX}} \frac{(c_{HIGH} - K_c)}{(K_c - c_{LOW})}\right]^{-1}. \tag{3.74}$$

Stability

Since the density-dependent factor $D(N)$ is always positive, the stability of the (f, c) subsystem is determined by the corresponding reduced 2x2 Jacobian matrix at the quasi-equilibria (f^*, c^*):

$$\tilde{J}(f^*, c^*) = \begin{bmatrix} \frac{\partial \dot{f}}{\partial f}(f^*, c^*) & \frac{\partial \dot{f}}{\partial c}(f^*, c^*) \\ \frac{\partial \dot{c}}{\partial f}(f^*, c^*) & \frac{\partial \dot{c}}{\partial c}(f^*, c^*) \end{bmatrix} \tag{3.75}$$

to establish their stability.

For the exponential phase quasi-equilibrium (Eqs. 3.68 and 3.69), the reduced Jacobian matrix $\tilde{J}$ reads:

$$\tilde{J}_E = \begin{bmatrix} -[\alpha_+(c_E^*) + \alpha_-(c_E^*)] & (1 - f_E^*)\frac{\partial \alpha_+}{\partial c}(c_E^*) + f_E^* \frac{\partial \alpha_-}{\partial c}(c_E^*) \\ 0 & -\left(\frac{b}{K_c} + r\right) \end{bmatrix} \tag{3.76}$$

If the concentration increases to the point that it reaches its maximum, regulated value before the population enters stationary phase, then the stationary phase Jacobian matrix is given by:

$$\tilde{J}_S = \begin{bmatrix} -\left(1 - \frac{N}{K}\right)[(\alpha_+(c_S^*) + \alpha_-(c_S^*)] & \left(1 - \frac{N}{K}\right)\left[(1 - f_S^*)\frac{\partial \alpha_+}{\partial c}(c_S^*) + f_S^* \frac{\partial \alpha_-}{\partial c}(c_S^*)\right] \\ 0 & -\left[\frac{b}{K_c} + \left(1 - \frac{N}{K}\right) r\right] \end{bmatrix} \tag{3.77}$$

Since the switching rates α_+ and α_- are linear functions of c when $c \in [c_{LOW}, c_{HIGH}]$, their partial derivatives $\frac{\partial \alpha_+}{\partial c}$ and $\frac{\partial \alpha_-}{\partial c}$ are always independent of c. Moreover, both $\tilde{J}_E$ and $\tilde{J}_S$ are triangular matrices, which means that their eigenvalues correspond to the elements on the principal diagonal: being both smaller than zero for any allowed value of the parameters, I can conclude that the (f, c) quasi-equilibria in exponential and stationary phase are stable nodes. Therefore, the undershoot in the frequency dynamics cannot be explained in terms of oscillatory behaviour of the reduced subsystem. to acknowledge the resemblance between this model and the FitzHugh-Nagumo one [37]: as in excitable systems, in our model there exist nonlinearities (the exponential increase of c during lag) pushing the system away from the (quasi-)steady state on a fast time scale (the overshoot), and a slow "recovery" mechanism (dilution through cell division) relaxing the system to its asymptotic state.

3.4 Fitting the overshoot experiment

Following the evolution and first characterization of the phenotypic switch in *Pseudomonas fluorescens* "switchers" (Chapter 1), the "overshoot experiment" provided further information about the complexity behind the expression of alternative phenotypes in a growing population of switching bacterial cells.

The goal of this experiment (conceived, designed and performed by Dr. Philippe Remigi at Rainey Lab, Massey University, Auckland) was to quantify and understand the role of demography and of past growth conditions in the switching behaviour: indeed, although the population demographic and phenotypic states were already known to be tightly linked in "switchers" populations (Chapter 1, Section 1.3.3), the extent and the eventual time dependence of their reciprocal interaction were still unknown.

This could be achieved by tracking the dynamics of the phenotypic composition of the population (i.e. the change of the relative frequency of the two alternative phenotypes cells can express) via flow cytometry across several generations. During this time, and at the same time points, optical density measurements were performed to track the dynamics of the population size. The role of previous growth conditions was, on the other hand, investigated by changing the time spent by the inoculum population in a microcosm with limited resources during a preliminary stage of growth.

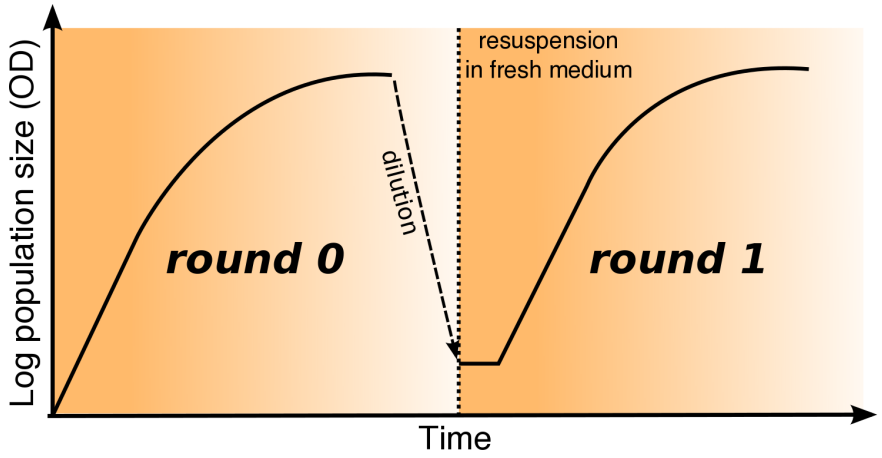

Figure 3.8: Scheme of the protocol of the overshoot experiment (1). Cells are prepared through a preculture stage (round 0), during which population growth causes the nutrients' concentration in the microcosms to get progressively exhausted (corresponding to the colour gradient). Once the desired population size is reached along the growth curve in round 0, cells get diluted and transfered into fresh medium to start round 1.

Two rounds of growth to study the effect of history on population phenotypic heterogeneity

The experiment consists of two successive stages, or *rounds*. During "round 0" three populations of switchers are grown from inocula obtained from a common night culture in sustained exponential phase. When cells from "round 0" are bottlenecked

and resuspended into fresh medium, a new stage of the experiment, called "round 1", starts: cells resume division, possibly after a lag phase, resulting in an exponential, then saturating population growth. The population phenotypic composition at the time of sampling during round 0 and the size of the bottleneck set the initial conditions of round 1 (Fig. 3.8).

Different initial conditions for frequency (but same population size)

Before resuspension, samples from populations that attained different densities in round 0 are diluted to the same optical density. Such bottleneck is no as small as to make stochastic fluctuations in sampling significant. The populations corresponding to the three treatments observed in round 1 ('low', "mid" and "high", detailed in the caption of Fig. 3.10) thus differ in the phenotypic composition and in the demographic and environmental conditions that their cells have experienced during the preparation stage (round 0). Importantly, during round 0 cells belonging to the "low" cell density sample never exit exponential phase, while the "high" cell density population approached stationary phase.

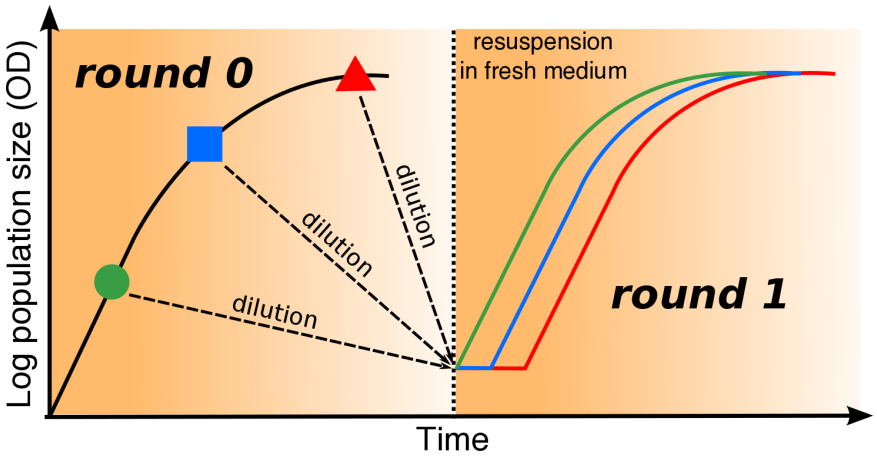

Figure 3.9: Scheme of the protocol of the overshoot experiment (2). To investigate the role of past environmental and demographic conditions on the dynamics of the expression of the alternative phenotypes, a growing population of switchers is sampled at different time points (cell densities) during round 0, diluted to the same cellular density and resuspended into fresh medium. Samples from later time points show a longer lag phase but the same growth rate in exponential phase. Symbols and colors are the same as those used later to identify the three treatments.

3.4.1 Qualitative features of the experimental observations

The results of the measurements of population size and of CAP+ frequency during round 1 are shown in Figure 3.10.

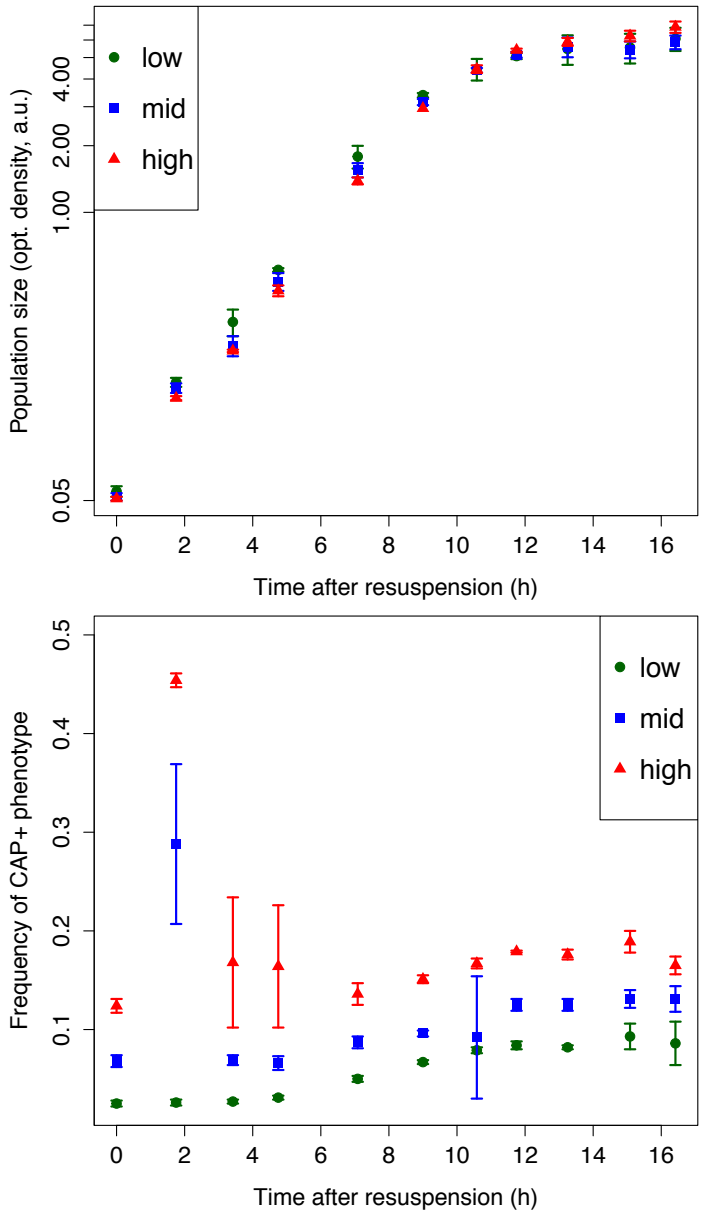

Figure 3.10: Demographic and phenotypic dynamics of a *Pseudomonas fluorescens* switchers population over several cellular generations (round 1). After resuspension into fresh medium, population size is measured through optical density (top panel), and CAP+ frequency through flow cytometry (bottom panel). Three different initial conditions, corresponding to different round 0 treatments, are shown: "low" population density at the end of round 0 ($\mathrm{OD}_{\mathrm{R0}} \simeq 0.3$, green circles), "mid" population density at the end of round 0 ($\mathrm{OD}_{\mathrm{R0}} \simeq 1.0$, blue squares), "high" population density at the end of round 0 ($\mathrm{OD}_{\mathrm{R0}} \simeq 1.5$, red triangles). All treatments are diluted to the same population size at the beginning of round 1 ($\mathrm{OD}(0) = 0.05$). The points correspond to the mean value over three statistical replicates, error bars corresponding to standard deviation.

Here I resume the main qualitative features of the overshoot experiment that my model aims at reproducing:

DIFFERENT INITIAL PHENOTYPIC COMPOSITION The "low", "mid" and "high" populations differ in terms of their phenotypic composition at resuspension: the higher the population density reached in round 0, the higher the frequency of CAP+, in agreement with the known association between advanced phases of growth and higher percentages of CAP+ cells (Chapter 1, Section 1.3.3).

LONG-TERM MEMORY OF THE POPULATION PHENOTYPIC STATE The difference in the phenotypic composition at the end of round 0 / beginning of round 1 is conserved across the whole duration of round 1, as the three conditions maintain their order in terms of frequency of the capsulated phenotype $f_{low} < f_{mid} < f_{high}$ at each time point.

TWO QUALITATIVELY DIFFERENT PHENOTYPIC DYNAMICS Two qualitatively different behaviours are observed for different treatments: in the "low" treatment, the frequency of capsulated cells increases monotonically, while the "mid" and "high" treatments both display a non-monotonic time course.

OVERSHOOT/UNDERSHOOT In round 1, the populations of the higher density treatments ("mid", "high") present a fast increase in the percentage of cells expressing the CAP+ phenotype soon after resuspension (thus during lag and early exponential phases) before declining towards different levels corresponding to the initial composition (*overshoot*), and then increasing again when the population approaches stationary phase (*undershoot*).

SAME GROWTH RATE, DIFFERENT LAG The three treatments have very similar growth curves all along round 1: both the average growth rate during exponential phase and the level of the carrying capacity exhibited at the end of the experiment are almost the same across the three treatments. On the other hand, later treatments have (slightly) lower population density during exponential phase, suggesting a differential duration of the lag phase after resuspension.

3.4.2 Three-dimensional model: qualitative dynamics

The three-dimensional mathematical model of Section 3.3.4 captures the salient qualitative features of the overshoot experiment, that were listed in Section 3.4.1. In this Section, I discuss the consequences of the model assumptions and present numerical simulations.

I coded the numerical system in Python, making use of the *odeint* routine present in the ScyPy Python scientific package to simulate the system of ordinary differential equations (Eqs. from 3.61 to 3.63). I then used Matplotlib to plot the results of the simulations (see Chapter 2, Section 2.3 for further details).

Choice of the initial conditions

In the model, the intracellular dynamics and resulting variation in the phenotypes' frequencies during round 0 is what underpins different frequencies of CAP+ across

the three treatments ("low", "mid", "high") at the beginning of round 1. Therefore, I need to discuss here which role may have the dynamics in round 0 on that of round 1, and in particular that of its initial and final conditions.

Sampling round 0 precultures at diferent time points or, equivalently, when they reach specific population densities, corresponds (if the sampling is independent of the cell phenotype and the dilution and resuspension processes do not affect the percentage of CAP+) to different initial conditions for round 1. By calling N_{R0} and f_{R0} the population size and corresponding CAP+ frequency at the moment of sampling during round 0, the initial conditions for the demographic and frequency variables $N(0),\ f(0),\ c(0)$ for round 1 are given by:

$$N(0) = N_{R0}\ d \tag{3.78}$$

$$f(0) = f_{R0} \tag{3.79}$$

$$c(0) = c_{R0} \tag{3.80}$$

where d is the dilution factor applied before resuspension in fresh medium at the beginning of round 1. I moreover make the assumption that the intracellular concentration is not altered when cells are transferred to new medium.

It should be noticed that, to make the three treatments start from the same population density $N(0)$ at resuspension, different values of d must be appropriately chosen. This was one of the choices at the basis of the experimental design, aimed at excluding possible effects of population size from those possibly due to different phenotypic compositions and population histories. Indeed, being initialized at the same cell density, the three treatments are expected to experience the same density-dependent interactions.

Unlike the initial population size in round 1 $N(0)$, which can be arbitrarily modified by acting on the dilution factor d, the CAP+ frequency at the beginning of round 1 $f(0)$ cannot be independently controlled but only "selected" by choosing an appropriate sampling time. In round 0, f varies following Equation 3.62, but it is not known how (no measurements were performed at this stage). Round 0 precultures are started from exponential phase inocula, and it can thus be safely assumed that no lag phase takes place in round 0. This is not, however, the only mechanism potentially giving rise to variations in the CAP+ frequency: the CAP+ frequency can increase as population size approaches the carrying capacity, or due to a difference between the initial conditions of round 0 and the quasi-equilibria associated to exponential phase.

While the sampling time is measurable and, in principle, controllable by the experimenter, the initial conditions of round 0 c_i and f_i are free parameters of the model whose role in the determination of the behaviour of the system in round 1 must be understood. I thus address the questions: How do different initial conditions for round 0 (in terms of frequency of CAP+ f_i and intracellular concentration of the molecule X c_i) affect the initial conditions in round 1 and, thus, the following dynamics? And is the magnitude of this effect dependent on when, during round 0, the preculture gets sampled?

The initial condition for the frequency in round 0 (in principle manipulable by enriching the precultures of CAP+, e.g. through flow cytometry) f_i affects the system's behaviour in round 1 only if the sampling occurs on a faster time scale than that of the

relaxation towards the exponential phase equilibrium f_E^* (Eq. 3.70). Indeed, all other parameters being equal, and set $c_i = c_E^*$ (*cf.* Eq. 3.71) to rule out transient intracellular dynamics, two populations characterized by different phenotypic compositions at the beginning of round 0 would soon converge to the same phenotypic frequencies.

Hence, only by sampling before the CAP+ frequency reaches its quasi-steady state f_E^* (Fig. 3.11, top row), the dynamics of round 1 can be altered. Furthermore, different initial conditions at the beginning of round 1 have an effect only shortly after resuspension, provided that all other parameters are equal (Fig. 3.11, bottom row).

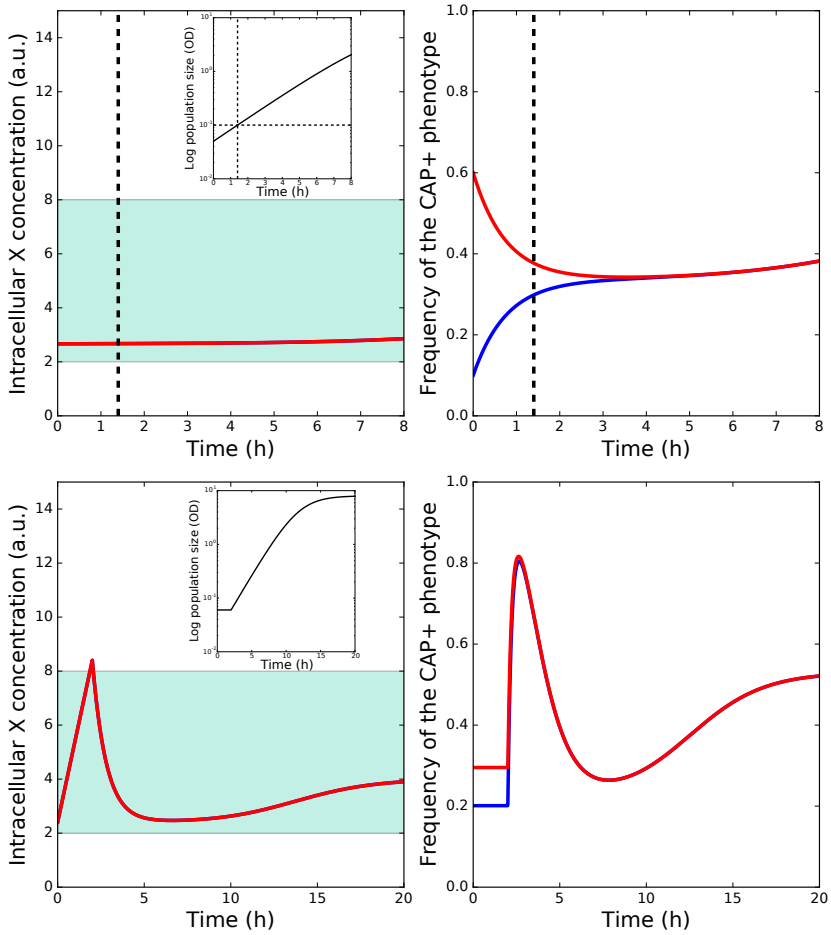

Figure 3.11: The CAP+ frequency at the beginning of round 0 (top row) affects the round 1 dynamics (bottom row) only when sampling early in round 0. Blue curve: $f_i = 0.1$; red curve: $f_i = 0.6$. No experimental data of this (in principle measurable) observable is available for the overshoot experiment. In the following, $f_i = f_E^*$ (see main text). The initial intracellular concentration of X c_i is set to $c_E^* = \frac{bK_c}{b+rK_c}$ for both populations. Other parameters: $r = 0.5$, $K = 8$, $\alpha_+^{MAX} = 4$, $\alpha_-^{MAX} = 1$, $b = 3$, $K_c = 4$, $c_{LOW} = 2$, $c_{HIGH} = 8$.

Also c_i, the initial intracellular concentrations at the beginning of round 0, can affect the initial conditions of round 1 (and thus the behaviour of the system in round 1) only if the sampling is performed before that the intracellular and phenotypic dynamics have relaxed to their exponential phase quasi-equilibria c_E^* and f_E^* (Fig. 3.12).

In other words, if the difference in c_i is such that the two subsystems are in different regimes of switching rates at the beginning of round 0, they may diverge in terms of CAP+ frequency, but will ultimately reach their common exponential phase quasi-equilibrium (c_E^*, f_E^*) set by the value of the parameters, and the same in round 1 soon after resuspension.

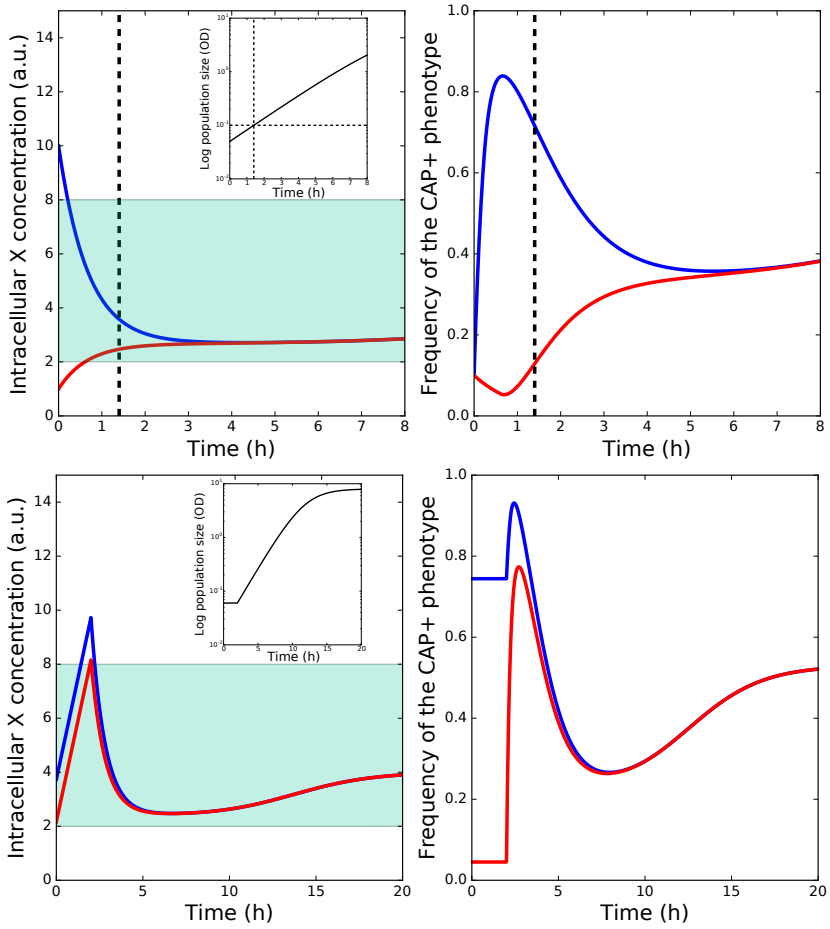

Figure 3.12: The intracellular concentration of X at the beginning of round 0 (top row) affects the round 1 dynamics (bottom row) only when sampling early in round 0. Blue curve: $c_i = 10$; red curve: $c_i = 1$. Being not directly accessible to measurements, c_i is one of the free parameters of the model. In the following, $c_i = c_E^*$ (see main text). The initial CAP+ frequency f_i is set to f_E^* for both populations. Other parameters: $r = 0.5$, $K = 8$, $\alpha_+^{MAX} = 4$, $\alpha_-^{MAX} = 1$, $b = 3$, $K_c = 4$, $c_{LOW} = 2$, $c_{HIGH} = 8$.

In conclusion, since round 0 is started from exponentially growing cultures, there is no reason to believe that at the beginning of round 0 the proportion of capsulated cells is very offset from its exponential equilibrium value. Therefore, in the following I assume $f_i = f_E^*$, with f_E^* defined by Equation 3.70. This choice is not unrealistic, as the frequency of CAP+ typically converges fast, as the population is maintained in exponential phase, to its quasi-steady state value.

The intracellular concentration cannot be directly assessed, but the model allowed to study what may be the effect of a difference in the initial condition for round 0 on the round 1 dynamics. If the population has remained in exponential phase long enough after being diluted, the memory of the initial concentration is lost. Alike phenotypic frequencies, c in round 0 approaches the equilibrium value c_E^* (Eq. 3.71), usually on a faster time scale than that of sampling. Therefore, in the following Sections I will assume $c_i = c_E^*$.

Long-term "memory" of the population history

Trans-generational persistence of the phenotypic composition of the population was observed in the overshoot experiment: populations started from different preculture treatments (round 0) kept their order in terms of the CAP+ frequency all along the measurement stage (round 1), notably at the end of the experiment (more than 16 hours after resuspension in fresh medium).

Such "splitting", corresponding to different treatments having different equilibria in stationary phase, cannot be obtained in the three-dimensional system (at least, as long as the intracellular and switching dynamics are faster than the demography) unless the set of parameters is different among the three treatments. Indeed, the stationary-state equilibria defined by Equation 3.81 only depend on the system's parameters and not on the initial conditions, which are, together with the lag duration, what differentiates the three treatments in round 1. A different conclusion is in principle possible when the time scales are not sufficiently separated, so that the vanishing of the population growth freezes the system before it can reach the equilibrium. However, numerical integration and the analysis of the stability of the stationary equilibrium suggest that this is approached sufficiently fast so that after few hours, the distance from the stationary-state equilibrium is so small that it cannot account for the large differences observed in the experiments.

When the time scales are separated, the value attained by the frequency at the end of round 1 depends on the ratio between the maximum switching rates $\alpha_+^{MAX}/\alpha_-^{MAX}$ (Fig. 3.13), and on the value of the maximum intracellular concentration K_c relative to the boundaries of the bistability region $[c_{LOW}, c_{HIGH}]$ (Fig. 3.14). Indeed, if the concentration reaches its maximum, regulated value K_c before the population enters stationary phase (which would otherwise progressively halt the phenotypic dynamics due to the "switch at cell division" assumption of the model) then the Equation 3.72 back in Section 3.3.5 provides a prediction for the (quasi-)equilibrium for the frequency of CAP+ at late times:

$$f_S^* = \left[1 + \frac{\alpha_-^{MAX}}{\alpha_+^{MAX}} \frac{(c_{HIGH} - K_c)}{(K_c - c_{LOW})}\right]^{-1}, \tag{3.81}$$

with $K_c \in [c_{LOW}, c_{HIGH}]$.

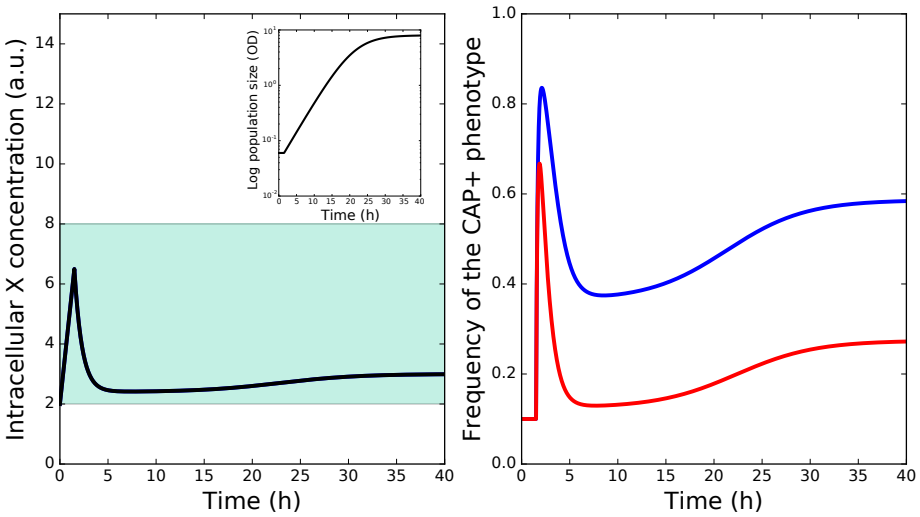

Figure 3.13: Higher $\alpha_+^{MAX}/\alpha_-^{MAX}$ ratios result in lower frequencies of the CAP+ phenotype at the end of round 1 (right panel), without affecting the intracellular dynamics (left panel). Blue curve: $\alpha_-^{MAX} = 4$; red curve: $\alpha_-^{MAX} = 1$. Other parameters: $r = 0.25\ \mathrm{h}^{-1}$, $K = 8$, $\tau = 1.5$, $c_{R0} = 2$, $\alpha_+^{MAX} = 8$, $b = 3$, $K_c = 3$, $c_{LOW} = 2$, $c_{HIGH} = 8$.

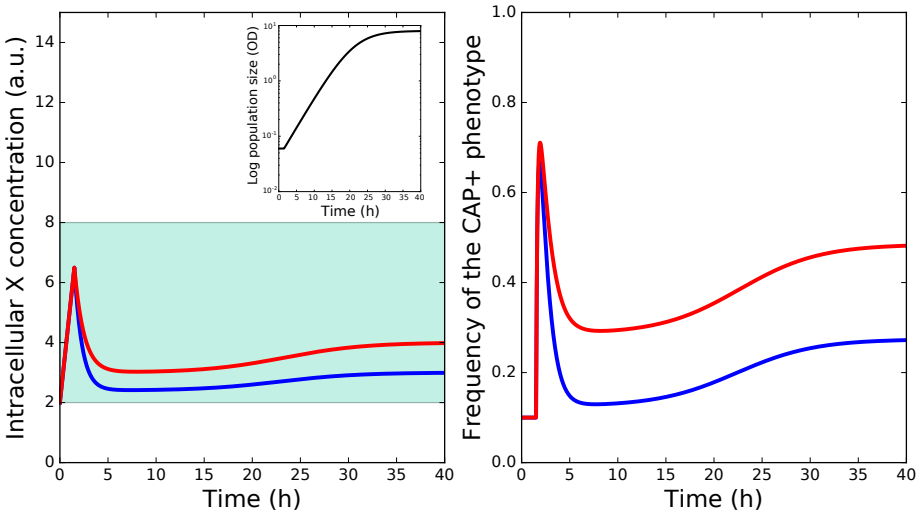

Figure 3.14: Higher maximum intracellular concentrations K_c yield higher frequencies of the CAP+ phenotype at the end of round 1 (right panel), by affecting the intracellular dynamics (left panel). Blue curves: $K_c = 3$; red curves: $K_c = 4$. Other parameters: $r = 0.25$, $K = 8$, $\tau = 1.5$, $c_{R0} = 2$, $\alpha_+^{MAX} = 8$, $\alpha_-^{MAX} = 4$, $b = 3$, $c_{LOW} = 2$, $c_{HIGH} = 8$.

The model hence suggests that the trans-generational persistence of the phenotype might be underpinned by some regulatory mechanism resulting in the differential modification, in the three treatments, of parameters defining the properties of the intracellular dynamics, e.g. the switching rates or the maximum concentration of the X metabolite. The quantitative fit of the experimental data will test these predictions (Section 3.5).

Qualitatively different transient variations of the phenotypic state

At the beginning of round 1, not only the proportion of capsulated cells differs among treatments, but the internal concentration (or its "physiological state") is also larger for later pre-cultures. This means that the initial switching rate towards capsulation will be higher the later is the pre-culture, thus providing the potential for an initial boost in the fraction of CAP+ cells. This effect is enhanced by the existence (or not) of a lag phase, whereby the deregulated production and accumulation of the compound X is not compensated by growth-induced dilution (Eq. 3.63). Qualitative different switching regimes can be therefore obtained, depending on whether the lag phase lasts enough for the internal concentration c to reach values for which the switching behaviour gets unbalanced toward the CAP+ state, and fast enough for its effect to be visible before the system reaches stationary phase.

In order for a gradual and slow increase in the CAP+ frequency to be observed, however, the concentration in exponential steady-state needs to be close to the lowest concentration for which bistability is possible, as to provide a corresponding equilibrium frequency that corresponds to the initial value f_{R0}^{LOW}. Indeed, for exponentially growing cultures remaining at steady-state also during dilution, the switching towards the capsulated state will not increase until cells approach stationary phase, and density-dependent effects start to displace the fast equilibrium.

On the contrary, older cultures, accumulating the intracellular compound during lag phase, will see a rapid, although temporary, increase in the probability of switching ot the capsulated state. Such increase will be larger (and thus the overshoot will be bigger), when the lag phase lasts longer, as occurs in "mid" and "late" cultures (Fig. 3.15).

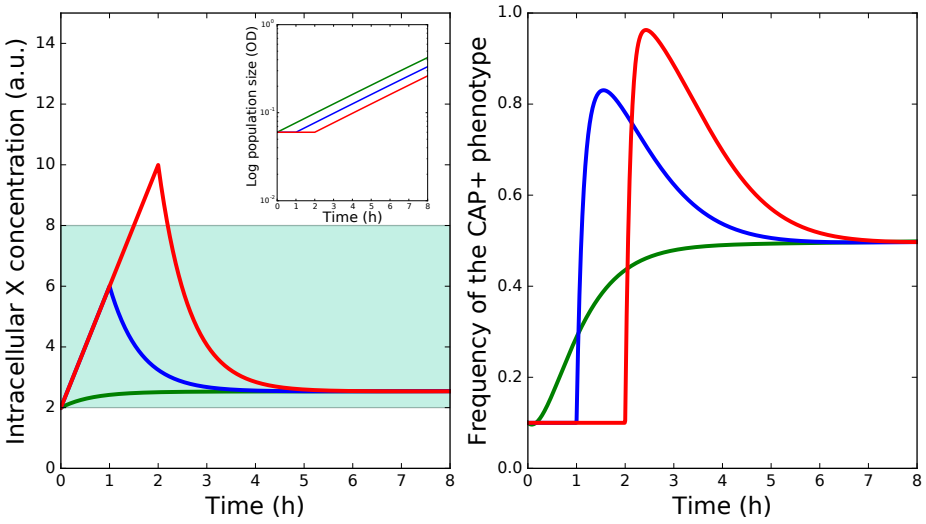

Figure 3.15: Differential duration of the lag phase affects the transient intracellular dynamics (left panel) and the corresponding of the CAP+ frequency dynamics in exponential phase (right panel). Green curves: $\tau = 0$; blue curves: $\tau = 1$; red curves: $\tau = 2$. Other parameters: $r = 0.25$, $K = 8$, $c_{R0} = 2$, $\alpha_+^{MAX} = 8$, $\alpha_-^{MAX} = 4$, $b = 3$, $K_c = 3$, $c_{LOW} = 2$, $c_{HIGH} = 8$.

Overshoot and exponential phase (quasi-)equilibrium

In the previous paragraphs I discussed the relationship between the values of some of the parameters and the qualitatively different responses that can be obtained from the mathematical model.

One of the most striking observations done on *Pseudomonas fluorescens* switchers was the (treatment-dependent) non-monotonic dynamics in the frequency of the capsulated phenotype f, characterized by an "overshoot" (i.e. a positive difference between the final frequency at the end of round 1 f_S^* and the maximum of the dynamics) in two out of the three treatments.

In the mathematical model, the non-monotonic dynamics of the frequency of the CAP+ frequency is the result of a similar non-monotonic intracellular dynamics (Eq. 3.63). During the lag phase at the beginning of round 1, the production term gets deregulated, which provides a mechanism of fast variation of the switching rates α_+ and α_-. Figure 3.16 shows the intracellular and phenotypic dynamics of two populations differing only in terms of the ratio between maximum switching rates $\alpha_+^{MAX}/\alpha_-^{MAX}$: the higher is this ratio, the higher get both the maximum CAP+ frequency reached and the succeeding quasi-steady value of the CAP+ frequency in exponential phase f_E^*.

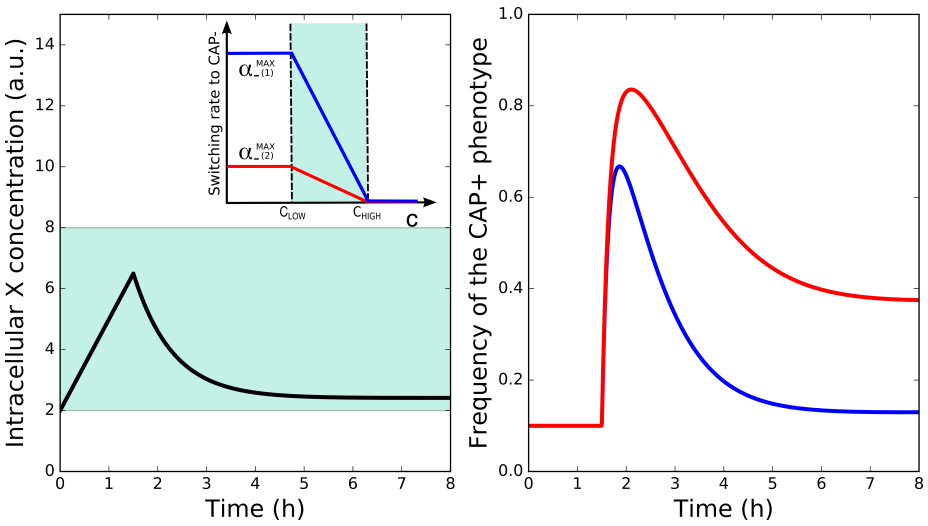

Figure 3.16: Higher $\alpha_+^{MAX}/\alpha_-^{MAX}$ ratios (left panel, inset) result in higher maxima in the CAP+ frequency in round 1 and higher quasi-steady equilibria for the frequency of CAP+ in exponential phase (right panel), without affecting the intracellular dynamics (left panel). Blue curves: $\alpha_-^{MAX} = 4$; red curves: $\alpha_-^{MAX} = 1$. Other parameters: $r = 0.25$, $K = 8$, $\tau = 1.5$, $c_{R0} = 2$, $\alpha_+^{MAX} = 8$, $b = 3$, $K_c = 3$, $c_{LOW} = 2$, $c_{HIGH} = 8$.

Undershoot

The undershoot in the phenotypic dynamics is defined by the difference between the stationary phase final value of the frequency f_S^* and the quasi-steady state in exponential phase:

$$f_S^* - f_E^* = f(c_S^*) - f(c_E^*) \tag{3.82}$$

which, given Eqs. 3.69 and 3.73, yields:

$$f_S^* - f_E^* = \left[1 + \frac{\alpha_-^{MAX}}{\alpha_+^{MAX}} \frac{(c_{HIGH} - K_c)}{(K_c - c_{LOW})}\right]^{-1} - \left[1 + \frac{\alpha_-^{MAX}}{\alpha_+^{MAX}} \frac{\left(c_{HIGH} - \frac{bK_c}{b+\rho K_c}\right)}{\left(\frac{bK_c}{b+\rho K_c} - c_{LOW}\right)}\right]^{-1}. \tag{3.83}$$

In other words, an undershoot following the overshoot can be obtained provided that the final intracellular concentration $c_S^* = K_c$ is higher than the exponential phase quasi-steady state $c_E^* = \frac{1}{\frac{1}{K_c} + \frac{r}{b}}$. Indeed, as the population keeps growing exponentially on a time scale longer than the duration of the overshoot, the frequency of capsulated cells will eventually converge towards its exponential steady-state. The approach to this limit will be then interrupted by the growth slowdown, whose effect through dilution will eventually become prevalent, thus causing the frequency to increase again.

Therefore, two populations identical in their initial conditions of round 1 and in their maximum capacity in terms of concentration of X K_c may present undershoots of different magnitude if the ratio between the average growth rate in exponential phase ρ and the production rate b are different 3.17.

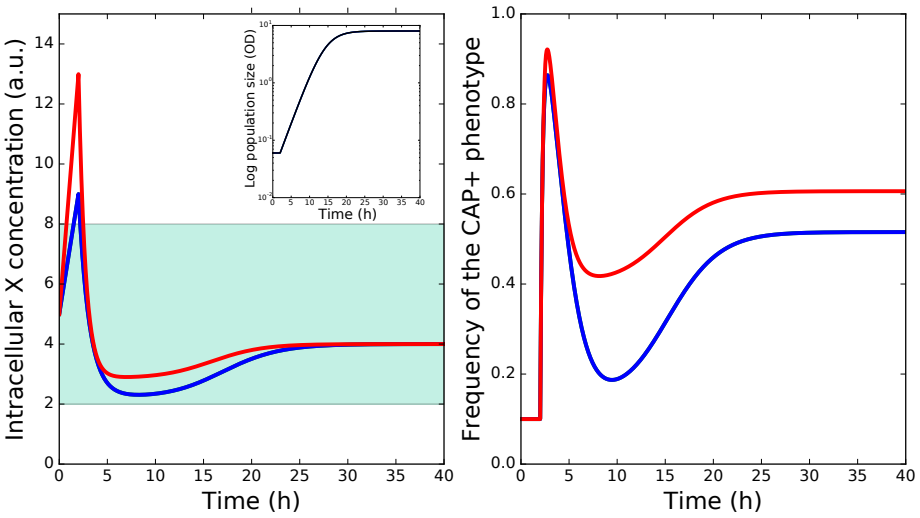

Figure 3.17: The ratio between the rate of production of b and the maximum growth rate ρ affects the balance between production and dilution (left panel), resulting in different depths of the undershoot in the phenotypic dynamics in round 1 (right panel). Blue curves: $b = 2$; red curves: $b = 4$. Other parameters: $r = 0.4$, $K = 8$, $\tau = 2$, $c_{R0} = 5$, $\alpha_+^{MAX} = 4$, $\alpha\_MAX = 1$, $K_c = 4$, $c_{LOW} = 2$, $c_{HIGH} = 8$. In the "switch at birth" hypothesis, the lower the ρ/b ratio, the higher the final frequency at the end of round 1.

The difference in the final CAP+ frequency in Figure 3.17, not predicted by Eq. 3.83 if all other parameters are constant, is due to the logistic factor dampening the switching rates as population approaches stationary phase ("switch at birth" hypothesis). By removing the logistic factor in the ODE for the temporal evolution of the frequency of the CAP+ phenotype (Eq. 3.62), therefore allowing the switching rates

to share the same value for the same intracellular concentration c irrespective of the population size $N(t)$, the two populations actually reach the same final stationary phase equilibrium (Fig. 3.18).

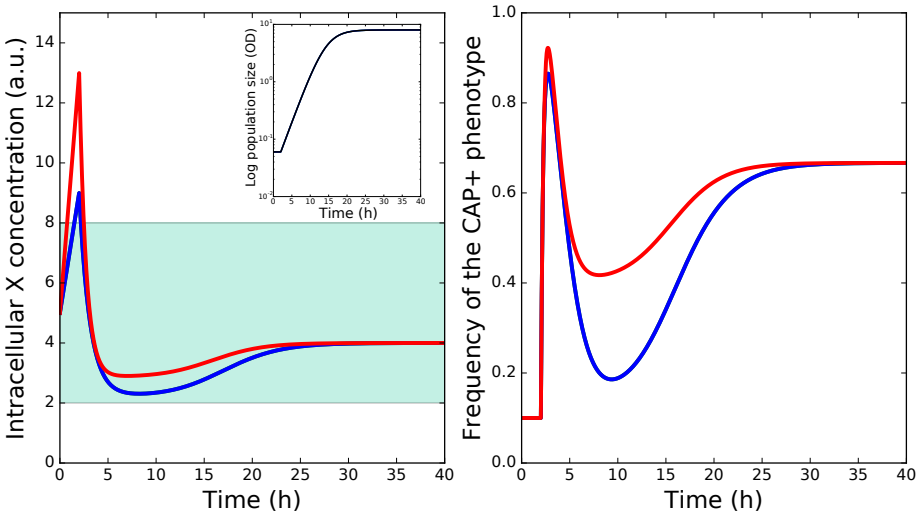

Figure 3.18: The ratio between the rate of production of b and the maximum growth rate ρ affects the balance between production and dilution (left panel), resulting in different depths of the undershoot in the phenotypic dynamics in round 1 (right panel). In the "switch at any time" hypothesis, the final frequency at the end of round 1 is independent of ρ/b. Blue curves: $b = 2$; red curves: $b = 4$. Other parameters: $r = 0.4$, $K = 8$, $\tau = 2$, $c_{R0} = 5$, $\alpha_+^{MAX} = 4$, $\alpha\_MAX = 1$, $K_c = 4$, $c_{LOW} = 2$, $c_{HIGH} = 8$.

In the next Section, the results of the overshoot experiment will be analyzed quantitatively, so to inform the mathematical model with quantitative values for the measurable parameters (the average growth rate of the populations ρ and the duration of the lag period at the beginning of round 1 τ). Since the experimental measures are not sufficient to fully parametrize the system, I will discuss the results of the quantitative fit of the model on the experimental data of the overshoot experiment (Section 3.5).

3.4.3 Estimate of the measurable parameters

The data from the overshoot experiment can be used to inform the 3-D mathematical model, in the form presented in Section 3.3.4. Indeed, the value of some of the parameters for each one of the three initial conditions ("low", "mid", "high" population density at the end of round 0) can be obtained from the growth curves of round 1: this is the case of the average growth rate in exponential phase ρ and the lag phase duration τ.

Instead, other parameters (e.g. the production rate b, the maximum switching rates α_+^{MAX} and α_-^{MAX}, the maximum X concentration K_c) are inaccessible through direct or indirect measurements and their values will thus be fitted (next Section). This reflects the nature of the additional state variable added to couple demography and phenotypic dynamics: c, the internal concentration of X, is a "hidden variable"

working as a proxy for the cell response to the ensemble of the environmental cues determining its phenotype. Since the hypothetical compound X has not yet been identified (beside the fact that it does not need to correspond to an actual concentration at all), its value cannot be measured.

For the average growth rate in exponential phase ρ, an exponential fit was performed on the first six time points (from 0 to 540 minutes after resuspension into fresh medium) of the mean growth curves for each of the three preculture conditions (Table 3.3). The mean value of the exponential phase growth rate $\bar{\rho}$ over the three treatments and its standard error can be computed:

$$\bar{\rho} = (0.45 \pm 0.02)\ \mathrm{h}^{-1}. \tag{3.84}$$

The very small variance associated with the mean growth rate $\bar{\rho}$ suggests that (1) the preculture difference does not generate an important difference in the average growth rate in exponential phase, and (2) there cannot be a very high growth rate difference between CAP+ and CAP-. For these reasons, I attribute the fitted value of ρ to the parameter r of the 3-D mathematical model.

Preculture	**Growth rate ρ (h^{-1})**	R^2
low (final $OD_{R0} = 0.3$)	0.45 ± 0.02	0.993
mid (final $OD_{R0} = 1.0$)	0.45 ± 0.02	0.993
high (final $OD_{R0} = 1.5$)	0.44 ± 0.02	0.995

Table 3.3: Results of the exponential fit of the growth curves in the overshoot experiment. Only the first 6 time points (from $t = 0$ to $t = 540'$ after resuspension), corresponding to the early exponential phase, are taken into account. The exponential fit provides a very good agreement with data for all three preculture conditions, as shown by the coefficient of determination R^2.

By comparison of the intercept of the exponential fit of the growth curves, it is possible to compute the duration of the lag period. The optical density at the beginning of round 1 is set to the value of 0.05 through dilution: any variation of the optical density extrapolated at the beginning of round 1, OD_0, from this value involves a deviation from fully exponential growth at the beginning of round 1, likely due to the lag phase. The duration of such lag can then be computed by evaluating the time at

Preculture	**Fitted $\mathbf{OD_0}$**	**Lag duration τ (h)**
low (final $OD_{R0} = 0.3$)	0.066 ± 0.002	0
mid (final $OD_{R0} = 1.0$)	0.059 ± 0.002	0.24 ± 0.03
high (final $OD_{R0} = 1.5$)	0.056 ± 0.002	0.35 ± 0.03

Table 3.4: Duration of the lag phase computed from the difference between the fitted initial optical density and the actual, imposed initial value (0.05). The computation permits an estimate of the time when exponential growth is resumed relative to the quickest population to resume exponential growth (the "low" treatment), whose lag phase duration is set to zero.

which the population should have had an optical density equal to 0.05. Results in Table 3.4 show that the "low" preculture condition has a higher fitted OD_0 with respect to that of the "mid" one, which in turn is higher than that of the "high" population. This is the order we expected: populations experiencing more advanced stages of growth take longer to restore their exponential growth after resuspension into fresh medium.

3.5 Quantitative fit of the free parameters

In the previous Sections I showed that the 3-D mathematical model reproduces the main features of the demographic and phenotypic dynamics of the overshoot experiment (Section 3.4.2). In this Section, I address the possibility of obtaining a quantitative fit of the experimental data (Section 3.5.1), and discuss how relaxing some hypotheses of the mathematical model affects its fitting power (Section 3.5.2).

The fitting method consisted in finding the best combination of the free parameters (the production rate b, the maximum internal concentration K_c, the maximum switching rates α_+^{MAX} and α_-^{MAX}) and initial conditions for round 0 (number of cells and frequency of the CAP+ phenotype at the beginning of the preculture stage) corresponding to the minimum deviation between the experimental data and the curve predicted by the model.

The original goal was to fit the trajectories of all the three treatments with the same set of parameters, but once noticed that, in that way, it was impossible to obtain differences in the final population composition comparable to those observed in the experiments, I decided to fit independently the data relative to different treatments, and to examine later which of the best fit parameters were similar or different across treatments.

To all non-free parameters (the optical density at which the three populations were sampled in round 0, the bottleneck size, the lag phase duration τ, the average growth rate in exponential phase ρ) I attributed the values estimated as explained in Section 3.4.3. Since the units of the intracellular concentration c is arbitrary, one of the parameters c_{LOW} can be set to an arbitrary value. In the following, for the sake of a greater efficiency in the fit procedure, c_{HIGH} is fixed as well.

The two-rounds system was simulated and fitted through Python routines for minimizing mean-square distance from the measured trajectories (for further details see Chapter 2).

3.5.1 Results of the fit

A preliminary run of the fit showed that the least variable parameter in the fit was the maximum switching rate to the CAP- state α_-^{MAX}. In order to speed up the fit, I decided to fix it to a value close to the optimal ones, and checked numerically that small changes in such value did not significantly alter the behaviour of the system.

The impossibility of fitting the three phenotypic dynamics with a common set of parameters indicates that, although the model qualitatively recapitulates the behaviour of the system, more biological detail should be implemented to get a complete, consistent description of the overshoot phenomenology. Nonetheless, if the

rationales of this model are correct, some intuitions about the mechanisms underpinning the switch may be obtained through the comparison of the fitted values of the parameters across the three preculture treatments, summarized in Table 3.5. The simulation of the dynamical system informed with these values of the free parameters is shown in Figure 3.19 (only round 1 presented).

Preculture	α_+^{MAX} **(h^{-1})**	α_-^{MAX} **(h^{-1})**	b **(h^{-1})**	K_c **(a.u.)**
low	2.7 ± 0.4	0.60 ± 0.07	11.9 ± 0.7	0.831 ± 0.002
mid	4.6 ± 0.6	0.60 ± 0.06	11.6 ± 1.7	0.830 ± 0.003
high	6.3 ± 0.8	0.60 ± 0.08	11.9 ± 2.2	0.833 ± 0.004

Table 3.5: The best fit parameters corresponding to the least sum of the squared residuals for each treatment. Other (arbitrarily fixed or measured) parameters: $\rho = 0.45$ h^{-1}, $K = 8$, $\tau_{low} = 0$, $\tau_{mid} = 0.24$ h, $\tau_{high} = 0.3$ h, $c_{LOW} = 0.8$, $c_{HIGH} = 1.6$.

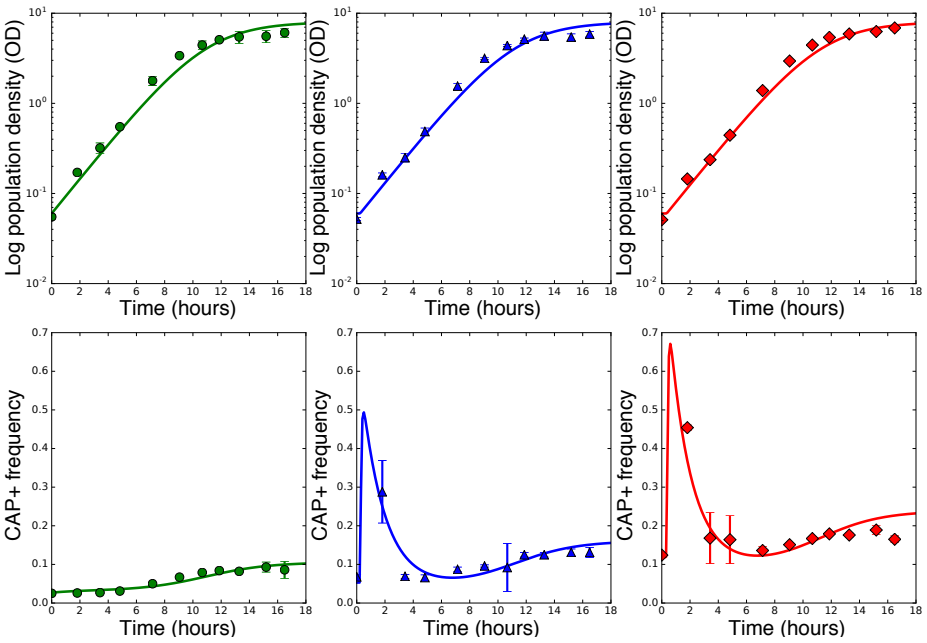

Figure 3.19: Best fit of the demographic (top row) and phenotypic dynamics (bottom row) in round 1 for the three preculture conditions ("low", left column; "mid", central column; "high", right column).

The model quantitatively reproduces the experimental measures. With this set of parameters the demographic dynamics is best fitted in early exponential phase and towards the end of the experiment, while population size is underestimated in late exponential phase. In Section 3.5.2 this aspect will be further discussed as a possible effect of a growth rate difference between CAP+ and CAP-.

Unlike α_-^{MAX}, the maximum switching rate to the CAP+ state α_+^{MAX} has to significantly differ across the three treatments to obtain their different trajectories. The

results of the fit propose values of α_+^{MAX} increasing with the final density reached by the preculture in round 0, suggesting that, if the model grasps the main mechanism at the basis of the capsulation switch, differences in the preculture growth regime likely affect the rate of switch to the CAP+ state more than that to the CAP-.

The intracellular dynamics, which links the demographic and the phenotypic ones through the "hidden" variable c, is at this stage inaccessible to direct experimental investigations. The results of the fit, however, suggest that neither the instantaneous rate of synthesis of X b, nor the maximum concentration of X K_c, need to vary much to account for the different phenotypic dynamics in the three treatments.

The role of K_c and of the rapid accumulation of X within the duration of the lag phase τ can be better appreciated in Figure 3.20, representing the dynamics of the system soon after the beginning of round 1 (lag and early exponential phases of growth). In the "low" treatment, a very short (or inexistent) lag phase prevents the internal concentration of X from crossing the c_{HIGH} threshold associated to a maximal switching rate to the CAP+ state and a switching rate to the CAP- state equalling zero. In the "mid" and "high" treatments, on the other hand, the concentration of X increases linearly with rate b during lag, before relaxing to its maximum allowed value K_c soon after exponential growth is resumed.

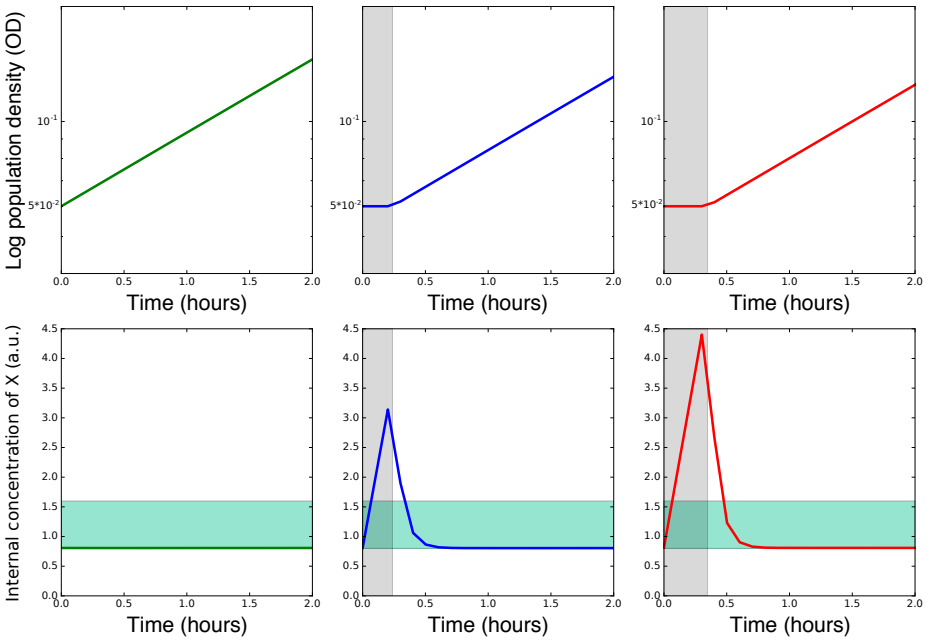

Figure 3.20: Demographic (top row) and intracellular dynamics (bottom row) at the beginning of round 1 for the three preculture treatments ("low", left column; "mid", central column; "high", right column). The horizonthal green band corresponds to the concentration range associated to bistability $[c_{LOW}, c_{HIGH}]$, wherein both switching rates are non-zero. The vertical grey band corresponds, for the "mid" and "high" populations, to the lag phase.

Just as discussed in Section 3.4.2, K_c has to be slightly higher than the threshold c_{LOW} to let f reach an appropriate quasi-steady state in later phases of the dynamics, and the differential lag phase duration explains the difference in the transient pheno-

typic dynamics between the "mid" and the "high" conditions in terms of the overshoot magnitude during early exponential phase.

3.5.2 Relaxation of some modelling assumptions

The three-dimensional model studied in the previous paragraphs was based on several assumptions. On the one hand, such working hypotheses made the model more tractable; on the other, some of them might have reduced the possibilities of a better agreement between the model and the experimental observations. In this Section, I address the robustness of my results when some of these assumptions are relaxed.

Decoupling of cell cycle and switch

As discussed in Section 3.3.3, in my mathematical model the switching terms are weighed by a density dependence term $(1–N/K)$ corresponding to the hypothesis that the switch only happens during specific phases of the cell cycle (e.g. at cell division), whereas cells do not switch when not dividing. By removing this factor from Equation 3.62, the phenotypic dynamics is described by:

$$\dot{f} = [\alpha_+(c)(1-f) - \alpha_-(c)f]\,\theta(t-\tau). \tag{3.85}$$

In this case, the arrest in the demographic dynamics taking place when population size reaches the carrying capacity does not prevent the system from reaching the steady-state in the phenotypic composition given by Equation 3.81 once the intracellular dynamics has relaxed to $c_S^* = K_c$.

In Figure 3.21 a comparison between these alternative hypotheses ("switch at birth" and "switch at any time") is shown, using the set of parameters that best fitted the "mid" treatment of the overshoot experiment. Coupling switch to cell division dampens the magnitude of CAP+ frequency increase at the entrance of stationary phase, without any change in the earlier dynamics (i.e. the overshoot). Density-dependence of the switch thus allows to better reproduce the levelling-off of f that occurs as the population enters stationary phase (Fig. 3.19).

Nonlinear switching rates

The switching rates were chosen as stepwise-linear functions of the intracellular concentration c, corresponding to the relative extension of the basins of attraction of the alternative stable equilibria in a Z-shaped bifurcation diagram (Section 3.3.1). However, the generic shape of the bifurcation diagram of a bistable dynamical system is rather S-shaped, whereby the bistability region is bounded by two fold bifurcations of the equilibria. In this case, the switching rates are expected to depend nonlinearly from the concentration c, and thus possibly alter the phenotypic dynamics, especially when the system approaches the thresholds of the bistability region $[c_{LOW}, c_{HIGH}]$.

I compared the phenotypic dynamics obtained in the previous Section (best fit for the "mid" treatment of the overshoot experiment) with the one obtained by replacing the stepwise-linear switching rates with stepwise-exponential ones characterized by infinite absolute values of their derivatives at $c = c_{LOW}$ and $c = c_{HIGH}$ (Fig. 3.22).

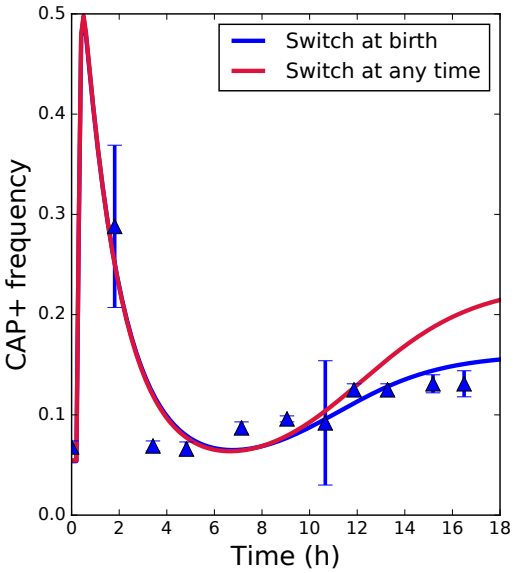

Figure 3.21: Comparison between the phenotypic dynamics in round 1 generated by the 3-D model under the alternative hypotheses "switch at birth" and "switch at any time". The values of the parameters are chosen according to the best fit of the "mid" treatment of the overshoot experiment (Tab. 3.5).

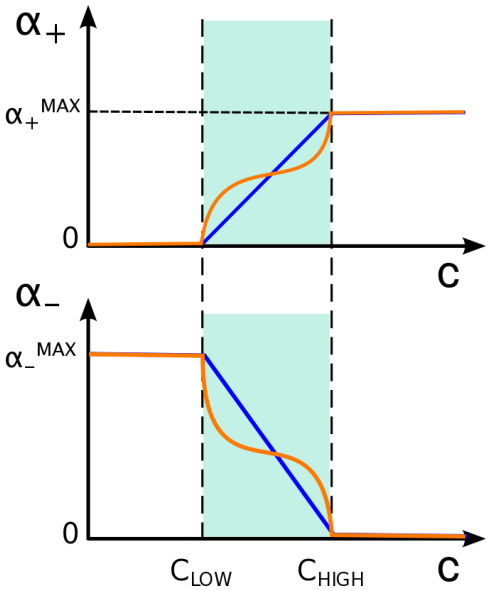

Figure 3.22: Linear vs nonlinear switching rates as functions of the internal concentration c (blue and orange lines, respectively). In both cases, switching rates are defined as piecewise functions, to allow them to be both nonzero only for values of c belonging to the bistability region $[c_{LOW}, c_{HIGH}]$, corresponding to CAP+ and CAP- coexistence. A very extreme instance of nonlinearity is chosen, that is piecewise-exponential functions with the maxima of derivatives near the boundaries of the region of coexistence. This way, small deviations of c near the boundaries yield very high switching rate variations, which should push the system to sudden transitions.

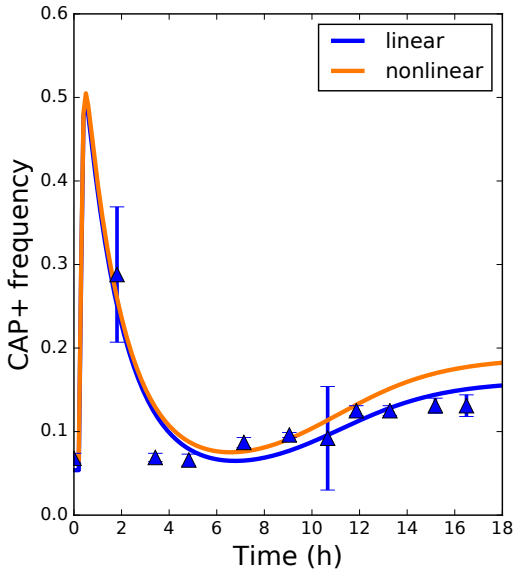

Figure 3.23: Comparison between the phenotypic dynamics in round 1 generated by the 3-D model with linear and nonlinear switching rates (blue and orange lines, respectively). The values of the parameters are chosen according to the best fit of the "mid" treatment of the overshoot experiment (Tab. 3.5).

Results are shown in Figure 3.23: no major change in the dynamics of the frequency of CAP+ in the population was obtained. As expected, the difference between the two can be better appreciated during the undershoot, that is when the internal concentration c relaxes to its quasi-steady state (slightly higher than c_{LOW}) and thus where the effects of the nonlinearities are maximal.

3.6 Effect of growth rate on phenotypic diversity in exponential phase

The mathematical model presented in this Chapter satisfactorily describes the transient dynamics of the phenotypic composition of a population of *Pseudomonas fluorescens* cells performing the capsulation phenotypic switch. I now aim to verify its validity and predictive power on a different problem, that is the link between CAP+ expression and growth rate. Indeed, the fundamental hypothesis on the context-dependence of phenotypic switchers is that the rate of phenotypic change depends on cell growth. Beside the case when it is affected by population demography, growth might be altered in different manners, while maintaining the population in the same demographic regime. For instance, it is known that different genetic backgrounds or different environmental conditions correspond to different growth rates in exponential phase.

As I will more extensively treat in the next Chapter, Section 4.1.2, a statistically significant negative correlation can be observed between the fraction of capsulated cells in a population of switchers and the mean growth rate of the population, when these two quantities are measured in the exponential regime of growth.

In this Section, I address the question: Do the theoretical models presented in this Chapter predict an explicit mutual dependence between the phenotypic composition of the population and the rate of population growth? And do the predictions account

for the negative correlation between these two quantities?

The first two null models of Section 3.2 ("pure switch" and "differential growth") did not predict any kind of mutual dependence between the CAP+ frequency and the mean growth rate of the population, while the third one ("constant switching rates with growth rate difference") predicted that the equilibrium frequency of the CAP+ phenotype in the population depended on the mean growth rate of the population following Equation 3.35, which can be rewritten as:

$$f^* = \left[1 + \frac{\alpha_-}{\alpha_+ + \rho - r_-}\right]^{-1}, \tag{3.86}$$

suggesting that higher values of the mean growth rate ρ would correspond to higher values of the frequency of CAP+ at equilibrium f^* (Fig. 3.24, left panel).

On the other hand, the 3-D mathematical model of context-dependent phenotypic switch of Section 3.3 provides a formula linking the exponential phase quasi-equilibrium for the CAP+ frequency in exponential phase f_E^* and the maximum growth rate ρ:

$$f_E^* = \left[1 + \frac{\alpha_-^{MAX}}{\alpha_+^{MAX}} \frac{c_{HIGH} - \frac{1}{\frac{1}{K_c} + \frac{\rho}{b}}}{\frac{1}{\frac{1}{K_c} + \frac{\rho}{b}} - c_{LOW}}\right]^{-1}. \tag{3.87}$$

By plotting the expected fraction of CAP+ cells during exponential phase f_E^* against the effective parameter $\frac{\rho}{b}$ (the ratio between the average growth rate and the maximum rate of production of the X metabolite) and using in Equation 3.87 the values of the parameters corresponding to the best fit (Section 3.5.1), it can observed that the relation is in this case qualitatively opposite with respect to that previously predicted by the third null model: the higher the mean growth rate ρ, the lower the equilibrium frequency of CAP+ f^* (Fig. 3.24, right panel).

In the next Chapter, I present my experimental tests on the topic: indeed, by disposing of a number of genetically different mutants all displaying switching between the CAP+ and CAP- phenotypes obtained by re-playing the evolutionary experiment in Beaumont et al. [11] (Chapter 1, Section 1.3.2), I can measure their maximum growth rate and frequency of the CAP+ in full exponential phase. Later in the next Chapter, I present experimental evidence of a negative correlation between the two quantities, and investigate whether Equation 3.87 predicts the right degree of variability in the CAP+ frequency when I manipulate the mean growth rate ρ by changing the switching genotype or by controlling the temperature of the environment.

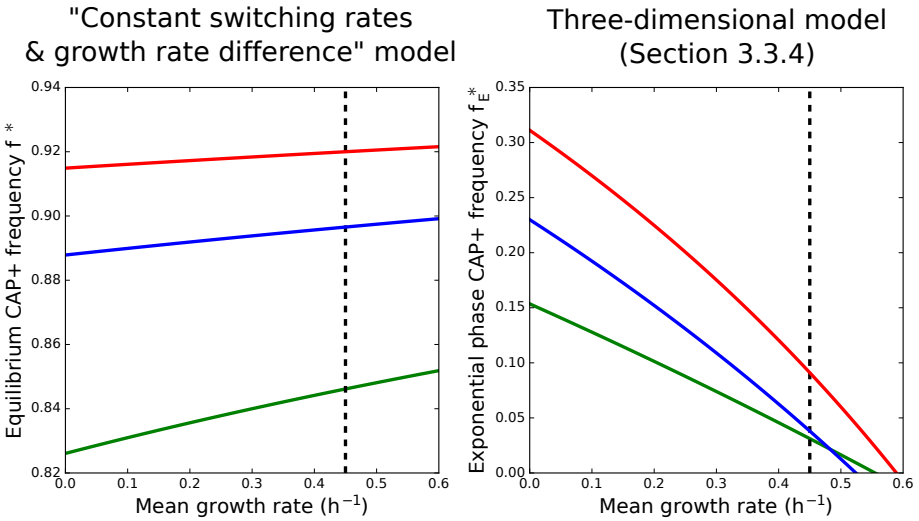

Figure 3.24: Correlation between the CAP+ frequency and the mean growth rate in exponential phase as predicted by the "constant switching rates with growth rate difference" (left panel) and by the three-dimensional (right panel) models. The two models predict the correlation to assume opposite sign. Colors correspond to the three treatments of the overshoot experiment, each obtained by informing Eqs. 3.86 and 3.87 with the corresponding parameters obtained providing the best fit of the demographic and phenotypic dynamics of the overshoot experiment (Table 3.5). The intersection between each curve and the vertical, dashed black straight line corresponding to the fitted value of ρ gives the expected equilibrium fraction of CAP+ during exponential phase.

3.7 Summary of the results and biological interpretation

The relevance of the bidirectional switch in *Pseudomonas fluorescens* switchers resides in being context-dependent. Indeed, along a normal population growth trajectory, the percentage of cells expressing the CAP+ phenotype changes dramatically in time if the preculture is sampled sufficiently close to the stationary state.

Models wherein the switch is context-independent do not encompass such a behaviour, while the 3-D model introduced in this work, where temporal variations in the intracellular concentration of a generic metabolite "translate" differential growth regimes in switching rates modulations, can reproduce the observed dynamics of the phenotypic composition of the population.

The qualitative difference between populations replicated from different preculture treatments and the extent of the overshoot and undershoot can be interpreted as the effect of intracellular dynamics being influenced by growth rate through dilution. The closer to stationary phase the cells get to during the preculture stage (round 0), the longer the lag period at resuspension (beginning of round 1), and the higher the concentration of X and its rate of increase at the beginning of round 1, ultimately causing cells to massively switch to the CAP+ state. On the other hand, cultures that are maintained in exponential phase maintain their phenotypic composition until they

reach stationary phase.

A quantitative comparison between data and model was performed, and it was found that the three trajectories corresponding to the three preculture treatments could not be fitted with just one set of parameters. This suggests that precultures at different stages of growth may be composed of cells that, beside having experienced different demographic histories, are characterized by different patterns of gene regulation related to the switching behaviour. The parameters that most vary among the different treatments are the duration of the lag period τ (measured), and the switching rate to the CAP+ state α_+^{MAX} (fitted). On the contrary, the preculture conditions seem not to have a strong influence on the growth rate in exponential phase, which might be a purely genotypic-driven observable, nor on the maximum switching rate to the CAP- phenotype α_-^{MAX}.

The trans-generational persistence of the levels of expression of CAP+ in the population (i.e. the fact that the difference in phenotypic composition at the beginning of round 1 is conserved across several generations, until the end of round 1) cannot be quantitatively explained only in terms of different initial conditions, but it seems to be mediated by the CAP- to CAP+ maximum switching rate α_+^{MAX}: the longer the preculture round, the higher the switching rate α_+^{MAX}.

Possible physiological basis of the parameter variation

During the course of the thesis, further work on the physiology and molecular underpinnings of the switching strains was realized in Paul Rainey's lab by Dr. Philippe Remigi, Dr. Gayle Ferguson (unpublished data). In their view, switchers have a misregulated production of ribosomes, that would be in particular up-regulated upon entering the stationary phase of growth. High ribosome levels would compete with RmsA/E genes for the translation of a positive regulator of capsule biosynthesis. Such gene, named "A", would encode for a protein whose concentration is responsible for the bistability in capsule expression.

One possible interpretation provided our model is that the product of gene "A", which triggers the switching behaviour via a threshold mechanism, is described by the concentration c of the product X. GFP fluorescence would measure, in experiments such that presented above, the translation of A (or X).

On the other hand, the model does not deal with more detailed levels of description, like the quantification of the concentration of ribosomes or that of the post-transcriptional repression of gene A by RsmA/E. Instead, I make use of growth rate as a proxy for the ensemble of the regulations acting on A (like the ratio between the concentration of ribosomes and that of RmsA/E). This choice allows me to simplify the description of the dynamics observed in the overshoot experiment.

The parameter b represents the maximum rate of production of X by the cell. In the mathematical model the intracellular concentration of X saturates (with the exception of the lag phase) to a maximum value K_c which represents the maximum amount of protein X that the cell can produce and store. This term encompasses all the possible regulations that control the maximum level of X. During lag, I suppose such a regulation is relieved, allowing c to get to values greater than K_c.

One can imagine that, as the concentration of ribosomes in the cell gets higher in older cultures, the production term, determining the accumulation of X after cells are diluted, increases too. If the growth rate is unaffected, the effect of having a higher ribosomal concentration may result in an increase of b and/or K_c: more ribosomes could make the maximum translation rate higher and/or to allow the cell to store more units of protein A/X. I modelled the second scenario but the first should be explored as well in future work.

Finally, it seems reasonable that, if it has a direct effect on the switching behaviour, the concentration of ribosomes should more likely affect the α_+^{MAX} rate, rather than the α_-^{MAX}. Indeed, α_+^{MAX} is related to the synthesis of huge amount of cellulose, whereas α_-^{MAX} is more dependent on degradation, which is not performed by ribosomes.

Conclusions

The three-dimensional mathematical model introduced here qualitatively reproduces the non-monotonic dynamics of the frequency of the capsulated phenotype. The model also fits quantitatively the transient behaviour, but in order to account for all the differences among preculture conditions ("low", "mid", "high"), each of such treatments needs to have different parameters, notably in terms of the maximal rate of switching α_+^{MAX}. The model moreover predicts a negative correlation between the average growth rate of the population and the frequency of the CAP+ phenotype, with the correlation coefficient depending on the microscopic parameters.

The experimental tests of this prediction will be the main focus of Chapter 4. In Section 4.1, I present my experimental results on the negative correlation between the level of expression of the CAP+ phenotype in the population and the growth rate of the population in exponential phase. Section 4.2 is dedicated to compare the model prediction with the measured variability in CAP+ frequency across strains and for the same strain at different temperatures. Finally, in Section 4.3, I propose a biologically reasonable further hypothesis on the switching rates, which allows to improve the fitting power of the model on the growth-capsulation data.

CHAPTER 4

THE ROLE OF GROWTH RATE IN *P. FLUORESCENS* SWITCHING DYNAMICS

Linking growth rate and switching through internal concentrations, the mathematical model presented in Chapter 3 succeeds in reproducing the phenotypic dynamics of *Pseudomonas fluorescens* "switchers" populations. The model predicts moreover the existence of quasi-equilibria of the CAP+ frequency in exponential phase, for which it offers a predictive formula where the quasi-equilibrium directly decreases with the mean growth rate of the population.

This Chapter tackles the following questions:

1. Do variations in the mean growth rate of *Pseudomonas fluorescens* populations influence the degree of phenotypic heterogeneity in exponential phase?

2. Does the mathematical model quantitatively predict the CAP+ frequency in exponential phase as a function of mean growth rate?

In this Chapter I present the results of experimental assays aimed at answering these questions: a negative correlation between the mean CAP+ frequency in exponential phase and the mean growth rate of the population is indeed obtained – both by testing different genotypes characterized by different mean growth rate and by controlling the growth rate through culture temperature (Section 4.1).

Even though the experimental protocol has to be refined in order to obtain more reliable statistics, my observations point to a quantitative mismatch with the predictions of the model, based on growth rate as an independent control parameter. When informing the aforementioned predictive formula with the parameters of the best fit of the overshoot dynamics, we cannot account quantitatively for the measured CAP+ frequency – which appears to be larger than predicted. Such an underestimation of the CAP+ frequency in exponential phase suggests that the switching rates might be explicit functions of the mean growth rate (Section 4.2).

The correct relation can be indeed obtained by having the maximum switching rates scale with the mean growth rate in a way that is compatible with the hypothesis that such rates are affected by ribosomal differential concentration between CAP+ and CAP- (Section 4.3).

4.1 The CAP+ frequency negatively correlates with the mean growth rate

The goal of this Section is to answer the question: Do controlled variations in the mean growth rate of *Pseudomonas fluorescens* populations influence the degree of phenotypic heterogeneity in exponential phase?

Such an inquiry is indeed motivated by the fact that both a simple growth-and-switch null model (Chapter 3, Section 3.2.3) and the mathematical model conceived to reproduce and explain the history-dependent dynamics of the phenotypic composition of the population (Chapter 3, Section 3.3.5) forecast the CAP+ frequency to vary as a function of the mean growth rate.

In particular, for the "constant switching rate with growth rate difference" null model I obtained a positive linear relation between the CAP+ frequency equilibrium and the average growth rate (Eq. 3.35). The mathematical model describing the overshoot dynamics, on the other hand, provided a quantitative prediction for the CAP+ frequency during exponential phase f_E^* (Eq. 3.70), from which a negative nonlinear relation between mean growth rate and an exponential phase CAP+ frequency quasi-equilibrium follows.

In the following pages, experimental tests of the relationship between growth rate and degree of phenotypic heterogeneity in *Pseudomonas fluorescens* are presented, and their relation with the different mathematical models discussed. First of all, I show experimental evidence supporting the hypothesis that the main determinant of the growth rate in exponential phase is the genotype rather than the phenotype (Section 4.1.1). The mean growth rate can be therefore taken as the independent variable to compare the levels of CAP+ expression in exponential phase across the different switching genotypes, firstly grown in KB (Section 4.1.2) and then in KBS (Section 4.1.3). Finally, one switching strain (1w4xGFP) will be exposed to different culture temperatures to control the mean growth rate and the CAP+ frequency in exponential phase, which are both known to respond to temperature (Section 4.1.4).

4.1.1 The growth rate depends on the genotype

The mean growth rate of one *Pseudomonas fluorescens* switching population depends on the (*a priori*, different) division rates of its two phenotypes CAP+ and CAP- and on the phenotypic composition of the population. Time-lapse experiments allow to measure growth rate at the microcolony level while ideally tracking the exact phenotypic composition of the microcolony itself, which can provide another measure of the growth rate of the different *Pseudomonas fluorescens* switchers and should in principle yield to the determination of the eventual difference in the division time between CAP+ and CAP-.

In the following paragraphs, time-lapse measurements of the increase in the area of microcolonies founded by CAP+ or CAP- individuals are presented. For this analysis, only those microcolonies whose cells never displayed a switch to the CAP+ state are considered "-" microcolonies, while "+" microcolonies will be those founded by a CAP+ cell, without keeping exact track of the individual phenotype of all cells (which revealed to be impossible in our experimental setup due to experimental issues). An example of microcolony growth data is provided by Figure 4.1. Further details on the experimental and image analysis protocols can be found in Chapter 2, Section 2.2.2.

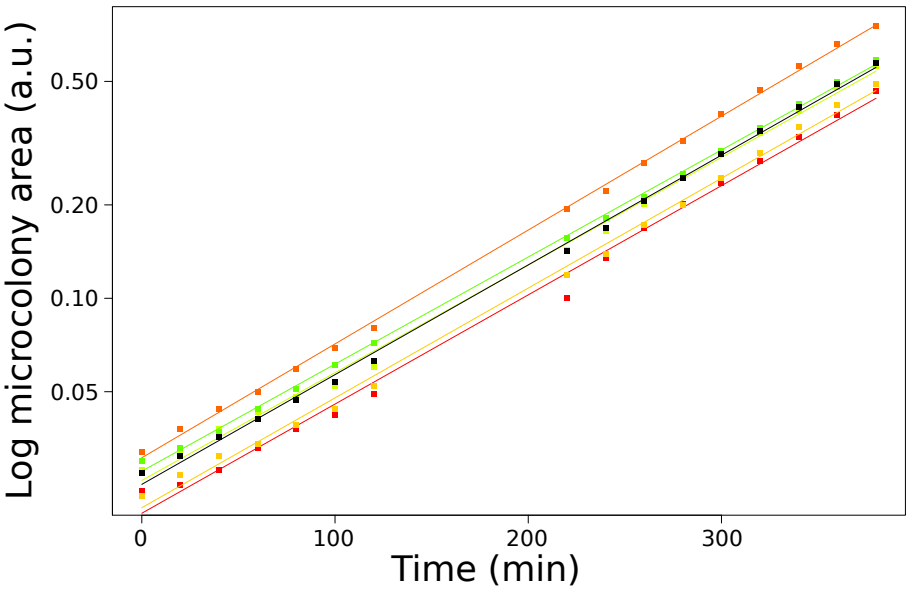

Figure 4.1: Example of microcolony growth data from a time-lapse experiments. Different colors represent different microcolonies monitored during the same experiment (in this case, five Re1.4xGFP microcolonies founded by CAP- cells). Solid lines are the exponential fit of data.

First, I compared "-" microcolonies (by far the most numerous) of strains 1w4xGFP, Re1.4xGFP, and Re1.5xGFP, the latter two being chosen because the fastest and the slowest growing in bulk, respectively. In Figure 4.2 it can be noticed that the expected order $\rho(Re1.4) < \rho(1w4) < \rho(Re1.5)$ is respected at the microcolony level, and on agar pad, too. The differences between the three strains are statistically significative (Table 4.1).

To understand whether the phenotype of the founding individual has an impact on the growth of *Pseudomonas fluorescens* colonies, time-lapse data about microcolonies started from either CAP+ or CAP- cells for the same genotype (Re1.4xGFP) were collected. Again (Figure 4.2 and Table 4.1), such microcolonies have a significantly different growth rate with respect to those of 1w4xGFP or Re1.5xGFP, but they are *not* significatively different from one another.

In conclusion, at least for the three strains here analysed, different switching genotypes show a significant difference in the mean growth rate on agar plates, too. In turn, a significative difference between the two phenotypes (CAP- and CAP+) of the same

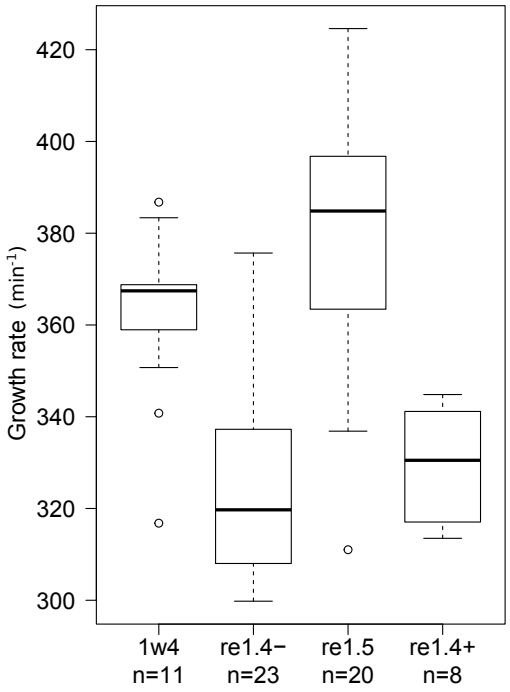

Figure 4.2: Distribution of the mean growth rate in exponential phase for three different "switchers" (1w4xGFP, Re1.4xGFP, Re1.5xGFP). Growth rate is measured by fitting the increase in the surface covered by microcolonies over time. For 1w4xGFP and Re1.5xGFP strains only microcolonies whose individual cells never expressed the CAP+ phenotype were taken in consideration, while Re1.4xGFP both "-" and "+" microcolonies could be observed. The number n of analysed microcolonies for each class is indicated.

	1w4 (-)	**Re1.4 (-)**	**Re1.5 (-)**
1w4 (-)	-	$1.1\ 10^{-4}$	0.043
Re1.4 (-)	-	-	$3.3\ 10^{-8}$
Re1.4 (+)	$3.9\ 10^{-4}$	0.67	$4.5\ 10^{-7}$

Table 4.1: Statistical significance of the difference in the exponential phase population growth rate between CAP- cells from 1w4xGFP, Re1.4xGFP and Re1.5xGFP, and CAP+ cells from Re1.4xGFP (P-values of the Student's t-test). The growth rate was measured as the rate of increase of the surface covered by micocolonies founded by one individual expressing the given phenotype. Differences between "-" microcolonies from the three different genotypes are statistically significant if the threshold is 5%. Re1.4xGFP "+" colonies are significantly different from those of 1w4xGFP and Re1.5xGFP "-", but not from Re1.4xGFP "-", i.e. from microcolonies founded by individuals of the same strain but expressing a different phenotype.

genotype (Re1.4xGFP) could not be appreciated. These results support the assumption that the division rate could be treated as a variable independent of the phenotype, and that, on the other hand, its main determinant is the genotype of the strain.

4.1.2 Switching genotypes differ in both growth and CAP+ expression

During a visit at Rainey Lab, Massey University (Auckland, New Zealand), I measured the growth rate in exponential phase for 1w4 and the other re-evolved switchers Re1.2, Re1.4, Re1.5, Re1.8, Re2, and Re12 (see Chapter 2, Section 2.2.2). By plotting such growth rates against previous measurements of CAP+ frequency in exponential phase performed by Jenna Gallie, I obtained a statistically significant negative correlation between these two quantities. The strains growing faster during exponential phase tend to have a lower percentage of CAP+ (Fig. 4.3).

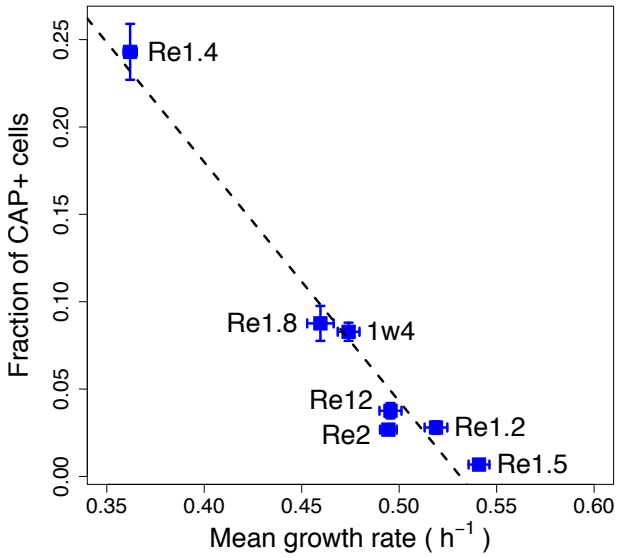

Figure 4.3: Mean growth rate and CAP+ frequency from seven switching genotypes growing in exponential phase in KB culture medium medium negatively correlate. Growth rates are computed by fitting optical density measurements obtained through an automated TiCan plate reader. CAP+ frequency measurements are those performed by Jenna Gallie and published for the first time in [41]. Each point corresponds to one of the seven different switching *Pseudomonas fluorescens* genotypes with the insertion of the *gfp* gene under the control of promoter of *CarAB* (1w4, and the six switchers re-evolved from 1w4 immediate precursor, see Chapter 2 for further details). Error bars on both dimensions correspond to standard error of the mean among replicate measures (growth measures: 3 replicates per strain; counting assays: 2500 cells per strain). Linear correlation coefficient $\rho = -0.981$, $P_{value} = 9.245\ 10^{-5}$.

The genetic transformation of the switchers (Chapter 2), paved the way to a more precise characterization of the *Pseudomonas fluorescens* CAP phenotypic switch: the frequency of the CAP+ state, now marked by the *gfp* gene, became measurable by flow cytometry, thus in a much higher throughput fashion than by the previous, laborious method consisting in staining cells with indian ink and then manualling counting the two phenotypes out of microscopy observations.

4.1.3 The culture medium affects both growth and CAP+ expression

By changing the amino acid source among the ingredients of the standard growth medium KB (King's B), Rainey and collaborators could induce a significant increase in the frequency of the CAP+ state across *Pseudomonas fluorescens* CAP switching populations when plated on agar plates. The new formula, called KBS ("King's B Switcher"), is the same culture medium used in the overshoot experiment (Chapter 3), and it differs from KB in that tryptone substitutes peptone III: although these compounds supply the same nutritional power, the switching behaviour appears to be different in the two media.

Growth rate measurements

To measure the switchers' exponential phase average growth rate in KBS, optical density was assayed in TiCan 96-plate reader, and the mean exponential phase growth rates obtained through exponential fit of the collected data. As an example, one growth curve for the 1w4 strain is shown in Figure 4.4.

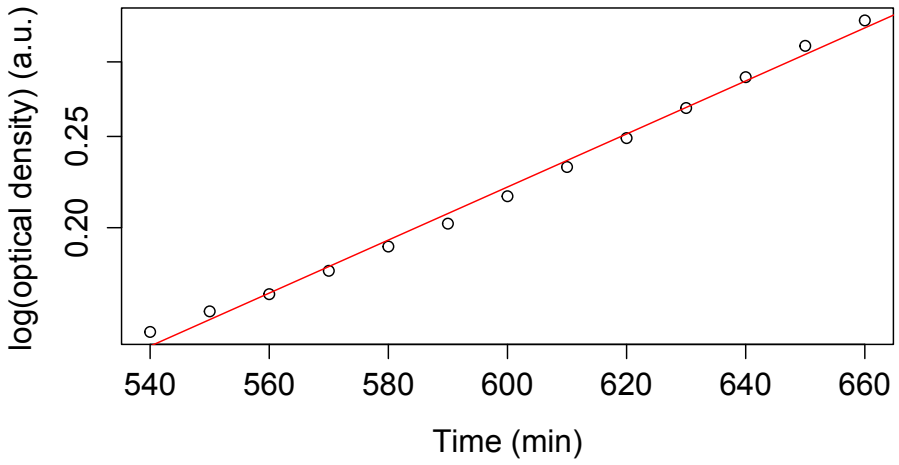

Figure 4.4: 1w4xGFP optical density data correspond to the expected exponential growth. Optical density (black circles) is measured by TiCan 96-plate reader (3 replicates per genotype, only one shown in figure). The exponential fit (red solid line) is performed on thirteen time points belonging to a time window of two hours, so to select the early exponential phase.

One non-GFP control (1w4) and the line 6 switching genotype with GFP insertion (6w4xGFP) were added to the pool of the assayed strains for these tests in KBS. The difference between every re-evolved switching genotype and its corresponding GFP version consists just in the insertion of the *gfp* gene downstream the *carAB* operon, under the control of its same promoter. Although it was shown that the response to external agents such as antibiotics can be different [4], the expression of the GFP protein only weakly affects growth rate in bacteria. Data support the evidence that the insertion of GFP slightly lowers the growth rate (*cf.* 1w4 vs 1w4xGFP in Table 4.2). The fastest growing strain (Re1.5xGFP) grows more than twice as fast as the slowest

one (Re1.4xGFP), as well as the fact that genotypes sharing the same switch-triggering mutation (1w4xGFP and Re1.8xGFP) present very similar growth rates.

	KB		KBS	
Strain	ρ **(OD h^{-1})**	$\bar{\sigma}_\rho$ **(OD h^{-1})**	ρ **(OD h^{-1})**	$\bar{\sigma}_\rho$ **(OD h^{-1})**
1w4 (control)	-	-	0.389	0.009
1w4xGFP	0.474	0.006	0.365	0.005
6w4xGFP	-	-	0.329	0.009
Re1.2xGFP	0.519	0.006	0.359	0.002
Re1.4xGFP	0.362	0.003	0.218	0.005
Re1.5xGFP	0.541	0.005	0.544	0.007
Re1.8xGFP	0.460	0.007	0.381	0.004
Re2xGFP	0.494	0.004	0.467	0.003
Re12xGFP	0.496	0.006	0.323	0.004

Table 4.2: Mean growth rate and standard error of the mean for the switching *Pseudomonas fluorescens* strains - experiments performed in both KB and in KBS culture media. Results were obtained by fitting TiCan growth curves with an exponential law in a time window of 2 hours during early exponential phase.

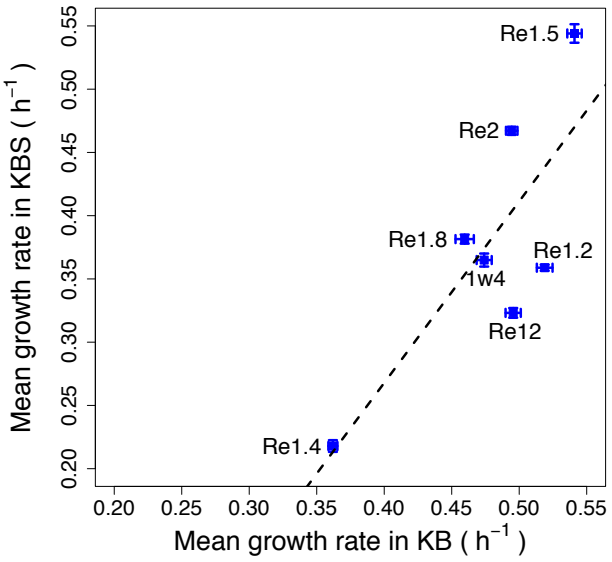

Figure 4.5: Measurements of the mean exponential growth rate in KBS and in KB culture media correlate. The medium change from KB to KBS introduces a sistematic change in the growth rate, which can quantified via the intercept of the linear fit with the y axis. Error bars on both dimensions correspond to standard error of the mean across the three replicates performed per strain. Linear fit: $\rho_{KBS} = 1.435 * \rho_{KB} - 0.306$. Linear correlation coefficient $\rho = 0.798$, $P_{value} = 0.031$.

Growth rate measurements in KBS correlate well with those previously performed in KB (Fig. 4.5). The two sets are significantly different ($P_{value} \simeq 0.05$), meaning that the difference between the two groups can be ascribed to the medium change. The *Pseudomonas fluorescens* switching strains grow slower in KBS than in the old medium recipe (all points are under the main diagonal of the graph). The (negative) intercept of the linear fit quantifies the bias induced by the medium change. On the other hand, inter-strain variability in KBS is higher than that measured in KB (the slope of the linear fit is greater than 1).

CAP+ frequency measurements

The frequency of the CAP+ phenotype in the populations of our *Pseudomonas fluorescens* switching strains was measured through flow cytometry (see Chapter 2, Section 2.2.2 for details). The results of the measurements (mean values and standard error over the three replicas for every strain) are shown in Table 4.3 and Figure 4.6. Here again, we observe that the genotypes sharing the same switch-triggering mutation (1w4xGFP and Re1.8xGFP) present similar frequencies of the CAP+ phenotype.

	KBS	
Strain	**CAP+ freq.**	$\sigma_{\textbf{CAP+ freq.}}$
1w4 (control)	0.004	-
1w4xGFP	0.780	0.015
6w4xGFP	0.904	0.022
Re1.2xGFP	0.294	0.028
Re1.4xGFP	0.147	0.004
Re1.5xGFP	0.010	0.001
Re1.8xGFP	0.792	0.014
Re2xGFP	0.370	0.038
Re12xGFP	0.389	0.028

Table 4.3: Mean CAP+ frequency and standard error of the mean for each of the 9 different switching strains (flow cytometry measurements). Three replicates were performed for each strain, with the exception of the negative control (1w4) for which only one replicate was performed.

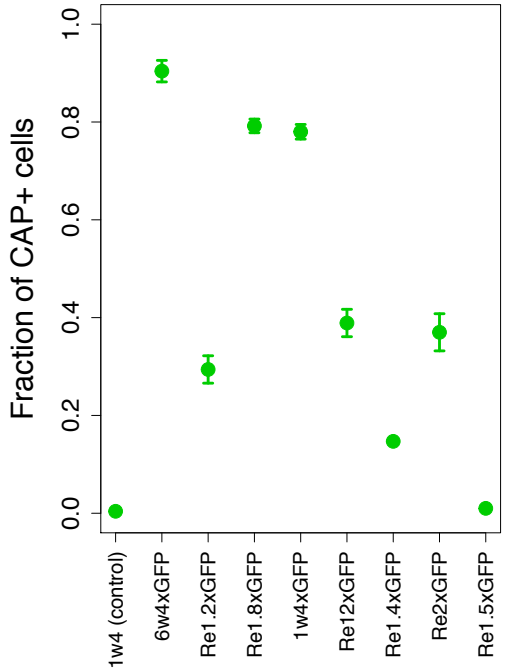

Figure 4.6: Mean CAP+ frequency measured through flow cytometry varies across the switching genotypes. Error bars represent standard error of the mean. Three replicates were performed for each strain, with the exception of the negative control (1w4) for which only one replicate was performed.

Growth rate / CAP+ frequency scatterplot

Data from growth and capsulation assays in KBS can be aggregated to verify if the negative correlation between average growth rate in exponential phase and frequency of the CAP+ state still holds (Fig. 4.7). Despite having significantly changed the culture environment, the negative correlation between the two observables is conserved, although it is less strong.

Unlike previous measures where they scored the highest frequency of CAP+ phenotype across the different switchers, Re1.4xGFP cultures presented in KBS a very low CAP+ frequency, instead of being positively affected by the medium change. This might be due to the particular mutation endowing Re1.4 with the capsulation switch, which might have cells respond differently to the amino acid change, or to clumping of cells preventing a precise measure through flow cytometry.

In conclusion, KBS (which was found to enhance the frequency of the CAP- to CAP+ switch on agar plates), corresponds to higher CAP+ frequency in bulk culture, while significantly slowing down population growth in exponential phase. Finally, a negative correlation between the mean growth rates and the CAP+ frequencies is always obtained, and appears to be irrespective of the growth medium and of the experimental protocol. Indeed, measuring the CAP+ frequency by flow cytometry (rather than indian ink staining) increases the sample size of several orders of magnitude without altering the relative differences between strains, with the exception of Re1.4xGFP.

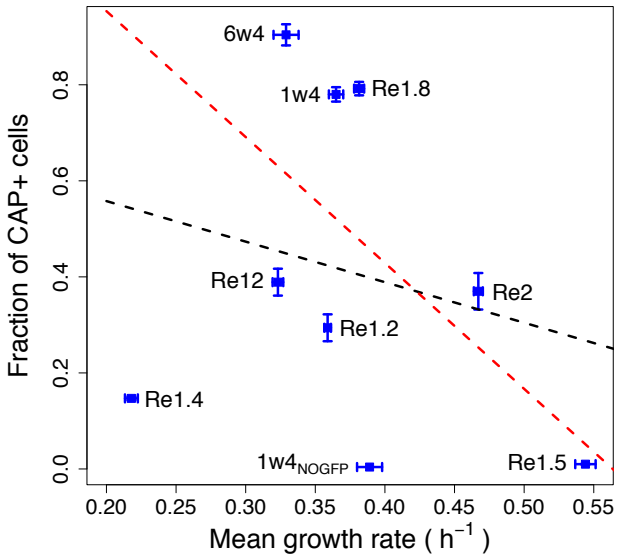

Figure 4.7: Mean growth rate and CAP+ frequency from different switching genotypes growing in exponential phase in KBS culture medium negatively correlate. Each point corresponds to one of the switching *Pseudomonas fluorescens* genotypes with the insertion of the *gfp* gene 1w4xGFP, 6w4xGFP, Re1.2xGFP, Re1.4xGFP, Re1.5xGFP, Re1.8xGFP, Re2xGFP, Re12xGFP, plus 6w4xGFP and the negative control 1w4 without the *gfp* insertion. Linear correlation coefficient $\rho = -0.227$, $P_{value} = 0.559$ (black dashed line). When excluding the negative control 1w4 and Re1.4xGFP (whose growth curves were strongly affected by cellular clumping): $\rho = -0.561$, $P_{value} = 0.148$ (red dashed line).

4.1.4 Temperature alters both growth and CAP+ expression

The results of the previous Sections indicate that, though differing in the genetic basis of the switching behaviour, the phenotypic state of different strains follows a pattern of co-variation with the growth rate: fastest-growing strains tend to have less capsulated cells than slower-growing ones. If there was a direct link between switching rates and growth rate similar to what assumed in the model presented in Chapter 3, one could expect that the same conclusion should hold if growth rate is altered otherwise than by genetic means. It is known that bacteria adjust their generation time according to the temperature of their growth environment.

I thus decided to control the mean growth rate of one specific strain by exposing it at different temperatures (the same during the night culture and the measurements phase). To this avail, 1w4xGFP cultures were grown at 20, 22, 25, 28, 31 and 34° C, and their growth rate and CAP+ frequency in exponential phase assessed.

If changes in the mean growth rate of the population are indeed the main cause of variability in the typical frequency of the CAP+ phenotype in *Pseudomonas fluorescens* populations sustained in exponential phase, I expect to obtain the same negative correlation between the two quantities, no matter how the growth rate is manipulated.

Nevertheless, I cannot rule out the fact that stress response could affect switching rates in ways that are independent of the "passive" dilution effect induced by growth rate change.

Growth rate measurements

After a night culture round, each of the three replicates was diluted to the same optical density (OD $= 0.1$) and cell density measured every 60 minutes (for the 20, 25 and 31° C samples), or every other hour (22, 28 and 34° C) through optical density. Although the measurements continued longer, the exponential fit necessary to estimate the exponential phase growth rate for each of the replicates was performed on an early time window (between two and six hours after resuspension), before the culture approached saturation. Results are presented in Table 4.4 and plotted in Figure 4.8.

Temp. (° C)	**Repl.**	$\rho\ (\mathbf{h}^{-1})$	$\bar{\sigma}_\rho\ (\mathbf{h}^{-1})$	**Temp. (° C)**	**Repl.**	$\rho\ (\mathbf{h}^{-1})$	$\bar{\sigma}_\rho\ (\mathbf{h}^{-1})$
20	R1	0.316		28	R1	0.443	
20	R2	0.308		28	R2	0.456	
20	R3	0.314		28	R3	0.405	
20		0.313	0.003	28		0.435	0.019
22	R1	0.310		31	R1	0.465	
22	R2	0.416		31	R2	0.471	
22	R3	0.335		31	R3	0.465	
22		0.354	0.039	31		0.467	0.002
25	R1	0.335		34	R1	0.046	
25	R2	0.367		34	R2	0.101	
25	R3	0.378		34	R3	0.140	
25		0.360	0.016	34		0.096	0.034

Table 4.4: Mean exponential phase growth rate of 1w4xGFP populations grown at different temperatures in KBS. An exponential fit of the optical density data between 2 and 6 hours after resuspension was performed for each of the replicates. For each temperature, the mean value and the standard error of the mean over the three replicates are also presented.

In Figure 4.9 the mean growth rate is plotted against temperature for six different temperatures between 20 and 34° C. Growth curves are highly reproducible (except the one at 22° C) and show quantitative differences as temperature is varied. It can be noticed that the positive effect of culture temperature on population growth during exponential phase seems to cease for cultures grown at temperatures higher than 31° C: the 34° C samples are indeed sick, and observation under the microscope proved their inability to grow associated to a very serious change of the cells' appearence. For this reason, they were excluded from the subsequent analysis.

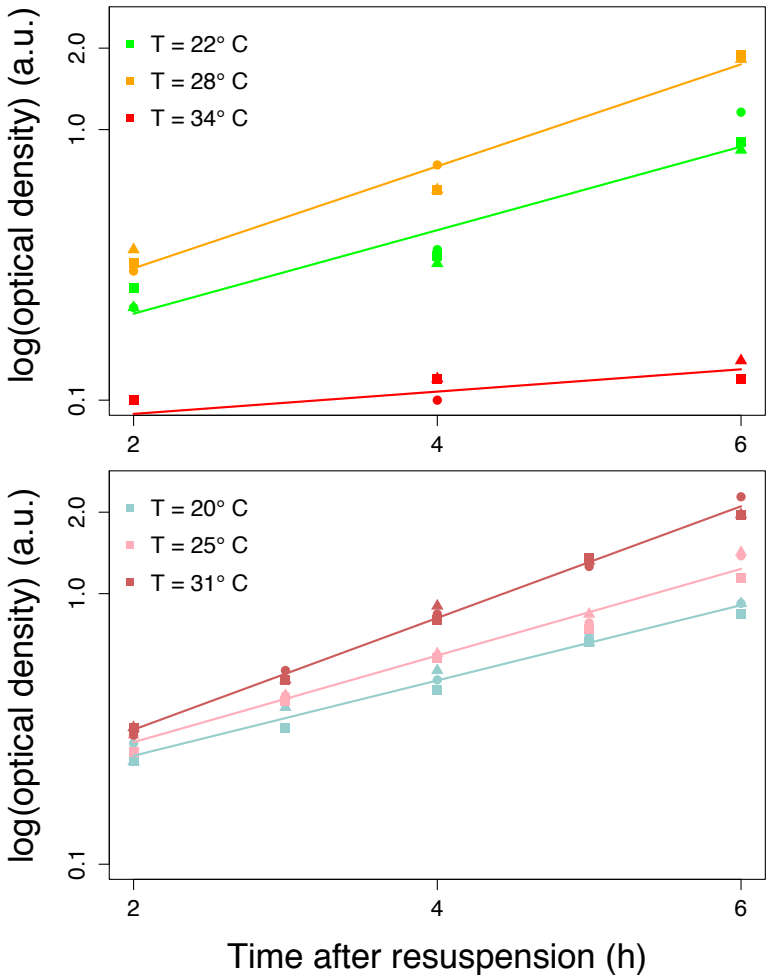

Figure 4.8: Optical density measurements of 1w4xGFP cultures grown at 22, 28, 34° C (top panel) and 20, 25 and 31° C (bottom panel). For each temperature, three identical replicates were grown, and the mean and standard error of the mean computed. The exponential fit of the mean OD across the three replicates was performed (solid lines).

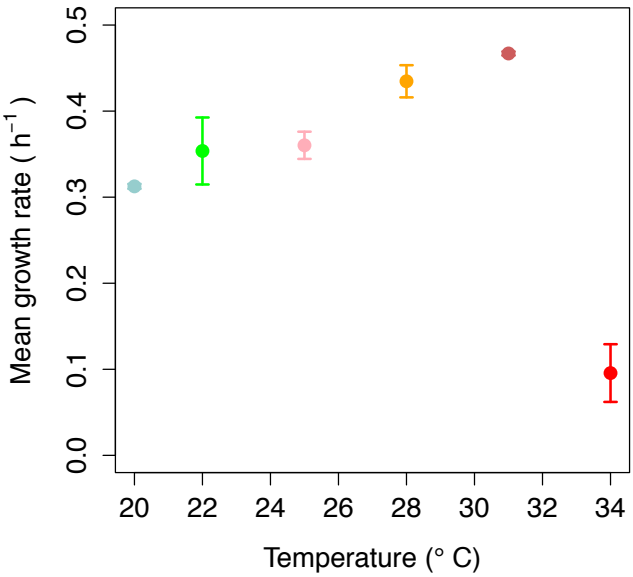

Figure 4.9: Temperature affects exponential growth in *Pseudomonas fluorescens* 1w4xGFP populations. Three independent populations were grown at each of the tested temperatures (20, 22, 25, 28, 31, and 34° C) and the growth rate computed by exponential fit of the corresponding optical density data. For each temperature, error bars correspond to the standard error of the mean growth rate over the three replicates.

CAP+ frequency measurements

The frequency of CAP+ cells in exponential phase was assayed by fluorescent microscopy. At 3 hours (20, 25, and 31° C) or 4 hours after resuspension (22 and 28° C), a $\sim$ 1 µl sample of each of the grown cultures was plated on a microscopy slide and 20 pictures taken at different locations in both phase contrast and GFP fluorescence. An automated Fiji image analysis procedure allowed us to gather data about the total number of cells (phase contrast channel) and the number of CAP+ cells (GFP fluorescence channel). Table 4.5 recapitulates the results of the counting assays. For further details about the experimental protocol, see Chapter 2, Section 2.2.2.

Temperature (° C)	Repl.	Counted cells	Counted CAP+	CAP+ frequency
20	R1	273	124	0.454
20	R2	362	77	0.213
20	R3	720	379	0.526
20		1355	580	0.428
22	R1	159	117	0.736
22	R2	404	212	0.525
22	R3	59	18	0.305
22		622	347	0.558
25	R1	254	133	0.524
25	R2	318	23	0.072
25	R3	545	154	0.283
25		1117	310	0.278
28	R1	153	25	0.163
28	R2	359	16	0.045
28	R3	102	26	0.255
28		614	67	0.109
31	R1	390	4	0.010
31	R2	430	1	0.002
31	R3	281	2	0.007
31		1101	7	0.006
34	R1	1	0	0
34	R2	2	0	0
34	R3	65	3	0.046
34		68	3	0.044

Table 4.5: Results of the counting assays for 1w4xGFP populations grown at 20, 22, 25, 28, 31, and 34° C. Data for each replicate are shown along the total number of cells, total number of CAP+ cells and CAP+ frequency for each of the temperatures.

Growth rate / CAP+ frequency scatterplot

When plotting the measured CAP+ frequency against the mean growth rate for the five temperatures, I again find a statistically significant negative correlation between these two observables, irrespectively of considering the data from different replicates at the same temperature individually or lumped together (Fig. 4.10).

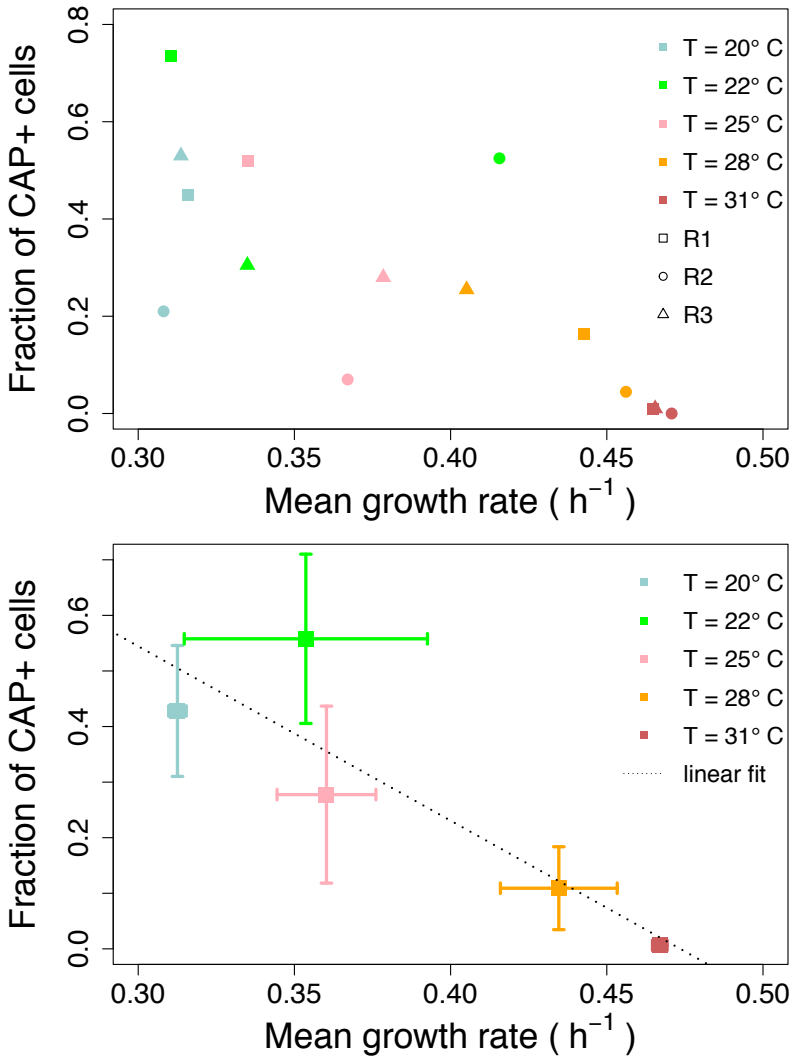

Figure 4.10: The fraction of CAP+ cells and the mean growth rate in exponential phase of 1w4xGFP populations grown at five different temperatures negatively correlate — one point per replicate (top panel) and aggregated results (bottom panel, error bars corresponding to the standard error of the mean across three replicates). Linear correlation coefficient $\rho = -0.881$, $P_{value} = 0.048$.

4.1.5 High variability might be due to protocol limitations

The high degree of intra- and inter-replicate variability obtained in the fluorescent microscopy assays (Fig. 4.10) casts some doubts about the reliability of the experimental protocol for reliably obtaining quantitative measures. Henceforward some considerations about the main experimental issues and the way to improve the protocol are discussed.

More data is needed to obtain reproducible results on CAP+ frequency

For each temperature, three different replicates were performed: for each replicate $\simeq 20-30$ microscopy images were taken to gather sufficient data about the frequency of the CAP+ phenotype in 1w4xGFP populations (see Chapter 2), corresponding to $\simeq 500-1000$ cells. Data display extremely high inter-replicate variability (*cf.* Table 4.5 and Figure 4.10), resulting in a high variance on the estimation of the frequency of CAP+ f. Here I aim at estimating how many different replicates should be performed to reduce the relative uncertainty on the CAP+ frequency below a desired level.

Table 4.6 recapitulates the minimum number of replicates $R_{20\%}$ needed to obtain a relative error on the CAP+ frequency of 20% for all the temperatures tested so far. The corresponding number of cells is obtained by multiplying the needed number of replicates by the average number of cells assayed per replicate $N/3$.

Temp. (° C)	R	N	N_+	f	σ_f	$\bar{\sigma}_f/f(\%)$	$R_{20\%}$	$N_{20\%}$
20	3	1355	580	0.428	0.167	27.6	5	2171
22	3	622	347	0.558	0.215	27.2	5	977
25	3	1117	310	0.278	0.225	57.2	17	6470
28	3	614	67	0.109	0.105	68.1	24	4953
31	3	1101	7	0.006	0.006	70.7	26	9542

Table 4.6: More independent replicates are needed to decrease the dispersion of the results of the frequency measurements to the 20% threshold. For each of the five different temperatures, the relative error on the frequency depends on the square root of the number of replicates minus one, which allows us to find the minimum number of replicates $R_{20\%}$ needed to get a relative error on f of 20%. The expected total number of cells to be assayed is finally obtained by multiplying $R_{20\%}$ by the average number of cells per replicate $N/3$.

When is exponential phase? Choosing the right timing

Of crucial importance is fixing the moment when the fluorescent microscopy measurement is performed: indeed, cultures must be in exponential phase, and at the same time frequencies must have reached a quasi-steady state. This means that enough time must have elapsed after the overshoot, where the fluctuations of the CAP+ frequency reach their maxima (*cf.* Chapter 3, Section 3.4). This aspect concerns not only the moment when pictures of the cultures are taken under the microscope, but also the preparation phase (e.g. when the first preculture gets diluted).

For these reasons, a preliminary experiment is needed to verify that the mean growth rate at 2 hours after resuspension into fresh KBS is a good proxy for the exponential phase quasi-equilibrium. To allow quantitative comparison with the model, the growth rate and the population composition must both be stable across replicates and irrespective of the number of previous dilutions (Figure 4.11).

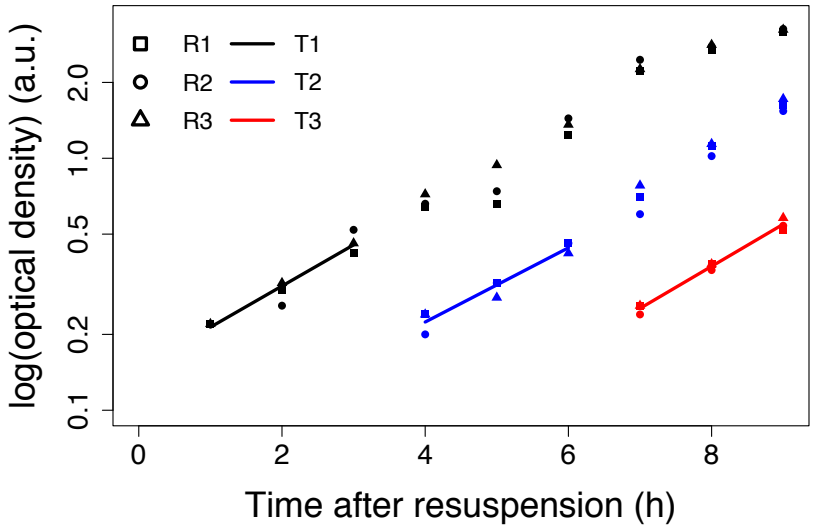

Figure 4.11: The mean growth rate in 1w4xGFP populations is stable across successive dilutions of the same population. Three identical 1w4xGFP cultures are started (T1, from R1 to R3, black points), and three hours later each of the three replicate cultures is diluted to OD = 0.01 into fresh KBS medium (T2, from R1 to R3, blue points). The procedure is then repeated three hours later, founding the three T3 populations (red points). The mean growth rate is obtained through an exponential fit of the optical density data between 1 and 3 hours after the foundation of each culture (solid lines).

Table 4.7 shows the series of three mean growth rates obtained by fitting the three successive optical density time series from one to three hours after foundation, for each replicate. In general, intra-replicate variability (by comparing the standard deviation of the results of the fit for T1, T2, T3 belonging to the same replicate) is higher than inter-replicate variability for a given dilution (in 7 out of the 9 pairwise combinations), meaning that the procedure followed to perpetuate a population through successive dilution does not introduce an uncertainty in the exponential phase growth rate greater than the one that we can already observe between different replicates of cultures of a same strain.

1w4xGFP at 28° C	**KBS**		
Repl.	**Dilution T1**	**Dilution T2**	**Dilution T3**
R1	0.323	0.325	0.347
R2	0.430	0.417	0.406
R3	0.369	0.280	0.401

Table 4.7: The 1w4xGFP mean growth rate does not vary much between successive dilutions. Standard deviations: $\sigma^2_{T1} = 0.054$, $\sigma^2_{T2} = 0.070$, $\sigma^2_{T3} = 0.033$, $\sigma^2_{R1} = 0.013$, $\sigma^2_{R2} = 0.012$, $\sigma^2_{R3} = 0.063$.

4.2 The model predicts only part of the variability in CAP+ frequency

The experimental results presented in the last Section prove that variation in mean growth rate translates into variation of the alternative phenotypes' frequencies during exponential phase, but also that this variation depends on a number of factors, including experimental protocol, culture medium, time of observation. It is not clear yet to what extent it is possible to describe these different situations within a unified framework, where the population state is mostly controlled by growth rate differences.

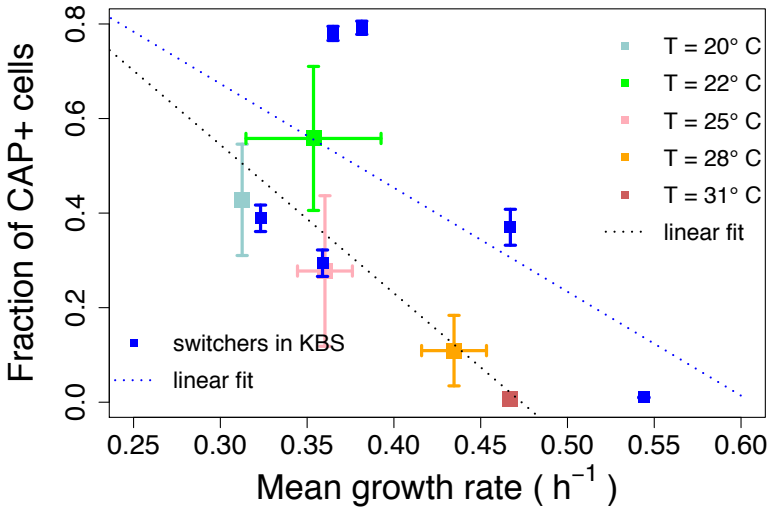

Figure 4.12: The fraction of CAP+ cells and the mean growth rate in exponential phase negatively correlate irrespective of how the latter is varied. Data from switchers in KBS (except 6w4xGFP and Re1.4xGFP, whose cultures were susceptible to clumping and therefore did not provide accurate measurements) and from 1w4xGFP exposed at 20, 22, 25, 28 and 31° C are shown. Linear correlation coefficient $\rho = -0.600$, $P_{value} = 0.051$.

Data about different *Pseudomonas fluorescens* switching genotypes and those about 1w4xGFP cultures grown at different temperatures both display a negative correlation between mean growth rate and percentage of CAP+ cells in the population. Figure 4.12 compounds the measures for different strains with those for different temperatures. To the level of resolution reached in these experiments, it appears that the two sources of growth variation cannot be distinguished on the sole basis of their effect on population composition.

A negative correlation between CAP+ frequency and growth rate could already be predicted by the model presented in Chapter 3. In this Section I aim at answering a further question: Does the mathematical model *quantitatively* account for the CAP+ frequency in exponential phase as a function of mean growth rate?

The focus of Chapter 3, the mathematical model (conceived to reproduce and explain the history-dependent dynamics of the phenotypic composition of the population) provides a quantitative prediction for the CAP+ frequency during exponential phase f_E^* (Eq. 3.70):

$$f_E^* = \left[1 + \frac{\alpha_-^{MAX}}{\alpha_+^{MAX}} \frac{\left((\frac{r}{b} + \frac{1}{K_c}) c_{HIGH} - 1 \right)}{\left(1 - (\frac{r}{b} + \frac{1}{K_c}) c_{LOW} \right)} \right]^{-1} . \tag{4.1}$$

Being f_E^* a monotonously decreasing function of the average growth rate $r = \rho$ (I consider the case where the two phenotypes are equal in terms of the cells' division time), this results in the prediction of a particular functional form for the negative correlation between these two observables.

4.2.1 The model underestimates the measured CAP+ frequency

When informed with the parameters that best fit the phenotypic dynamics (Table 3.5), the Equation 4.1 underestimates the frequency of CAP+ corresponding to low mean growth rates in exponential phase (Fig. 4.13).

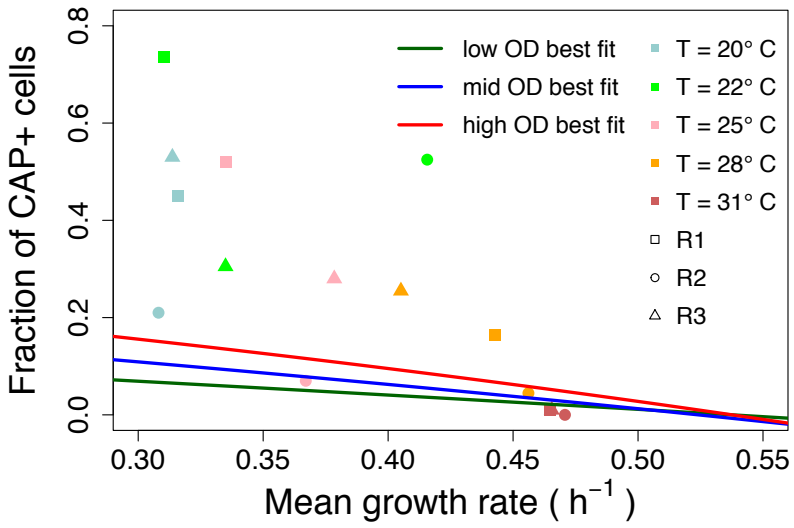

Figure 4.13: The mathematical model of Chapter 3 cannot explain the degree of CAP+ expression in 1w4xGFP populations exposed at different culture temperatures. The three solid lines (green, blue and red) correspond to the growth rate - frequency of CAP+ curves obtained by informing Equation 4.1 with the different sets of parameters that best fit the phenotypic dynamics under the three preculture conditions ("low", "mid", "high", respectively).

Indeed, while the measurements taken at 31° C fall close to the curve obtained informing Equation 4.1 with the parameters of the fit of the "low" preculture conditions, the other measurements appear not to be predicted by the model. Taking the aggregated data (one point per temperature obtained by summing the countings and

averaging the mean growth rates over the three replicates), the divergence between model and data seems to increase as temperature decreases apart from the point at 22° C (Figure 4.14).

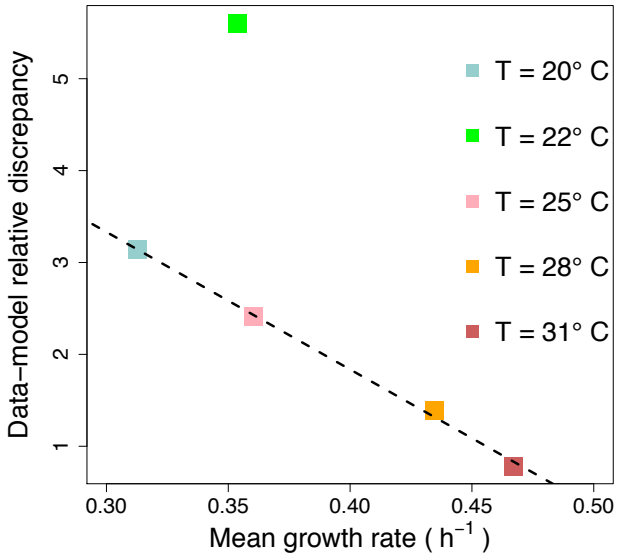

Figure 4.14: The deviation of the experimental data about CAP+ frequency deviation from the theoretical prediction issued from the overshoot model decreases with the mean growth rate. Such deviation was computed as $\frac{|f_i - f_E^*(r_i)|}{f_E^*(r_i)}$, where $f_i(r_i)$ and $f_E^*(r_i)$ are the measured and expected values of the fraction of CAP+ cells. Expected values are computed by Equation 4.1 by using the mean growth rates r_i for any given temperature, and parameters from the best fit of the overshoot experiment, "mid" preculture condition (Section 3.5.1). With the exception of the point at 22° C, the decrease of the computed deviation between model and data appears to scale linearly with the mean growth rate (dashed line).

In conclusion, I need to understand the origin of the discrepancy between model and data, and why the discrepancy increases as the mean growth rate decreases. The strategy I want here to follow consists in loosening some assumptions made so far:

- the ratio between the maximum switching rates $\alpha_+^{MAX}/\alpha_-^{MAX}$ is the same that best fits the overshoot experiment (Section 4.2.2),
- the switching rates depend linearly on the internal concentration c (Section 4.2.3), and
- the maximum switching rates α_+^{MAX} and α_-^{MAX} does not depend on the mean growth rate (Section 4.2.4).

4.2.2 Higher maximum switching rates ratios reduce the discrepancy

Measured CAP+ frequencies as a function of the mean growth rate in exponential phase do not concentrate around any of the curves set by Equation 4.1 when it is informed by the parameters that best fit the overshoot experiment. This discrepancy may be due to the fact that the switching rates are different under such different experimental conditions. Albeit effort was put into following the same protocol as the overshoot experiment, the fact of realizing measures in another lab and with different instruments might indeed have affected the quantitative reproducibility of the observations.

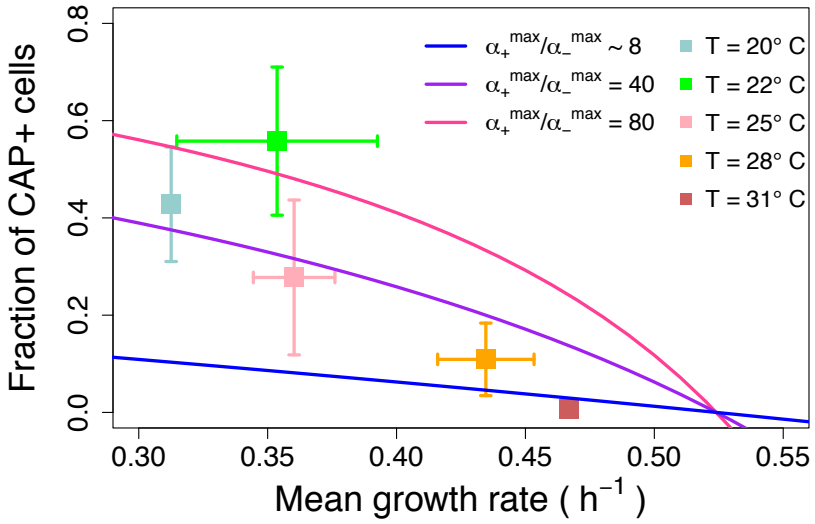

Figure 4.15: The fit of the relation between mean growth rate and CAP+ frequency in exponential phase is improved by increasing the ratio between the maximum switching rates α_+^{MAX} and α_-^{MAX} (solid lines). Although higher values of $\alpha_+^{MAX}/\alpha_-^{MAX}$ improve the correspondance between data and model prediction with respect to that corresponding to the best fit of the overshoot dynamics experiment (blue line), the unchanged scaling law does not appear to match the data distribution yet.

From the analysis of the model (Chapter 3, Section 3.3.5), it is known that, if the quasi-equilibrium f_E^* depends on most of the parameters of the model, the slope of the CAP+ frequency vs mean growth rate curve is particularly sensitive to changes in the ratio between the maximum switching rates $\alpha_+^{MAX}/\alpha_-^{MAX}$ (Equation 4.1). Please notice that, with α_-^{MAX} fixed, α_+^{MAX} appears to be the parameter that affects more sensitively the fit of the phenotypic dynamics across the three preculture conditions (Table 3.5). For growing values of the $\alpha_+^{MAX}/\alpha_-^{MAX}$ ratio, the curves generated by Equation 4.1 become steeper and reach higher values of the CAP+ frequency quasi-equilibrium f_E^* for low growth rates (Fig. 4.15).

In conclusion, the curves obtained by increasing the $\alpha_+^{MAX}/\alpha_-^{MAX}$ ratio of one order of magnitude do perform better than the previous ones, but they do not still seem

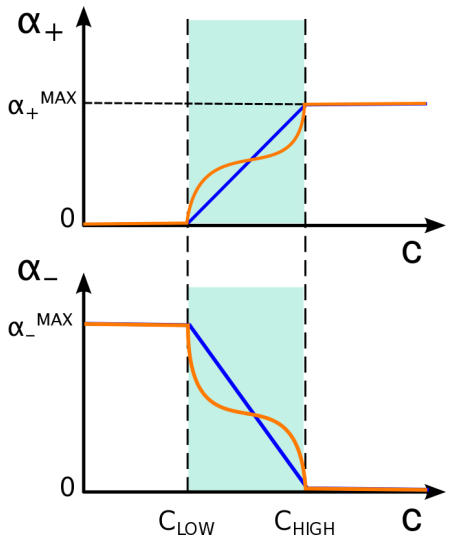

Figure 4.16: Linear vs nonlinear dependency of the switching rates on the internal concentration c (blue and orange lines, respectively). In both cases, switching rates are defined as piecewise functions, to allow them to be nonzero at once only for values of c belonging to an intermediate region (corresponding to CAP+ and CAP- coexistence). In this case a very extreme instance of nonlinearity is chosen, that is piecewise-exponential functions with the maxima of derivatives near the boundaries of the region of coexistence. This way, small deviations of c near the boundaries yield very high switching rate variations, pushing the system to sudden transitions.

to grasp how the CAP+ frequency scales with the mean exponential phase growth rate.

4.2.3 Nonlinear rates do not change the predicted functional shape

Another possible reason for the data-model discrepancy when dealing with the expected frequency of the CAP+ cells in exponential phase as a function of the mean growth rate of the population may consist in the simplistic functional form chosen in the model for the switching rates dependence on the internal concentration of X, c.

Therefore, for the switching rates $\alpha_+(c)$ and $\alpha_-(c)$ one can consider alternative functional forms, like piecewise- exponential functions corresponding to an S-like and not Z-like intracellular bifurcation diagram of c in the bistability region $c \in [c_{LOW}, c_{HIGH}]$ (Fig. 4.16). It is evident from Figure 4.17 that for any of the $\alpha_+^{MAX}/\alpha_-^{MAX}$ ratios, the piecewise-nonlinear functional form of the switching rates does not yield a sea change in the shape of the curves: the reason lies in the fact that at equilibrium the ratio is fixed. I conclude that we need the two switching rates $\alpha_+(c)$ and $\alpha_-(c)$ explicitly depend on r, and with a different scaling. In the next Section I analyse the case where the maximum switching rates α_+^{MAX} and α_-^{MAX} explicitly depend on the mean growth rate r.

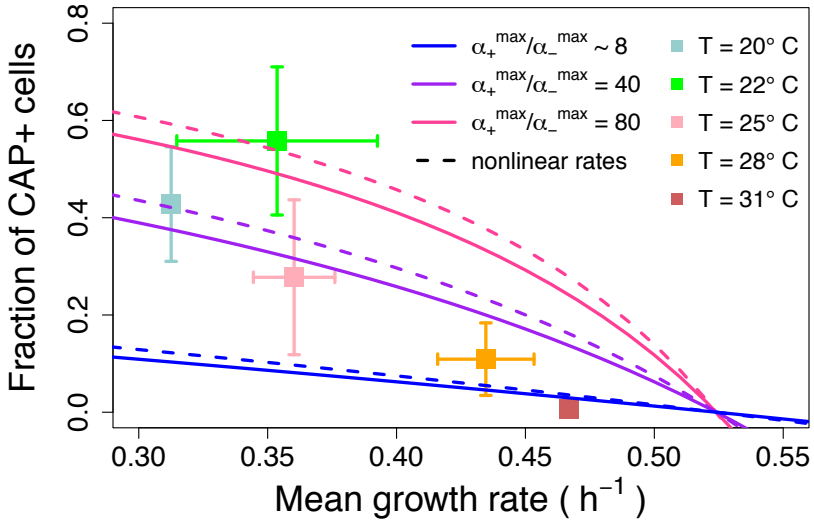

Figure 4.17: Highly nonlinear functional form of the switching rates do not change the scaling law for the growth rate - CAP+ frequency relation predicted by the model. With respect to the linear ones (solid lines), nonlinear switching rates (dashed lines) predict slightly higher CAP+ frequencies (especially at low mean growth rates) but do not account for a change in the scaling law of the dependency of the CAP+ frequency in exponential phase on the mean growth rate.

4.2.4 The switching rates ratio must scale with the growth rate

Equation 4.1 was derived from the more general Equation setting the quasi-equilibria for the frequency of the CAP+ given the values of the switching rates when the internal concentration c reaches its quasi-steady state:

$$f^* = \frac{\alpha_+(c^*)}{\alpha_+(c^*) + \alpha_-(c^*)},$$

which can be written as

$$f^* = \left[1 + \frac{\alpha_-(c^*)}{\alpha_+(c^*)}\right]^{-1}. \tag{4.2}$$

Furthermore, in Chapter 3 the switching rates were written as the product of a switch-characteristic time scale (the maximum switching rate) and a piecewise-linear function of the internal concentration c, in formula:

$$\alpha_+(c) = \alpha_+^{MAX} \frac{c - c_{LOW}}{c_{HIGH} - c_{LOW}} \tag{4.3}$$

$$\alpha_-(c) = \alpha_-^{MAX} \frac{c_{HIGH} - c}{c_{HIGH} - c_{LOW}}. \tag{4.4}$$

Let's now imagine that, instead of being constant parameters, the maximum switching rates scale with the mean growth rate r:

$$\alpha_+^{MAX} \sim r^{\gamma} \tag{4.5}$$

$$\alpha_-^{MAX} \sim r^{\delta}, \tag{4.6}$$

which yields

$$\frac{\alpha_-^{MAX}}{\alpha_+^{MAX}} \sim r^{\delta-\gamma}. \tag{4.7}$$

Substituting Eqs. 4.3, 4.4 and 4.7 in Eq. 4.2 yields:

$$f^* = \left[1 + \frac{\alpha_-^{MAX}}{\alpha_+^{MAX}} \frac{c_{HIGH} - c^*}{c^* - c_{LOW}} r^{\delta-\gamma}\right]^{-1}. \tag{4.8}$$

If α_+^{MAX} and α_-^{MAX} are made constant ($\delta = \gamma = 0$) or, more generally, if they scale with the average growth rate following the same functional law ($\delta - \gamma = 0$), than one obtains the previous results. On the other hand, one can try different scalings ($\delta \neq \gamma$) and compare the results with the data of the exponential phase CAP+ frequency quasi-equilibrium and the mean growth rates. In this case, it is possible to obtain a decrease in CAP+ frequency with growth rate that is faster than linear, whereas the previously discussed model predicted a concave function for the curve $f_E^*(\rho)$ (Figure 4.18).

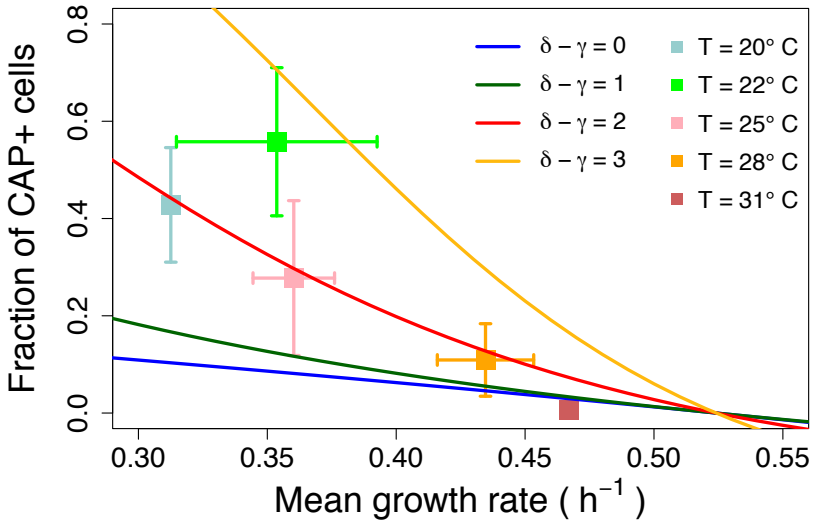

Figure 4.18: Significant improvements in the theoretical prediction of the quasi-equilibrium f^* can be achieved by increasing the exponent $\delta - \gamma$ of the power law scaling of the maximum switching rates ratio $\alpha_+^{MAX}/\alpha_-^{MAX}$ with respect to the mean growth rate. The theoretical expectation best reproduces the data when the $\alpha_-^{MAX}/\alpha_+^{MAX}$ maximum switching rates ratio scales as $r^{\delta-\gamma}$ with $\delta - \gamma \simeq 2$.

Figure 4.18 also shows how, to best fit the results of the experiment, $\delta - \gamma$ must be higher than 1, meaning that the $\alpha_-^{MAX}/\alpha_+^{MAX}$ maximum switching rates ratio must increase faster than linearly with the mean growth rate. A best agreement between data and prediction is obtained by taking $\delta - \gamma \simeq 2$: in Section 4.3.1 I discuss how this result could be explained in terms of differential internal ribosome concentration between CAP+ and CAP- cells (ribosomal interpretation of the switch, see Section 4.3.1).

4.3 Biological interpretation of the switching rates ratio scaling

As I reviewed in Chapter 1, Section 1.3.2, genetic studies showed the existence of a branching point along the pyrimidine pathway, downstream the operon whose expression triggers the expression of the CAP+ phenotype (Fig. 1.5). Such operon is indeed touched by genetic mutations increasing the occurrence of the expression of the CAP+ phenotype of around three orders of magnitude with respect to the wild type *Pseudomonas fluorescens* SBW25.

The effect of such genetic mutations has been attributed to the disequilibrium induced in the fluxes of UDP and UTP along the pyrimidine pathway [42], thus perturbing the partition of those metabolic products between two alternative branches of the pathway – one devoted to DNA and RNA synthesis, and the other to colanic acid production. As a consequence, the independently evolved *Pseudomonas fluorescens* switching genotypes (whose switching-related mutations are on different loci of either gene *carB* or gene *pyrH*) are found to differ for their mean growth rate and for their typical frequency of the CAP+ phenotype during exponential phase.

Following these findings (the existence of the branching point on the pyrimidine pathway and the effects of mutations along the pathway affecting the fluxes of UDP and UTP), it can also be assumed that a trade-off between cellular growth and capsulation may be in place in the *Pseudomonas fluorescens* "switchers": metabolic resources related to the pyrimidine pathway must be partitioned between cellular growth and capsule production, in ratios that depend on the specific mutation triggering the switch at high frequency ("checkpoint hypothesis").

The checkpoint hypothesis is supported by my experimental results on the relation between mean growth rate and frequency of the capsulated state across the population: whether I test different genotypes with different characteristic exponential phase growth rates, or expose one genotype to different temperatures to trigger a variation in its growth, I always obtain a negative correlation between the growth rate and the frequency of the capsulated phenotype.

The mathematical model of Chapter 3, Section 3.4 — developed to explain the highly nonlinear, history-dependent transient phenotypic dynamics of 1w4xGFP populations grown in KBS bulk cultures — predicts the negative relation between mean growth rate and frequency of the capsulated state through Equation 4.1. Nevertheless, the model is not able to quantitatively account for the degree of heterogeneity observed for slowly-growing populations, nor to qualitatively explain the scaling law connecting the CAP+ frequency and the mean growth rate in exponential phase.

By considering the maximum switching rates as explicit functions of the mean growth rate of the population, and letting them scale differently with it, a better imitation of the measured negative relation between mean growth rate and frequency of the capsulated state can be obtained. The ratio between the switching rate from CAP+ to CAP- and that from CAP- to CAP+ must scale superlinearly with the growth rate, yielding the best agreement with the experimental results when it scales with the second-power of r.

4.3.1 Bimodal expression of ribosomal genes and switching rates

In Chapter 3, Section 3.7 the results of the fit of our mathematical model are interpreted in terms of a theory elaborated by Dr. Philippe Remigi, Dr. Gayle Ferguson and Prof. Paul Rainey. Rainey and collaborators assume the existence of a competition between high ribosome levels and RmsA/E genes for the translation of a positive regulator of capsule biosynthesis. This gene, called "A", would encode for a protein whose concentration is responsible for the bistability in capsule expression. This "ribosomal hypothesis" is in agreement with what our mathematical model proposes to explain the results of the overshoot experiment: the concentration c of the product X is endowed with the same function of that of the product of gene "A", that is triggering the switching behaviour via a threshold mechanism.

The hypothesis of the existence of a mechanism linking ribosomal concentration and the cellular switching behaviour can indeed help in finding a coherent interpretation of one of the major results of this Chapter (Section 4.2.4): the maximum switching rates' ratio superlinear scaling with the mean growth rate might be due to a higher concentration of ribosomes in CAP+ cells. This would result both in a faster-than-linear increase of the timescale of the switch to the CAP- state for higher amounts of ribosomes (e.g. due to a higher mean growth rate of the strain [53])

Supporting this line of reasoning, Dr. Philippe Remigi's has recently measured a higher expression of ribosomal genes in CAP+ with respect to CAP- in 1w4 (unpublished data, personal communication). Moreover, it is known that, as the concentration of ribosomes strongly increases with the growth rate in physiological conditions [28, 53], the concentration of ribosomes inside CAP+ cells belonging to a fast-growing population must be much higher than the concentration of ribosomes inside CAP+ cells of a slow-growing population, regardless of the origin of the growth rate difference.

As a consequence, CAP+ cells from a fast-growing population will be characterized by faster cellular processes with respect to the same processes taking place in CAP+ cells from a slow-growing population. The switch from CAP+ to CAP- would make no exception. On the contrary, CAP- cells, having less ribosomes than the CAP+, might be less susceptible to the effect of variations in ribosome concentration related to growth rate. As a result, the ratio between the maximum switching rates $\alpha_-^{MAX}/\alpha_+^{MAX}$ might scale more than linearly with the mean growth rate.

CHAPTER 5

DISCUSSION AND CONCLUSIONS

Artificially evolved *Pseudomonas fluorescens* "switchers" are a model system for the study of binary polymorphism in cellular phenotypes, a particular instance of phenotypic heterogeneity displayed by several isogenic populations of microbes.

Clonal *Pseudomonas fluorescens* populations perform a phenotypic switch between a normal cellular state and a rare capsulated phenotype. The phenotypic switch, already present at low frequency in the wild type, can be better appreciated in the so-called "switchers": these are strains that were artificially evolved under a regime of alternating growth conditions staggered by single-colony bottleneck, when phenotypic novelty was selected at the colony scale. This experimental evolution protocol yielded mutated genotypes whose expression rates of the rare capsulated state across the population were at least three orders of magnitude higher than in the wild type (from 10^{-4} to 10^{-1}).

The switchers are a particularly useful model system for addressing transitions between alternative phenotypes because of the possibility of assessing the frequency of the two states (and, in principle, the switching rates) through microscopy observations. The experimental protocols progressed from Indian ink staining and manual counting in bright field images, to automatic routines able to distinguish the CAP+ phenotype, marked with GFP, and produce time-resolved, high-throughput surveys of populations during their demographic variations.

Genetic, environmental and stochastic factors all concur in the determination of the phenotype and its variability

As I reviewed in the Introduction, instances of phenotypic switching are often dichotomously classified as purely stochastic or environment-driven. Indeed, many are the examples of phenotypic switches whose main determinant is an intrinsic bistability. The transition between alternative states is interpreted as the consequence of number fluctuations of the molecules involved in the decision point, which can re-

spond or not to environmental cues. One of the neatest examples of noise-driven expression of alternative phenotypes is genetic competence in *Bacillus subtilis*, whose phenotype is expressed by about 10% of cells in stationary phase due to noise in the expression of the *comK* gene. On the other hand, other microorganisms sense the environment and tune their phenotype accordingly. Such sensing strategies can consist in adjusting the phenotype as the environmental conditions change (acclimation), or in varying the degree of heterogeneity at the population level, like *Klebsiella oxytoca* isogenic populations able to adapt to nutrient limitation and fluctuation by shaping phenotypic heterogeneity in metabolism [86].

Alternative scenarios of switch at the cellular level pave the way for different population-level manifestations, hence leading the researcher to focus on different observables. On the one hand, when the switching is purely stochastic, the population is at any given time a mixture of phenotypes (some of which potentially maladapted): the relevant observable is in this case the distribution of the phenotypes' frequencies across the population, and their time variation is neglected as the system is assumed to be ergodic. On the other hand, responsive switching results in homogeneous populations for most of the observation times, and the system is described in terms of the variation of the mean phenotype in time.

From an evolutionary standpoint, the existence of different strategies has been connected to the time scale of the environmental variation that microorganisms face. As pointed out by Kussell & Leibler, pure stochastic switching is optimal for organisms whose environment changes in a hardly or not at all predictable fashion, while acclimation is preferable when the cost of producing and maintaining sensing mechanisms is not very high and the environment not completely unpredictable or characterized by extreme changes. Other strategies can relate to the evolution of an internal clock that can be synchronized to the environmental change when the latter is regular or highly predictable.

In this Thesis, I inquired how the interplay of stochasticity and environmental sensing affects the dynamics of phenotypic heterogeneity in populations of cells able to perform a phenotypic switch.

Environmental dependence of the phenotypic switch in *Pseudomonas fluorescens*

The fact that the alternative, capsulated phenotypic state is always expressed in the population, and not only for specific values of the environmental parameters, indicates that the "decision" of expressing the capsule must have a stochastic component. Measurements on agar pads of the timescale associated with transitions between the alternative phenotypic states, obtained through time-lapse fluorescent microscopy, revealed that this is longer than the cell lifetime and sufficiently short not to be negligible on the time scale (hours) of population demography. Moreover, a qualitative asymmetry between the switching rates from or to the capsulated cellular state was evidenced, indicating the existence of mechanisms, likely rooted in intracellular regulation pathways, able to bias the switch.

At the same time, Jenna Gallie showed in her Ph.D. thesis that several environmental signals can influence the variation of the relative frequencies of the two phe-

notypes: temperatures lower than the standard growth temperature (28° C) and higher concentration of uracil in the culture medium were both shown to cause a significant increase of the frequency of the capsulated phenotype across the population. In stationary phase, too, the capsulated state is expressed at a higher frequency, suggesting the capsulation transition to be impacted by the demographic state of the population.

Therefore, *Pseudomonas fluorescens* switchers can hardly be treated as collections of purely stochastically switching units, or of responsive cells all acclimating to the environment as it changes. Only by considering both the genetic background and the role of the environment on the stochastic switch the observed phenomenology in *Pseudomonas fluorescens* can be put into a coherent framework.

In this sense, the most similar example in the literature is antibiotic persistence, first interpreted in terms of phenotypic switch and bet-hedging strategies by Balaban *et al.* [8]. Contrary to persisters, in *Pseudomonas fluorescens* switchers there is no clear-cut adaptive role known at this point for the capsulated phenotype, and capsulated cells grow at rates that are comparable to the non-capsulated ones.

In a modelling perspective, the temporal variation of the degree of phenotypic heterogeneity within a population (i.e. the alternative phenotypes' frequencies) becomes a relevant observable, and opens novel questions about how much of such variation is genetically or environmentally controlled. As done in Balaban *et al.* for persisters, systems of ODEs provide a simple but efficient framework to the end of describing such dynamics.

Population growth alone can provide the sufficient information on the environmental context to explain transient variation in population phenotypic composition

The gentotype of *Pseudomonas fluorescens* switching strains does not define qualitatively the degree of phenotypic heterogeneity. The frequencies of the alternative phenotypes CAP- and CAP+ indeed vary in time. Moreover, even the qualitative nature of their variation depends on the history of the population.

Early observations by Dr. Jenna Gallie revealed that the frequency of the capsulated phenotype was different if cultures were in exponential rather than in stationary phase. Dr. Philippe Remigi subsequently proved, through flow cytometry experiments, that the demographic history and the population frequency at the moment of sampling affect the degree of phenotypic variability of a population. He showed that, in cultures initialized at a same cell density, not only the frequency of different phenotypes was highly dynamic, but that such dynamics varied with the density at which the preculture was harvested. Cultures derived from "older" precultures showed a structured transient, where an overshoot in the frequency of the capsulated phenotype was followed by an undershoot.

To these results, I added the observation that a negative correlation existed between the average maximum growth rate and the frequency of the CAP+ cells across the different re-evolved switchers. Building on the hypothesis of a possible direct effect of growth rate on the switching behaviour, I developed a mathematical model aimed at exploring the possibility that population demography (quantified by the average population growth rate) could bear sufficient information to explain a non-

monotonic, history-dependent dynamics in the phenotypic composition of the population.

Dilution of an intracellular compound can couple a bistable switch to the demography of the cell population

In Chapter 3, I verified that context-independent models of populations of switchers are mathematically incompatible with the observation of an overshooting dynamics. Indeed, in models with constant switching rates the frequencies of the phenotypes can only change monotonously in time, even if a difference in growth rate is allowed between the two phenotypes.

Mathematically, such an inadequacy of these simple but general models of context-independent switch provided the justification to explore the context-dependence of the switching rates. Modelling the intracellular switch as a bistable system controlled by an intracellular concentration, I could couple the population composition to demography.

In this model, the inherent stochastic hallmark of the system (the switching rates) is bound to a macroscopic observable (the growth rate of the population), which "measures" the demographic state of the population as a whole. One way to provide a biologically reasonable mechanism for context-dependence consists in the introduction of a third variable, alongside the population size and the frequency of the capsulated phenotype: the intracellular concentration c of a compound produced by the cell and diluted through cell division.

If the stability of the alternative equilibria is controlled by c, then changes in the population growth rate as cells experience lag, exponential and eventually stationary phase modify, through changes in the internal concentrations, the probability of switching. In particular, slower growth in lag and stationary phase results in an increased probability of developing a capsule, whereas in exponential phase such probability decreases on a timescale set by the population growth rate.

The mathematical model proposed in Chapter 3 consists of a 3-D dynamical system that assumes no growth rate difference between phenotypes. Although an approximation of the more general case where the two phenotypes are not selectively equivalent, it is sufficiently simple for its dynamics to be investigated through an analytical approach, and can qualitatively reproduce the temporal dynamics data. In particular, it can produce history-dependent qualitatively different transients, whereby the overshoot and undershoot behaviour, as well as a larger initial fraction of capsulated cells, are associated to "old" precultures. Indeed, the delayed growth induced by the approach to stationary phase promotes the accumulation of the intracellular compound, and thus the transient increase of the switching rate towards the capsulated state. Such switching rate subsequently decreases as the intracellular compound is diluted out by exponential cell elongation, but increases again as growth slows down when the population approach the stationary phase. This generic feature is common, though to a different quantitative extent, in models whose demographic parameters and initial conditions are chosen so as to match the experimental measures. The other parameters (the maximal switching rates, the intracellular rates) have not been measured on this system, but were estimated through the fit of the overshoot experiment

data.

Quantitatively fitting the transient phenotypic dynamics in a consistent way across multiple experiments proved, however, challenging, even if a low number of free parameters was involved. One of the obstacles to explaining all behaviours with a single set of parameters is that, whereas overshooting dynamics is generic, qualitatively different history-dependent behaviour is only obtained when some initial conditions are at the brink of bistability. Moreover, the nonlinearities associated to the entry in stationary phase play a critical role in the slowing down of the phenotypic dynamics, but their effect on switching rates and on lag phase are naively described in the model discussed in Chapter 3.

The trade-off between genericity of the approach and inclusion of specific mechanistic details poses the question of how later phases of growth should be modelled in a mathematical description of a demography-dependent switch. In our model a good agreement between the fitted curves and the experimental data at late time points was achieved by supposing a fast accumulation mechanism during the lag phase, which gave rise to the overshoot at the beginning of the dynamics. Alternatively, to reproduce the experimentally observed convergence in stationary phase towards a phenotypic steady state without invoking a lag mechanism, I could have assumed that the maximal switching rates depended on population size in a highly nonlinear fashion.

As the biological system gets further characterized, the nature of the environmental switch-tuning will be made more precise, and the elaboration of mathematical models more adherent to the biological reality will be possible.

The mathematical model provides qualitative predictions about the relationship between growth and switch in exponential phase

Setting aside the problems associated to modelling the entry in stationary phase, the mathematical model articulated in Chapter 3 can be used as a predictive tool beyond the description and explanation of the non-monotonous history-dependent phenotypic dynamics. Indeed, the analytical study of the exponential phase equilibria provides a testable relationship between the average rate of population growth and the fraction of the alternative phenotypes. In exponential phase all environmental effects decreasing growth rate below its maximum value can be neglected, so that, according to the intracellular model, the population will reach a steady state. Such an equilibrium is defined as a function of a smaller number of parameters with respect to what is needed in order to encompass the transient dynamics, and is thus constrained by the optimal fit of the observations.

I have asked to what extent the fitted parameters predict the variation of the equilibrium phenotypic composition in different experimental settings, if the only control parameter was the rate of exponential growth. This question can be applied to populations of different genetic background, which in general display variations both in growth rate and in phenotypic composition, or to the same genotype, when the growth rate is modulated by changes in the environmental conditions (e.g. temperature).

My mathematical model predicts a negative correlation between the mean growth rate and the frequency of the capsulated state, and this irrespective of what under-

pins the growth rate change (as long as the basic regulatory mechanism remains the same). I proved such relation to hold true by assessing the percentage of capsulated cells among different strains, or in populations of the same strain grown at different temperatures. Although the qualitative agreement between the predictions of the model and the result of my experimental tests were good, the model could not quantitatively account for the degree of heterogeneity observed for the slowest growing strains, nor qualitatively explain the scaling law connecting the CAP+ frequency and the mean growth rate in exponential phase.

By supposing that the maximum switching rates are explicit functions of the mean growth rate (instead than fixed parameters) a better data-model agreement was obtained. In particular, I showed that the ratio between the maximum switching rates $\alpha_{-}^{MAX}/\alpha_{+}^{MAX}$ must scale superlinearly with the mean growth rate, and that the experimental results are best fitted when it scales with the second-power of the mean growth rate.

Changing the temperature might have been an invasive method for altering population growth. Indeed, affecting virtually all cellular processes, temperature may likely perturb those directly involved in the switch. The most conservative way of altering the switching rates may therefore be that of considering different genetic mutants, like the seven re-evolved *Pseudomonas fluorescens* switching strains. In perspective, it would moreover be interesting to genetically alter some other component of the translational or post-translational machinery, so as to slow down growth, without altering the production of one specific compound. These kind of experiments may help to refine our understanding of the essential ingredients determining the unbalance leading to capsulation, and in particular the role of deregulation in protein production during lag phase.

New questions and perspectives for further work

The mathematical model analysed in this work describes several aspects of phenotypic heterogeneity in *Pseudomonas fluorescens* switchers: the temporal variation of the phenotypic composition of the population, its history-dependence, and the response of populations of switchers to the environment under a steady exponential growth regime. In doing so, the model conjugates the approach of most models of purely stochastic switches with the one typically followed when dealing with responsive switching and acclimation.

The model was then "stretched" in order to fit both the overshoot experiment and the negative capsulation-growth correlation and, in doing so, I probably crossed the boundaries of the domain of its meaningful application. A more advanced knowledge of the molecular mechanisms involved in *Pseudomonas fluorescens* CAP phenotypic switch will likely allow to refine it, for example by establishing if the growth rate is the best variable to choose as a proxy for the environmental state perceived by the cells.

Different modifications may be considered for improving the predictions of the model on specific aspects. For example, the shape of the negative correlation between phenotypic composition and mean growth rate in exponential phase could be fine-tuned by acting on the scaling law of the maximum switching rates with re-

spect to the mean growth rate. This allowed to adjust the quantitative results, but did not touch the salient property needed to model the effect of population growth on a stochastic, environment-dependent phenotypic switch: the need for a feedback between the demographic state and the phenotypic repartition of the population, which can be obtained through an internal variable "sensing" the environment.

If further studies confirm the role of ribosomal concentration and regulation, adding another variable explicitly representing the ribosomal concentration may allow a better fit of the experimental results. Such a supplementary variable, explicitly coupled to the average growth rate, would accelerate or slow down the variations in the concentration c, therefore introducing another time scale. Although the manipulation of this other time scale might provide a higher degree of control over the overshoot dynamics in the model, it would nonetheless be associated to the introduction of additional parameters. Such complexification of the model would thus likely be useful if additional, molecular data were available to complement the experiments discussed in this Thesis.

From an experimental point of view, the limitations of considering the growth rate as the only proxy for the population demographic state are manifold. Indeed, there are different ways of affecting the growth rate, not all of which are expected to be equivalent in terms of regulation of the intracellular concentrations. One question is to what extent can growth rate be used, in a phenomenological perspective like that adopted by Terence Hwa and collaborators, to describe populations whose growth has been altered because of physical (temperature), genetic (mutants having different regulatory circuits), translational (mutants with mutations in the same gene), and post-translational (mutants that differ in the ribosomal content) modifications.

To conclude, the mechanism of switch modulation described by the model is potentially common, and the understanding of its consequences might be important not only on the ecological time scale, but also for understanding how the phenotypic dynamics can affect in the long-term, evolutionary fate of cellular populations. Indeed, the intrinsic time scale of the transient dynamics, intermediate between that of the individual and that of the population, might pave the way to the establishment of new levels of organismal organization.

ACKNOWLEDGEMENTS

I would like to thank my supervisor, Professor Silvia De Monte for the opportunity to conduct my research with her. Under her constant and attentive supervision I learned more than mere notions or methods, and I am grateful for the infinite patience she found when dealing with the ups and downs of my research activity, as well as those of my personal life. To my thesis director, Professor Chris Bowler goes all my gratefulness for having supported me when I most needed it and for all the interesting discussions we had. I would also like to warmly thank the Director of the Sciences du Végétal doctoral school, Professor Jacqui Shykoff for her substantial help and support.

Funding for this four-year-long project, without which all this work would not have seen the light of day, was provided by the Île-de-France region through the Institut des Systèmes Complexes and by the Labex MemoLife of the Institut de Biologie de l'École Normale Supérieure.

Professor Paul Rainey and Dr. Philippe Remigi introduced me to the world of cutting-edge experimental biology: under their guidance I was for the first time challenged by a variety of thrilling phenomena and techniques spanning from microbiology to genetics and evolution, all useful to understand the bigger picture. I am grateful to have had the opportunity to work with them, always in the spirit of a free sharing of hypotheses and results, and to have learned from them how the international scientific community works.

My two stays at Massey University were unvaluable experiences also thanks to all friends and colleagues: Andy Farr, Chhavi Chawla and her family, Elena Colombi, Chaitanya Gokhale, Honour McCann, Christina Straub, Luca Bütikofer and Professor Heather Hendrickson. I would also like to thank all the researchers (Dr. Maxime Ardré above all) of the Laboratoire de Biochimie at the École Supérieure de Physique et Chimie Industrielles (ESPCI) for having given me the possibility to perform my experimental work in their spaces and with their facilities.

The Éco-Évolution Mathématique group of the Institut de Biologie de l'École Normale Supérieure (IBENS) has been an extremely stimulating and friendly work environment. It has been a privilege to work (and to share passionate discussions at lunchtime) with such brilliant people that I deem friends more than just colleagues:

David Salthouse, Clara Champagne, Charles Bernard, Stéphane Debove, Célian Colon, Boris Sauteray, Elsa Abs, Linh Phuong Nguyen, Pierre-Antoine Precigout, Julia Clause, Vincent Le Bourlot, Jonathan Rault, Professor Sabrina B. L. Araujo and Professors David Claessen and Corinne Robert.

Dr. Sandrine Adiba deserves a special place: she won a place in my affections thanks to a rare combination of extraordinary scientific rigour, unique kindness and sense of humour. The long hours *à la paillasse* ran faster in her company and I owe to her tenacious teachings all that I can do in a microbiology laboratory.

To Professor Marco Cosentino Lagomarsino: thank you for having made me love scientific research in the first place, and for all the encouragement and the precious pieces of advice in the toughest moments of my doctorate!

"¡Muchas gracias!" also to my physiotherapist Dr. Beatriz del Barco, who managed to make me fully and rapidly recover from a bad fracture. Without my left hand back in shape I would not been able to complete the writing of this thesis.

For the last five years Paris has been a special place where to enjoy life, too, and this must be ascribed to really special people: a tremendous "thank you!" goes to my dearest friends Alberto, Claudio and Manon, Elisa, Enrico, Francesco (x2), Giovanni and M., Isabella, Lucilla and Samir, Matteo, Pietro and Esther, Telemaco and Ilaria, Vittore and Elizaveta.

Finally, I would like to thank my family, especially my father, my sister Sissi and my nephew Jacopo. All my deepest gratitude goes to my beloved mother, who suffered the most from my departure abroad: I wish I could rewind the tape of these five years and pay her one visit more. Last but not least, thank you Paola for having been at my side from day one and for endlessly making my life a wonderful adventure.

BIBLIOGRAPHY

[1] M. Acar, J. T. Mettetal, and A. van Oudenaarden, *Stochastic switching as a survival strategy in fluctuating environments.*, Nature genetics, 40 (2008), pp. 471–475.

[2] M. Ackermann, B. Stecher, N. E. Freed, P. Songhet, W.-D. Hardt, and M. Doebeli, *Self-destructive cooperation mediated by phenotypic noise.*, Nature, 454 (2008), pp. 987–90.

[3] P. Alberch, *From genes to phenotype: dynamical systems and evolvability*, Genetica, 84 (1991), pp. 5–11.

[4] D. G. Allison and M. A. Sattenstall, *The influence of green fluorescent protein incorporation on bacterial physiology: A note of caution*, Journal of Applied Microbiology, 103 (2007), pp. 318–324.

[5] U. Alon, *An Introduction to Systems Biology: Design Principles of Biological Circuits*, vol. 10, Chapman and Hall/CRC, 2006.

[6] V. I. Arnold, V. S. Afrajmovich, Y. S. Il'yashenko, and L. P. Shil'nikov, *Bifurcation Theory and Catastrophe Theory*, Lecture Notes in Computer Science, (2011).

[7] M. Arnoldini, R. Mostowy, S. Bonhoeffer, and M. Ackermann, *Evolution of stress response in the face of unreliable environmental signals.*, PLoS computational biology, 8 (2012), p. e1002627.

[8] N. Q. Balaban, J. Merrin, R. Chait, L. Kowalik, and S. Leibler, *Bacterial persistence as a phenotypic switch.*, Science (New York, N.Y.), 305 (2004), pp. 1622–5.

[9] Y. Bao, D. P. Lies, H. Fu, and G. P. Roberts, *An improved Tn7-based system for the single-copy insertion of cloned genes into chromosomes of gram-negative bacteria*, Gene, 109 (1991), pp. 167–168.

[10] J. Baranyi and T. Roberts, *A dynamic approach to predicting bacterial growth in food.*, Int J Food Microbiol., 23 (1994), pp. 277–294.

[11] H. J. E. Beaumont, J. Gallie, C. Kost, G. C. Ferguson, and P. B. Rainey, *Experimental evolution of bet hedging.*, Nature, 462 (2009), pp. 90–3.

[12] M. K. Belete and G. Balázsi, *Optimality and adaptation of phenotypically switching cells in fluctuating environments*, Physical Review E - Statistical, Nonlinear, and Soft Matter Physics, 92 (2015), pp. 1–8.

[13] G. Bertani, *Studies on lysogenesis. I. The mode of phage liberation by lysogenic Escherichia coli.*, Journal of bacteriology, 62 (1951), pp. 293–300.

[14] Z. D. Blount, C. Z. Borland, and R. E. Lenski, *Historical contingency and the evolution of a key innovation in an experimental population of Escherichia coli.*, Proceedings of the National Academy of Sciences of the United States of America, 105 (2008), pp. 7899–7906.

[15] A. Buckling, R. Kassen, G. Bell, and P. B. Rainey, *Disturbance and diversity in experimental microcosms*, Nature, 408 (2000), pp. 961–964.

[16] J. J. Bull, *Evolution of Phenotypic Variance*, Evolution, 41 (1987), pp. 303–315.

[17] T. Cağatay, M. Turcotte, M. B. Elowitz, J. Garcia-Ojalvo, and G. M. Süel, *Architecture-dependent noise discriminates functionally analogous differentiation circuits.*, Cell, 139 (2009), pp. 512–22.

[18] J. Choi, D. Shin, and S. Ryu, *Implication of quorum sensing in Salmonella enterica serovar typhimurium virulence: The luxS gene is necessary for expression of genes in pathogenicity island 1*, Infection and Immunity, 75 (2007), pp. 4885–4890.

[19] D. Cohen, S. Sallon, E. Solowey, Y. Cohen, R. Korchinsky, M. Egli, I. Woodhatch, O. Simchoni, M. Kislev, A. T. Austin, D. C. Murray, S. G. Pearson, R. Fullagar, B. M. Chase, J. Houston, J. Atchison, N. E. White, M. I. Bellgard, E. Clarke, M. Macphail, M. T. P. Gilbert, J. Haile, and M. Bunce, *Optimizing reproduction in a randomly varying environment.*, Journal of theoretical biology, 12 (1966), pp. 119–129.

[20] J. J. Collins, T. S. Gardner, and C. R. Cantor, *Construction of a genetic toggle switch in Escherichia coli*, Nature, 403 (2000), pp. 339–342.

[21] N. A. Cookson, S. W. Cookson, L. S. Tsimring, and J. Hasty, *Cell cycle-dependent variations in protein concentration*, Nucleic Acids Research, 38 (2009), pp. 2676–2681.

[22] N. L. Craig, *Tn7: a target sitespecific transposon*, Molecular Microbiology, 5 (1991), pp. 2569–2573.

[23] C. Darwin, *On the origin of species by means of natural selection, or the preservation of favoured races in the struggle for life*, John Murray, London, 1859.

[24] M. Diard, V. Garcia, L. Maier, M. N. P. Remus-Emsermann, R. R. Regoes, M. Ackermann, and W.-D. Hardt, *Stabilization of cooperative virulence by the expression of an avirulent phenotype.*, Nature, 494 (2013), pp. 353–6.

[25] E. Drenkard and F. M. Ausubel, *Pseudomonas biofilm formation and antibiotic resistance are linked to phenotypic variation.*, Nature, 416 (2002), pp. 740–743.

[26] D. Dubnau and R. Losick, *Bistability in bacteria*, Molecular Microbiology, 61 (2006), pp. 564–572.

[27] S. Dukan and T. Nystrom, *Bacterial senescence: stasis results in increased and differential oxidation of cytoplasmic proteins leading to developmental induction of the heat shock regulon*, Genes Dev., 12 (1998), pp. 3431–3441.

[28] M. Ehrenberg, H. Bremer, and P. P. Dennis, *Medium-dependent control of the bacterial growth rate*, Biochimie, 95 (2013), pp. 643–658.

[29] S. Einum and I. A. Fleming, *Environmental unpredictability and offspring size: Conservative versus diversified bet-hedging*, Evolutionary Ecology Research, 6 (2004), pp. 443–455.

[30] A. Eldar and M. B. Elowitz, *Functional roles for noise in genetic circuits*, Nature, 467 (2010), pp. 167–173.

[31] M. B. Elowitz, A. J. Levine, E. D. Siggia, and P. S. Swain, *Stochastic gene expression in a single cell.*, Science (New York, N.Y.), 297 (2002), pp. 1183–6.

[32] S. Enomoto, A. Chari, A. L. Clayton, and C. Dale, *Quorum Sensing Attenuates Virulence in Sodalis praecaptivus*, Cell Host & Microbe, 21 (2017), pp. 629–636.e5.

[33] J. L. Enos-Berlage and L. L. Mccarter, *Relation of Capsular Polysaccharide Production and Colonial Cell Organization to Colony Morphology in Vibrio parahaemolyticus*, PNAS, 182 (2000), pp. 5513–5520.

[34] J. Feng, D. a. Kessler, E. Ben-jacob, and H. Levine, *Growth feedback as a basis for persister bistability.*, Proceedings of the National Academy of Sciences of the United States of America, 111 (2013), pp. 544–549.

[35] D. H. Figurski and D. R. Helinski, *Replication of an origin-containing derivative of plasmid RK2 dependent on a plasmid function provided in trans*, Proceedings of the National Academy of Sciences, 76 (1979), pp. 1648–1652.

[36] R. Fisher, *The Genetical Theory of Natural Selection*, Oxford University Press, 1930.

[37] R. Fitzhugh, *Impulses and Physiological States in Theoretical Models of Nerve Membrane*, Biophysical Journal, 1 (1960), pp. 445–466.

[38] D. Fraser and M. Kærn, *A chance at survival: Gene expression noise and phenotypic diversification strategies*, Molecular Microbiology, 71 (2009), pp. 1333–1340.

[39] G. Fusco and A. Minelli, *Phenotypic plasticity in development and evolution: facts and concepts. Introduction.*, Philosophical transactions of the Royal Society of London. Series B, Biological sciences, 365 (2010), pp. 547–556.

[40] G. Galilei, *Il Saggiatore*, 1623.

[41] J. Gallie, *Evolutionary and molecular origins of a phenotypic switch in Pseudomonas fluorescens SBW25*, PhD thesis, Massey University, Auckland, New Zealand, 2010.

[42] J. Gallie, E. Libby, F. Bertels, P. Remigi, C. B. Jendresen, G. C. Ferguson, N. Desprat, M. F. Buffing, U. Sauer, H. J. E. Beaumont, J. Martinussen, M. Kilstrup, and P. B. Rainey, *Bistability in a Metabolic Network Underpins the De Novo Evolution of Colony Switching in Pseudomonas fluorescens*, PLOS Biology, 13 (2015), p. e1002109.

[43] S. J. Gould, *Ontogeny and phylogeny*, Harvard University Press, 1977.

[44] O. Häggström, *Finite Markov chains and algorithmic applications*, Cambridge University, 2002.

[45] K. Hammerschmidt, C. J. Rose, B. Kerr, and P. B. Rainey, *Life cycles, fitness decoupling and the evolution of multicellularity*, Nature, 515 (2014), pp. 75–79.

[46] Y. Ito, H. Toyota, K. Kaneko, and T. Yomo, *How selection affects phenotypic fluctuation.*, Molecular Systems Biology, 5 (2009), p. 264.

[47] E. Jablonka and M. J. Lamb, *Evolution in Four Dimensions: Genetic, epigenetic, behavioral, and symbolic variation in the history of life*, The MIT Press, Cambridge, Massachusetts, 2005.

[48] E. Jablonka, B. Oborny, I. Molnar, E. Kisdi, J. Hofbauer, and T. Czaran, *The Adaptive Advantage of Phenotypic Memory in Changing Environments*, Philosophical transactions of the Royal Society of London. Series B, Biological sciences, 350 (1995), pp. 133–141.

[49] F. Jacob and J. Monod, *Genetic regulatory mechanisms in the synthesis of proteins*, Journal of Molecular Biology, 3 (1961), pp. 318–356.

[50] F. Janzen and G. Paukstis, *Environmental Sex Determination in Reptiles: Ecology, Evolution, and Experimental Design*, Review Literature And Arts Of The Americas, 66 (2009), pp. 149–179.

[51] R. Kassen and G. Bell, *Experimental evolution in Chlamydomonas. IV. Selection in environments that vary through time at different scales*, Heredity, 80 (1998), pp. 732–741.

[52] E. King, M. Ward, and D. Raney, *Two simple media for the demonstration of pyocyanin and fluorescin*, J Lab Clin Med., 44 (1954), pp. 301–7.

[53] S. Klumpp, Z. Zhang, and T. Hwa, *Growth Rate-Dependent Global Effects on Gene Expression in Bacteria*, Cell, 139 (2009), pp. 1366–1375.

[54] E. Kussell and S. Leibler, *Phenotypic diversity, population growth, and information in fluctuating environments.*, Science (New York, N.Y.), 309 (2005), pp. 2075–8.

[55] P. Labhsetwar, J. A. Cole, E. Roberts, N. D. Price, and Z. a. Luthey-Schulten, *Heterogeneity in protein expression induces metabolic variability in a modeled Escherichia coli population*, Proceedings of the National Academy of Sciences, 110 (2013), pp. 14006–14011.

[56] G. Lambert and E. Kussell, *Memory and Fitness Optimization of Bacteria under Fluctuating Environments*, PLoS Genetics, 10 (2014).

[57] S. Leibler and E. Kussell, *Individual histories and selection in heterogeneous populations.*, Proceedings of the National Academy of Sciences of the United States of America, 107 (2010), pp. 13183–8.

[58] R. Lewontin, *The Genetic Basis of Evolutionary Change*, Columbia University Press, 1974.

[59] A. J. Lotka, *Analytical Note on Certain Rhythmic Relations in Organic Systems.*, Proceedings of the National Academy of Sciences of the United States of America, 6 (1920), pp. 410–415.

[60] H. Maamar and D. Dubnau, *Bistability in the Bacillus subtilis K-state (competence) system requires a positive feedback loop*, Molecular microbiology, 56 (2005).

[61] M. Madigan, J. Martinko, and J. Parker, *Brock biology of microorganisms*, Prentice-Hall, Upper Saddle River, NJ, 2000.

[62] D. Martin, *The oxygen consumption of Escherichia coli.*, J. Gen. Physiol., 15 (1932), pp. 691–708.

[63] N. Massin and A. Gonzalez, *Adaptive radiation in a fluctuating environment: Disturbance affects the evolution of diversity in a bacterial microcosm*, Evolutionary Ecology Research, 8 (2006), pp. 471–481.

[64] R. Mathis and M. Ackermann, *Response of single bacterial cells to stress gives rise to complex history dependence at the population level*, Proceedings of the National Academy of Sciences, 113 (2016), p. 201511509.

[65] J. Monod, *The growth of bacterial cultures*, Annual review of microbiology, 3 (1949).

[66] T. Mora and A. M. Walczak, *Effect of Phenotypic Selection on Stochastic Gene Expression*, The Journal of Physical Chemistry B, (2013).

[67] C. Mouslim and K. T. Hughes, *The Effect of Cell Growth Phase on the Regulatory Cross-Talk between Flagellar and Spi1 Virulence Gene Expression*, PLoS Pathogens, 10 (2014).

[68] E. R. Moxon, P. B. Rainey, M. a. Nowak, and R. E. Lenski, *Adaptive evolution of highly mutable loci in pathogenic bacteria.*, Current biology, 4 (1994), pp. 24–33.

[69] H. S. Moyed and K. P. Bertrand, *hipA, a newly recognized gene of Escherichia coli K-12 that affects frequency of persistence after inhibition of murein synthesis.*, Journal of Bacteriology, 155 (1983), pp. 768–75.

[70] M. Mueller, *Ueber den Einfluss von Fieber temperaturen auf die Wachstumsgeschwindigkeit und die Virulenz des Typhus Bacillus.*, Z. Hyg. Infektionskr., 20 (1895).

[71] M. A. Mulvey, *Adhesion and entry of uropathogenic Escherichia coli*, Cellular Microbiology, 4 (2002), pp. 257–271.

[72] T. M. Norman, N. D. Lord, J. Paulsson, and R. Losick, *Memory and modularity in cell-fate decision making.*, Nature, 503 (2013), pp. 481–6.

[73] E. M. Ozbudak, M. Thattai, H. N. Lim, B. I. Shraiman, and A. Van Oudenaarden, *Multistability in the lactose utilization network of Escherichia coli.*, Nature, 427 (2004), pp. 737–40.

[74] P. Patra and S. Klumpp, *Emergence of phenotype switching through continuous and discontinuous evolutionary transitions*, Physical Biology, 12 (2015), p. 046004.

[75] J. M. Pedraza and A. V. Oudenaarden, *Noise Propagation in Gene Networks*, Science, 1965 (2012).

[76] M. Pigliucci, *Genotype-phenotype mapping and the end of the 'genes as blueprint' metaphor.*, Philosophical transactions of the Royal Society of London. Series B, Biological sciences, 365 (2010), pp. 557–566.

[77] M. Pigliucci, C. J. Murren, and C. D. Schlichting, *Phenotypic plasticity and evolution by genetic assimilation.*, The Journal of experimental biology, 209 (2006), pp. 2362–7.

[78] P. B. Rainey and M. J. Bailey, *Physical and genetic map of the Pseudomonas fluorescens SBW25 chromosome.*, Molecular microbiology, 19 (1996), pp. 521–33.

[79] P. B. Rainey and B. Kerr, *Cheats as first propagules: a new hypothesis for the evolution of individuality during the transition from single cells to multicellularity.*, BioEssays : news and reviews in molecular, cellular and developmental biology, 32 (2010), pp. 872–80.

[80] P. B. Rainey and M. Travisano, *Adaptive radiation in a heterogeneous environment.*, Nature, 394 (1998), pp. 69–72.

[81] W. Ratcliff, R. Denison, M. Borrello, and M. Travisano, *Experimental evolution of multicellularity*, Proceedings of the National Academy of Sciences, 109 (2012), pp. 1595–1600.

[82] C. W. Reynolds, *Flocks, herds and schools: A distributed behavioral model*, ACM SIGGRAPH Computer Graphics, 21 (1987), pp. 25–34.

[83] M. D. Rolfe, C. J. Rice, S. Lucchini, C. Pin, A. Thompson, A. D. S. Cameron, M. Alston, M. F. Stringer, R. P. Betts, J. Baranyi, M. W. Peck, and J. C. D. Hinton, *Lag phase is a distinct growth phase that prepares bacteria for exponential growth and involves transient metal accumulation*, Journal of Bacteriology, 194 (2012), pp. 686–701.

[84] S. T. Rutherford and B. L. Bassler, *Bacterial quorum sensing: its role in virulence and possibilities for its control.*, Cold Spring Harbor perspectives in medicine, 2 (2012), pp. 1–25.

[85] K. Sato, Y. Ito, T. Yomo, and K. Kaneko, *On the relation between fluctuation and response in biological systems.*, Proceedings of the National Academy of Sciences of the United States of America, 100 (2003), pp. 14086–14090.

[86] F. Schreiber, S. Littmann, G. Lavik, S. Escrig, A. Meibom, M. M. M. Kuypers, and M. Ackermann, *Phenotypic heterogeneity driven by nutrient limitation promotes growth in fluctuating environments*, Nature Microbiology, (2016), pp. 1–7.

[87] J. Seger and H. J. Brockmann, *What is bet-hedging?*, Oxford Surveys in Evolutionary Biology, 4 (1987), pp. 182–211.

[88] M. Slatkin, *Hedging one's evolutionary bets*, Nature, 250 (1974), pp. 704–705.

[89] A. Solopova, J. van Gestel, F. J. Weissing, H. Bachmann, B. Teusink, J. Kok, and O. P. Kuipers, *Bet-hedging during bacterial diauxic shift.*, Proceedings of the National Academy of Sciences of the United States of America, 111 (2014), pp. 1–6.

[90] A. Spiers, A. Buckling, and P. B. Rainey, *The causes of Pseudomonas diversity*, Microbiology, (2000), pp. 2345–2350.

[91] R. Stanier, *Enzymatic adaptation in bacteria*, Annual review of microbiology, 5 (1951).

[92] G. M. Süel, R. P. Kulkarni, J. Dworkin, J. Garcia-Ojalvo, and M. B. Elowitz, *Tunability and Noise Dependence in Differentiation Dynamics*, Science, 1363 (2005), pp. 11–14.

[93] P. S. Swain, M. B. Elowitz, and E. D. Siggia, *Intrinsic and extrinsic contributions to stochasticity in gene expression.*, Proceedings of the National Academy of Sciences of the United States of America, 99 (2002), pp. 12795–800.

[94] J.-W. Veening, W. K. Smits, and O. P. Kuipers, *Bistability, epigenetics, and bet-hedging in bacteria.*, Annual review of microbiology, 62 (2008), pp. 193–210.

[95] J. M. G. Vilar, C. C. Guet, and S. Leibler, *Modeling network dynamics: The lac operon, a case study*, Journal of Cell Biology, 161 (2003), pp. 471–476.

[96] P. Visco, R. J. Allen, S. N. Majumdar, and M. R. Evans, *Switching and growth for microbial populations in catastrophic responsive environments*, Biophysical Journal, 98 (2010), pp. 1099–1108.

[97] C. Waddington, *Genetic Assimilation of the Bithorax Phenotype*, Evolution, 10 (1956), pp. 1–13.

[98] M. J. West-Eberhardt, *Phenotypic plasticity and the origins of diversity*, Annual Review of Ecology and Systematics, 20 (1989), pp. 249–278.

[99] ———, *Developmental Plasticity and Evolution*, Oxford University Press, 2003.

[100] J. S. Wolfson, D. C. Hooper, G. L. Mchugh, M. A. Bozza, and M. N. Swartz, *Mutants of Escherichia coli K-12 Exhibiting Reduced Killing by Both Quinolone and 3-Lactam Antimicrobial Agents*, Antimicrobial agents and chemotherapy, 34 (1990), pp. 1938–1946.

[101] F. H. Yildiz and G. K. Schoolnik, *Vibrio cholerae O1 El Tor: identification of a gene cluster required for the rugose colony type, exopolysaccharide production, chlorine resistance, and biofilm formation.*, PNAS, 96 (1999), pp. 4028–33.

[102] R. E. Zordan, D. J. Galgoczy, and A. D. Johnson, *Epigenetic properties of white-opaque switching in Candida albicans are based on a self-sustaining transcriptional feedback loop.*, Proceedings of the National Academy of Sciences of the United States of America, 103 (2006), pp. 12807–12.

[103] E. Zuckerkandl and R. Villet, *Concentration-affinity equivalence in gene regulation: convergence of genetic and environmental effects.*, Proceedings of the National Academy of Sciences of the United States of America, 85 (1988), pp. 4784–8.

université PARIS-SACLAY | ÉCOLE DOCTORALE Sciences du végétal : du gène à l'écosystème

Titre : Rôle des switch phénotypiques et de la mémoire non-génétique dans l'hétérogénéité des populations bactériennes

Mots clés : hétérogénéité, multistabilité, mémoire

Résumé : *Pseudomonas fluorescens* « switchers », souches évolués artificiellement au Rainey Lab, sont un système modèle pour les switch phénotypiques. Ces populations sont typiquement caractérisées par les fréquences de deux phénotypes alternatifs liés à la production d'une capsule d'acide colanique autour de la paroi cellulaire. Bien que on s'attende que telles fréquences soient définies d'une manière univoque par le génotype, elles varient au long de la croissance de la population, ce qui indique une possible dépendance des taux de transition à l'égard de la démographie. J'ai développé un modèle mathématique où les cellules sont représentées comme systèmes bistables contrôlés par une concentration intracellulaire et où les taux de transition dépendent de l'état de la croissance de la population. Le modèle reproduit quantitativement la dynamique de la composition phénotypique de la population (dépendante de l'histoire), et fournie des prédictions à propos de son quasi-équilibre en phase exponentielle en fonction du taux de croissance de la population — prédictions ensuite qualitativement confirmées par les résultats de mon travail expérimental. Pour conclure, on ne peux pas caractériser une population croissante de « switchers » que par l'état asymptotique des fréquences de ses phénotypes alternatifs, puisque le switch est étroitement lié à la démographie.
Dans une perspective évolutive, la persistance transgénérationnelle du phénotype, influencée par des concentrations intracellulaires, pourrait être à l'origine de l'émergence de stratégies comme le « bet-hedging ».

Title : Context-dependent phenotypic switching and non-genetic memory in heterogeneous bacterial populations

Keywords : heterogeneity, multistability, memory

Abstract : *Pseudomonas fluorescens* "switchers", artificially evolved in Rainey Lab, are a model system for phenotypic switching. Populations can be characterized by the frequencies of two alternative states related to the production of a colanic acid capsule around the cell wall. Expected to be at an equilibrium underpinned by the genetic background, such frequencies vary during population growth, hinting to a dependence of the switching rates on demography, and appear to be dependent on the history of the preculture. I thus developed a mathematical model with individual cells as bistable systems controlled by an intracellular concentration, where transition rates depend on the growth state of the population. The model quantitatively reproduces the history-dependent dynamics of the phenotypic composition of the population, and provides qualitative predictions on its quasi-steady state in exponential phase as a function of the growth rate — then corroborated by the results of my experimental work. I conclude that a growing population of switching cells cannot be fully characterized only by the asymptotic steady state of the phenotypes' frequencies, because phenotypic switching is inextricably intertwined with demography. From an evolutionary perspective, trans-generational inheritance of the phenotype mediated by internal concentrations may be at the basis of the emergence of bet-hedging-like strategies.

Université Paris-Saclay
Espace Technologique / Immeuble Discovery
Route de l'Orme aux Merisiers RD 128 / 91190 Saint-Aubin, France